Seismic Design of Rigid Wall-Flexible Diaphragm Buildings: An Alternate Procedure

FEMA P-1026/March 2015

FEMA

nehrp

Seismic Design of Rigid Wall-Flexible Diaphragm Buildings: An Alternate Procedure

FEMA P-1026/March 2015

Prepared for the Federal Emergency Management Agency of the U.S. Department of Homeland Security by the Building Seismic Safety Council of the National Institute of Building Sciences

The Building Seismic Safety Council
A council of the National Institute of Building Sciences
Washington, DC

National Institute of BUILDING SCIENCES
An Authoritative Source of Innovative Solutions for the Built Environment

NOTICE: Any opinions, findings, conclusions, or recommendations expressed in this publication do not necessarily reflect the views of the Federal Emergency Management Agency. Additionally, neither FEMA nor any of its employees make any warranty, expressed or implied, nor assume any legal liability or responsibility for the accuracy, completeness, or usefulness of any information, product, or process included in this publication.

The Building Seismic Safety Council (BSSC) was established in 1979 under the auspices of the National Institute of Building Sciences as a forum-based mechanism for dealing with the complex regulatory, technical, social, and economic issues involved in developing and promulgating building earthquake hazard mitigation regulatory provisions that are national in scope. By bringing together in the BSSC all of the needed expertise and all relevant public and private interests, it was believed that issues related to the seismic safety of the built environment could be resolved and jurisdictional problems overcome through authoritative guidance and assistance backed by a broad consensus.

The BSSC is an independent, voluntary membership body representing a wide variety of building community interests. Its fundamental purpose is to enhance public safety by providing a national forum that fosters improved seismic safety provisions for use by the building community in the planning, design, construction, regulation, and utilization of buildings.

This report was prepared under Contract HSFEHQ-09-D-0417 between the Federal Emergency Management Agency and the National Institute of Building Sciences.

For further information on Building Seismic Safety Council activities and products, see the Council's website (www.bssconline.org) or contact the Building Seismic Safety Council, National Institute of Building Sciences, 1090 Vermont, Avenue, N.W., Suite 700, Washington, D.C. 20005; phone 202-289-7800; fax 202-289-1092; e-mail bssc@nibs.org.

This report can be obtained free of charge from the the FEMA Publication Distribution Center at 1-800-480-2520. The report can also be downloaded in pdf form from the BSSC website at www.bssconline.org.

The National Institute of Building Sciences and its Building Seismic Safety Council caution users of this document to be alert to patent and copyright concerns especially when applying prescriptive requirements.

Foreword

The Federal Emergency Management Agency (FEMA) of Department of Homeland Security has committed under the National Earthquake Hazard Reduction Program (NEHRP) to support implementation of new knowledge and research results for improving seismic design and building practices in the nation. This FEMA NEHRP document, Seismic Design of Rigid Wall-Flexible Diaphragm Buildings: An Alternate Procedure is a new design resource that applies recent research and testing results in addressing the seismic performance issue of "big box" buildings. This type of buildings is typically used for warehouses or retail stores and has been reported for numerous earthquake damage or collapses in the past.

FEMA and the project officer wish to express the gratitude to the members of the Project Workgroup, the Project Management Committee, the Project Review Panel and BSSC Board of Direction, management, and staff for the development, review and completion of this alternate design procedure of rigid wall flexible diaphragm buildings. We are also delighted to see that this alternate procedure has also been adopted in Part III of the 2015 NEHRP Recommended Provisions for trial use by the design community and hopefully to be adopted by the national standards and code in the future.

Federal Emergency Management Agency

Preface

Single-story buildings with rigid walls and flexible diaphragms (RWFD buildings) are common throughout the United States and are often used for warehouse buildings and "big box" retail stores. These buildings have stiff walls constructed of reinforced concrete or masonry, or braced frames of structural steel, and relatively flexible diaphragms of metal deck or wood structural panels. The seismic response of this type of structure is dominated by the deformation of the large and relatively flexible diaphragms. The standard design methods used in current seismic codes for all building types, however, assume primary response occurs in deformation of the vertically oriented lateral force resisting elements - moment frames, braced frames, or shear walls. A design approach for the RWFD building type that is more technically correct than current code design methods, and that can be shown to meet accepted code performance, has been sought for some time.

This publication is the result of a Simplified Design Program study funded by the Federal Emergency Management Agency (FEMA) and administered by the National Institute of Building Sciences' Building Seismic Safety Council. For the RWFD building type, this study demonstrates that design provisions narrowly directed at a single building type can not only be simpler, but provide designs that more consistently meet expected performance objectives. The study also has formed the basis for developing improved design provisions for Part 3 of the 2015 edition of the NEHRP Provisions [FEMA, 2015].

With the alternate design provisions provided in this report, the seismic design community will be afforded a far greater understanding of the seismic response of RWFD buildings. It is anticipated that this methodology will be incorporated into future seismic design codes and standards. Until this occurs, some aspects of the alternate design method can be implemented within the context of current code procedures.

I wish to thank the subject matter experts listed in the Acknowledgments, who were instrumental in conducting the RWFD study and producing this publication.

Jim Sealy
Chair, Building Seismic Safety Council Board of Direction

Acknowledgments

Principal Authors

John Lawson, California Polytechnic State University, San Luis Obispo
Dominic J. Kelly, Simpson Gumpertz & Heger Inc.

Contributing Authors

Andre Filiatrault, University at Buffalo, New York
Maria Koliou, University at Buffalo, New York

Reviewers

Kelly Cobeen, Wiss, Janney, Elstner Associates, Inc.
David McCormick, Simpson Gumpertz & Heger Inc.

Project Management Committee

William Holmes, Rutherford and Chekene (Chair)
James R. Harris, JR Harris & Company
John D. Hooper, Magnusson Klemencic Associates
Dominic J. Kelly, Simpson Gumpertz & Heger Inc.
Barry H. Welliver, BHW Engineers, L.L.C.

Project Review Panel

Ryan Kersting, Buehler & Buehler Structural Engineers, Inc.
James Kramer, MHP Structural Engineers
Trent Nagele, VLMK Consulting Engineers
Joe Steinbicker, Steinbicker & Associates, LLC
Doug Thompson, STB Structural Engineers, Inc.

Project Review Panel Workshop Participants

Thomas Gangel, Wallace Engineering (Walmart)
Nathan Hauer, Structural Engineering Group, Target Stores
Philip Line, American Wood Council
Bonnie Manley, American Iron and Steel Institute
Lawrence Novak, Portland Cement Association

Project Oversight

Mai Tong, Federal Emergency Management Agency
Robert D. Hanson, Federal Emergency Management Agency
Philip Schneider, National Institute of Building Sciences

Table of Contents

Foreword i

Preface ii

Acknowledgments iii

Chapter 1 Introduction 1

1.1 The Need for a New Design Procedure for RWFD Buildings 2

1.2 Purpose of Report 2

1.3 Introduction to the Alternate Procedure and Comparison to Current Design Practice 3

1.4 Implementation of the Alternate Design Procedure 6

1.5 Scope and Limitation of the Alternate Procedure 6

1.6 Overview of Report Contents 7

Chapter2 Description of RWFD Buildings and Their Performance in Earthquakes 11

2.1 Description of Typical RWFD Structures 11

2.2 Seismic Performance History 12

Chapter 3 Current Design Practice Example 17

3.1 Example Building Description (current practice) 17

3.2 Determine Design Spectral Response Accelerations SDS and SD1 (current practice) 19

3.3 Determine Fundamental Building Period (current practice) 19

3.4 Base Shear Using the ELF Procedure (current practice) 20

3.5 Diaphragm Design Forces Using the ELF Procedure (current practice) 21

3.6 North/South Diaphragm Shear Design (current practice) 25

3.7 North/South Diaphragm Chord Design (current practice) 30

3.8 East/West Diaphragm Shear Design (current practice) 31

3.9 East/West Diaphragm Chord Design (current practice) 32

3.10 Shear Wall Force Using the ELF Procedure (current practice) 33

3.11 Shortcomings of Current Practice 36

Chapter 4 Development of an Alternate Seismic Design Procedure 37

4.1 Determination of Building and Diaphragm Period 38

4.2 Response Modification Coefficient, R, Selection 41

4.3 Deflection Amplification Factor, C_d, Selection 45

4.4 Overstrength Factor, Ω_o, Selection 45

4.5 Overview of the Alternate Seismic Design Procedure 46

Chapter 5 Implementation of the Alternate Seismic Design Procedure 49

5.1 A Two-Stage ELF Procedure 49

5.2 First Stage – Diaphragm Design 50

5.3 Diaphragm Design Coefficient C_s Using the ELF Procedure 50

5.4 Diaphragm Forces Using the ELF Procedure 54

5.5 North/South Diaphragm Shear Design 57

5.6 North/South Diaphragm Shear Transfer to Walls 62

5.7 North/South Diaphragm Chord Design 62

5.8 East/West Diaphragm Shear Design 63

5.9 East/West Diaphragm Shear Transfer to Walls 64

5.10 East/West Diaphragm Chord Design 65

5.11 Second Stage – Shear Wall Design 65

5.12 Shear Wall Force Using the ELF Procedure 66

5.13 Limitations and Adaptations of the Alternate Design Procedure 71

Chapter 6 Diaphragm Deflection Check 73

6.1 Deflection of North/South Diaphragm 73

6.2 Deflection of North/South Walls 77

6.3 Limits on Diaphragm Deflection – Deformation Compatibility 79

6.4 Limits on Diaphragm Deflection – Second Order Effects and P-Δ Instability 79

6.5 Limits on Diaphragm Deflection – Building Separations and Setbacks 81

Chapter 7 Comparison of Designs Using Current Practice and Alternate Design Procedure 83

Chapter 8 Future Studies for Design of RWFD Buildings 87

8.1 Steel Deck Diaphragms 87

8.2 Out-of-Plane Top of Wall Anchorage Forces 87

8.3 In-Plane Wall Yielding/Rocking 88

8.4 Irregular Plan Shapes and Abrupt Changes along Exterior Walls 88

8.5 Combining Connector Forces from Shear Acting in Two Orthogonal Directions 89

8.6 Forces on Continuity Ties 89

8.7 Three-Dimension Modeling Calibrated to the Response of Buildings and Tests 89

8.8 Deflection of Wood Diaphragms 89

8.9 Applicability to Buildings with Lightweight Enclosures and Steel Bracing 90

8.10 Applicability to Multi-Story Buildings 90

8.11 Implications of Diaphragm Deflections on Structural and Nonstructural Elements 90

8.12 Large-Scale Diaphragm Tests 91

Chapter 9 Conclusions 93

References 95

Appendices

A. Alternate Design Procedure Discussion and Commentary 99

A.1 Commentary on Alternate Design Procedure with Diaphragm Yielding 99

A.2 Limitations of the Alternate Design Procedure 103

A.3 Applicability of Alternate Design Procedure to RWFD Buildings with Steel Deck Diaphragms 104

A.4 Discussion of Diaphragm Yielding 105

A.5 Quality of Design, Construction and Inspection 105

A.6 Diaphragm Modifications and Deterioration 106

A.7 Possible Code Provisions 106

B. Evaluating RWFD Buildings Using FEMA P695 Methodology 111

B.1 Modeling Framework 113

B.2 Modeling Framework Validation 116

C. List of Connectors in Database 119
D. Evaluation of Current Design Procedure 121
D.1 Description of Archetypes 121
D.2 Summary of FEMA P695 Analysis Results for Current Design 123
D.3 Fundamental Period of the Archetypes 126
E. Description of Archetypes for Current Design Procedure 129
F. FEMA P695 Evaluation Results for Current Design Procedure 137
G. Evaluation of Alternate Design Procedure 145
G.1 Description of Archetypes 145
G.2 Summary of FEMA P695 Analysis Results for the Alternate Design Procedure 145
G.3 Overstrength and Deflection Amplification Factors for the Diaphragm 147
H. Description of Archetypes for Alternate Design Procedure 149
I. FEMA P695 Evaluation Results for Alternate Design Procedure 153
J. Out-of-plane Wall Anchorage Forces 157
J.1 Out-of-Plane Wall and Wall Anchorage Forces; Current Design 157
J.2 Out-of-Plane Wall Anchorage Force Study 158
J.3 Stiffness of Wall Anchorage Connectors 161
J.4 Transfer of Wall Anchorage Forces to Continuous Diaphragm Ties 161
K. Analysis of Archetypes Using Uniform Nailing 163

List of Tables

Table 3.1 Diaphragm Nailing Schedule (Cases 2 and 4) 28

Table 3.2 Diaphragm Nailing Zone Shear Checks 29

Table 3.3 Diaphragm Nailing Zone Shear Checks 32

Table 5.1 Diaphragm Nailing Schedule (Cases 2 and 4) 59

Table 5.2 Diaphragm Nailing Zone Shear Checks 61

Table 5.3 Diaphragm Nailing Zone Shear Checks 64

Table 6.1 Shear Deformation and Nail Slip Computation Table 75

Table 7.1 Common Features for Example Buildings 83

Table 7.2 Comparison of Diaphragm Design Using Current Practice and Alternate Design Procedure 83

Table 7.3 Comparison of Shear Wall Design Forces Using Current Practice and Alternate Design Procedure 85

Table B1 FEMA P695 Earthquake Ground Motion Ensemble 112

Table B2 Beta factors for determining acceptable collapse margin ratios 113

Table C1 Cyclic test data for nails 119

Table C2 Cyclic test data for steel deck sidelap connectors 119

Table C3 Cyclic test data for steel deck framing connectors 120

Table D1 Summary of collapse margin ratio results for wood diaphragm archetype performance groups for current design 125

Table D2 Summary of collapse margin ratio results for steel deck diaphragm archetype performance groups 125

Table D3 Summary of Elastic Periods for Archetypes 126

Table E1 Archetype Descriptions for Wood Diaphragms 129

Table E2 Archetype Descriptions for Steel Diaphragms for High-Seismic Risk – Existing Design 130

Table E3 Archetype Descriptions for Steel Diaphragms for Moderate-Seismic Risk – Existing Design 133

Table F1 Summary of collapse results for RWFD buildings incorporating wood roof diaphragm archetype designs 138

Table F2 Adjusted collapse margin ratios and acceptable collapse margin ratios for RWFD buildings incorporating wood roof diaphragm archetype designs 139

Table F3 Summary of collapse results for RWFD buildings incorporating steel roof diaphragm archetype designs 140

Table F4 Computed and acceptable adjusted collapse margin ratios for RWFD buildings incorporating steel roof diaphragm archetype designs 143

Table G1 Summary of collapse margin ratio results for wood structural panel diaphragm archetype performance groups 146

Table G2 Summary of Elastic Periods for Archetypes Designed Using the Alternative Design Procedure 146

Table G3 Range of building drift ratios (BDRs) for the wood diaphragm performance groups 147

Table H1 Archetype Descriptions for Wood Diaphragms for High- and Moderate-Seismic Risk – Alternate Design 149

Table I1 Summary of collapse results for RWFD buildings incorporating wood roof diaphragm archetype designs 153

Table I2 Adjusted collapse margin ratios and acceptable collapse margin ratios for RWFD buildings incorporating wood roof diaphragm archetype designs 154

Table I3 Overstrength and Deflection Amplification Parameters for the Alternate Design Procedure 155

Table I4 Ratio of the medial diaphragm drift caused by the design level ground motion to the median diaphragm drift at the “code” level force 156

Table K1 Comparison of archetypes 163

List of Figures

Figure 1.1 Comparison of design steps for the alternate and current procedures 5

Figure 2.1 Collapse of RWFD Buildings at Elmendorf Air Force Base, 1964 13

Figure 2.2 Partial Collapse of a RWFD Building with a steel deck diaphragm in Yucca Valley, 1992 14

Figure 2.3 Partial Collapse of a RWFD Building in the Northridge Earthquake, 1994 14

Figure 2.4 Evolution of Wall Anchorage Code Provisions 15

Figure 3.1 Example RWFD Building 17

Figure 3.2 Diaphragm Loading Model (both orthogonal directions shown) 23

Figure 3.3 Diaphragm Shear Distribution in both Orthogonal Directions 25

Figure 3.4 Sheathing Layout and Nailing for a Panelized Roof System 27

Figure 3.5 North/South Nailing Zone Layout 29

Figure 3.6 Diaphragm Chord Forces 30

Figure 3.7 North/South and East/West Nailing Zones Combined 32

Figure 3.8 North/South Lateral Design Forces acting on the Shear Walls (Lines A & J) 35

Figure 3.9 East/West Lateral Design Forces acting on the Shear Walls (Lines 1 & 5) 35

Figure 5.1 Diaphragm Loading Model (Alternate Procedure) 55

Figure 5.2 Diaphragm Shear Distribution 57

Figure 5.3 Shear Diagrams for the Diaphragm Design with the 1.5x Factor 58

Figure 5.4 North/South Nailing Zone Layout 61

Figure 5.5 North/South and East/West Nailing Zones Combined Layout 64

Figure 5.6 North/South Lateral Design Forces acting on the Shear Walls (Lines A & J) 70

Figure 5.7 East/West Lateral Design Forces acting on the Shear Walls (Lines 1 & 5) 71

Figure A1 Amplified Shear Boundary Zones for the Alternate Procedure 102

Figure A2 Deformations and Change in Angle between Roof Diaphragm and Wall 103

Figure B1 Three-step modeling framework 114

Figure B2 Illustration of hysteretic models: (a) Wayne-Stewart and (b) CUREE-SAWS 114

Figure B3 Comparison of hysteretic response for 10d common nail and wood deck: (a) example of experimental data and (b) best fit numerical model based on data from several tests 115

Figure B4 Comparison of hysteretic response for 2-ply-22-gauge framing welds to 0.25 in. plate: (a) experimental and (b) fitted optimal hysteretic models 115

Figure B5 In-plane displacement components of the analytical inelastic roof diaphragm model 116

Figure B6 Illustration of a simplified rigid wall flexible diaphragm (RWFD) building model developed in the RUAUMOKO2D platform 116

Figure B7 Validation/comparison of inelastic roof diaphragm for monotonic loading 117

Figure B8 Validation/comparison of inelastic roof diaphragm for cyclic loading 117

Figure B9 Incremental dynamic analysis results/comparison 118

Figure D1 Archetype Naming Convention 122

Figure D2 Comparison of fundamental periods from analyses of wood panel archetypes to those predicted by the proposed formula, ASCE 7-10 equations, a best fit curve, and those proposed by Freeman et. al. 127

Figure D3 Comparison of fundamental periods from analyses of steel deck archetypes to those predicted by the proposed formula, ASCE 7-10 equations, and a best fit curve 128

Figure J1 Median out-of-plane wall anchorage force for transverse direction of loading 159

Figure J2 Median out-of-plane wall anchorage force for longitudinal direction of loading 160

Acronyms

ACI	American Concrete Institute
ACMR	adjusted collapse margin ratio
ASCE	American Society of Civil Engineers
ASD	allowable stress design
AWC	American Wood Council
BDR	building drift ratio
CMR	collapse margin ratio
CUREE	Consortium of Universities for Research in Earthquake Engineering
DDR	diaphragm drift ratio
DE	Design Earthquake
DF/L	Douglas-Fir/Larch
DM	damage measure
EERI	Earthquake Engineering Research Institute
ELF	Equivalent Lateral Force
FEMA	Federal Emergency Management Agency
g	gravity
IBC	International Building Code
ICBO	International Conference of Building Officials
ICC	International Code Council
IDA	incremental dynamic analysis
IM	intensity measure
MCE	Maximum Considered Earthquake
NEHRP	National Earthquake Hazards Reduction Program
NIST	National Institute of Standards and Technology
NOAA	National Oceanic and Atmospheric Administration
NRC	National Research Council of National Academy of Sciences
o.c.	on center
OSB	oriented-strand board
P-Δ	axial load-deflection
PCF	pounds per cubic foot
PEER	Pacific Earthquake Engineering Research Center
PG	performance group

PGA	peak ground acceleration
Plf	pounds per linear foot
PSI	pounds per square inch
RWFD	rigid wall-flexible diaphragm
SAWS	Seismic Analysis of Woodframe Structures
SDC	Seismic Design Category
SDI	Steel Deck Institute
SDPWS	Special Design Provisions fo Wind and Seismic
SEAOC	Structural Engineers Association of California
SEAONC	Structural Engineers Association of Northern California
sec	seconds
SFRS	Seismic-Force-Resisting System
SRSS	square root sum of the squares
SSC	Seismic Safety Commission of the State of California
SSF	spectral shape factor
UBC	Uniform Building Code
WDR	wall drift ratio
WR Deck	wide rib deck

Chapter 1 Introduction

This report presents a proposed alternate design procedure for earthquake resistance of one-story buildings with stiff and strong concrete or masonry wall elements coupled with flexible roof diaphragms. In this report, these buildings are referred to as rigid wall-flexible diaphragm (RWFD) buildings.

This alternate design procedure resulted from one of three studies that were part of the Building Seismic Safety Council's Simplified Design Program, a larger project to explore means of simplifying the seismic design of buildings. The other two studies in this program were stand-alone seismic design provisions for Seismic Design Category (SDC) B structures and further simplification of the existing simplified procedure in Section 12.14 of ASCE 7 (ASCE, 2010). The goal of the RWFD study was to determine whether a set of stand-alone design provisions could be created for a single building type, in this case a "box" or RWFD building. This topic had the added potential to directly address the behavior of RWFD buildings that often includes yielding of the diaphragm rather than in-plane yielding of the walls.

The objectives of the study were:

- To develop an alternate design methodology for the horizontal roof diaphragm and the vertical elements of the seismic-force-resisting system (SFRS) that is relatively simple yet appropriately captures the unique behavior of single-story RWFD buildings in which a building's response is dominated by the diaphragm instead of the vertical portion of the SFRS, and

- To base the alternate design procedure on design parameters that are representative of the diaphragms response such as a period, a ductility coefficient, and an overstrength factor that account for diaphragm flexibility and performance.

The alternate design procedure was developed and evaluated using the procedure of *Quantification of Building Seismic Performance Factors* (FEMA P695) [FEMA, 2009] to confirm it would meet the intent of current code provisions. The results of these evaluations are presented in the appendices to this report.

In addition to this report, a preliminary version of the alternative procedure is included in Part 3 of the 2015 NEHRP Provisions [FEMA, 2015]. It is intended that the alternative design procedure be proposed for incorporation into a future edition of *Minimum Design Loads for Buildings and Other Structures* (ASCE 7) [ASCE, 2010].

1.1 The Need for a New Design Procedure for RWFD Buildings

Single-story buildings with concrete or masonry walls supporting lightweight wood or steel roof diaphragms are a very common building type across North America and other parts of the world. The walls are strong and stiff in their plane in comparison to the strength and stiffness of the diaphragm in its plane. The current building code provisions most frequently used for these buildings are those of the equivalent lateral force procedure in ASCE 7-10 (ASCE, 2010). This procedure, applicable to all buildings, incorporates the assumption that the primary flexibility and ductility occur in the vertical elements of the SFRS. The flexibility drives the dynamic amplification of the ground motion, and the ductility drives the dissipation of the energy of the dynamic response. The actual seismic behavior of these Rigid Wall-Flexible Diaphragm (RWFD) buildings is quite different. Evidence indicates that the dynamic behavior is largely dominated by the diaphragm's response instead of the walls' response. This is a significant departure from the underlying assumptions of the widely used equivalent lateral force procedure.

The past performance of RWFD buildings when subjected to moderate to strong earthquake shaking has demonstrated weaknesses. Building code design provisions have addressed specific known weaknesses of RWFD buildings, and in particular, the connections between the tops of walls and the diaphragms. Provisions specific to these buildings have evolved mostly as reactions to observed damage with little stated recognition of how these buildings respond differently to earthquakes than multi-story frame buildings or one-story buildings with rigid diaphragms. The RWFD buildings have diaphragms that often yield and dominate the building behavior while the walls typically remain mostly in the elastic range for in-plane loading.

There is a need to address the diaphragm yielding of RWFD buildings in applicable design requirements. Several design approaches were considered including a displacement based design approach, which would not have fit into the current framework of ASCE 7. However, the resulting alternate design procedure ended up being well aligned with current provisions of ASCE 7-10, but with the diaphragm yielding specifically considered. Many of the current provisions are still applicable when implementing the alternate design procedure. As such it is better suited for incorporation into ASCE 7 rather than being in a stand-alone document.

1.2 Purpose of Report

The purpose of this report is to present an alternate seismic design procedure for RWFD buildings that better captures actual building behavior, and in particular accounts for yielding of the diaphragm being predominant, rather than yielding in the vertical elements of the SFRS. The target audience is practicing engineers that design and retrofit this type of building. The intention of this report is to convey design principles to these practicing engineers that they may use in their designs to improve the seismic performance of RWFD buildings.

1.3 Introduction to the Alternate Procedure and Comparison to Current Design Practice

The alternate procedure is force based like existing design requirements for this type of building; however, unlike current provisions, the magnitude of the diaphragm design forces in the alternate procedure depends more on diaphragm properties than those of the vertical in-plane wall elements. The alternate procedure is similar to the two-staged analysis procedure of a multiple story building with a flexible upper portion and a stiff lower portion; however, for the one-story RWFD building, the diaphragm is the flexible upper portion, and the in-plane walls are the stiff lower portion.

In the alternate procedure, the diaphragm is designed using the equivalent lateral force procedure but with a period applicable to the diaphragm alone and a response modification coefficient applicable to the diaphragm, R_{diaph}. This is a departure from current design practice in which the diaphragm forces are computed using a period and response modification coefficient applicable to the vertical wall system. Also, the alternate procedure requires designing the end regions of a diaphragm for an amplified shear to better spread diaphragm yielding. Diaphragm chords are designed using forces computed with R_{diaph} but without the amplification in the end regions. Collectors for buildings assigned to SDC C to F are designed for a diaphragm force amplified by the diaphragm overstrength factor, Ω_o. At this time the alternative is limited to buildings constructed with wood structural panel diaphragms nailed to wood framing members or wood nailers.

The walls are then designed using a period appropriate for the in-plane walls and a response modification, R_{wall}, applicable to the wall SFRS. The period for the walls is based on an approximate period equation, Equation 12.8-10, in ASCE 7-10 applicable to masonry and concrete shear walls. Note that this is a different approximate period equation than equation 12.8-7 of ASCE 7-10 that is commonly used for this type of building. In addition, the value of R_{wall}/ρ_{wall} cannot be greater than $R_{diaph}/\rho_{diaph;}$ and if it is less, then the diaphragm force applied to the walls must be amplified by the ratio of $(R_{diaph}\times\rho_{wall})/(R_{wall}\times\rho_{diaph})$. Currently, the redundancy factor ρ_{diaph} is permitted to equal 1.0 per ASCE 7-10 Section 12.3.4.1. These variables are defined in Chapters 4 and 5 of this report.

In addition to designing the diaphragm and walls for lateral forces, the in-plane deflections of the diaphragm and walls must be checked. The diaphragm deformations are computed using the equation from the SDPWS-2008 (AWC, 2009) using a force level consistent with the design force level and then amplified by a defection amplification coefficient, C_d, applicable to the diaphragm. The wall deformations can be computed using their design level forces and then amplified by the C_d factor appropriate for the wall SFRS. These deflections are used to check deformation compatibility, P-Δ instability, and building separation or setbacks.

The alternate design procedure is outlined in Figure 1.1 along with an outline for current design practice. The list of design steps demonstrates both similarities and differences between the alternate design procedure and current design practice. Many of the difference have been discussed above. The similarities are substantial in that both procedures are force based and the steps for each procedure can be aligned with one another. Many provisions such as those for out-of-plane wall forces, wall anchorage and diaphragm cross-ties are essentially identical for larger diaphragms under current practice.

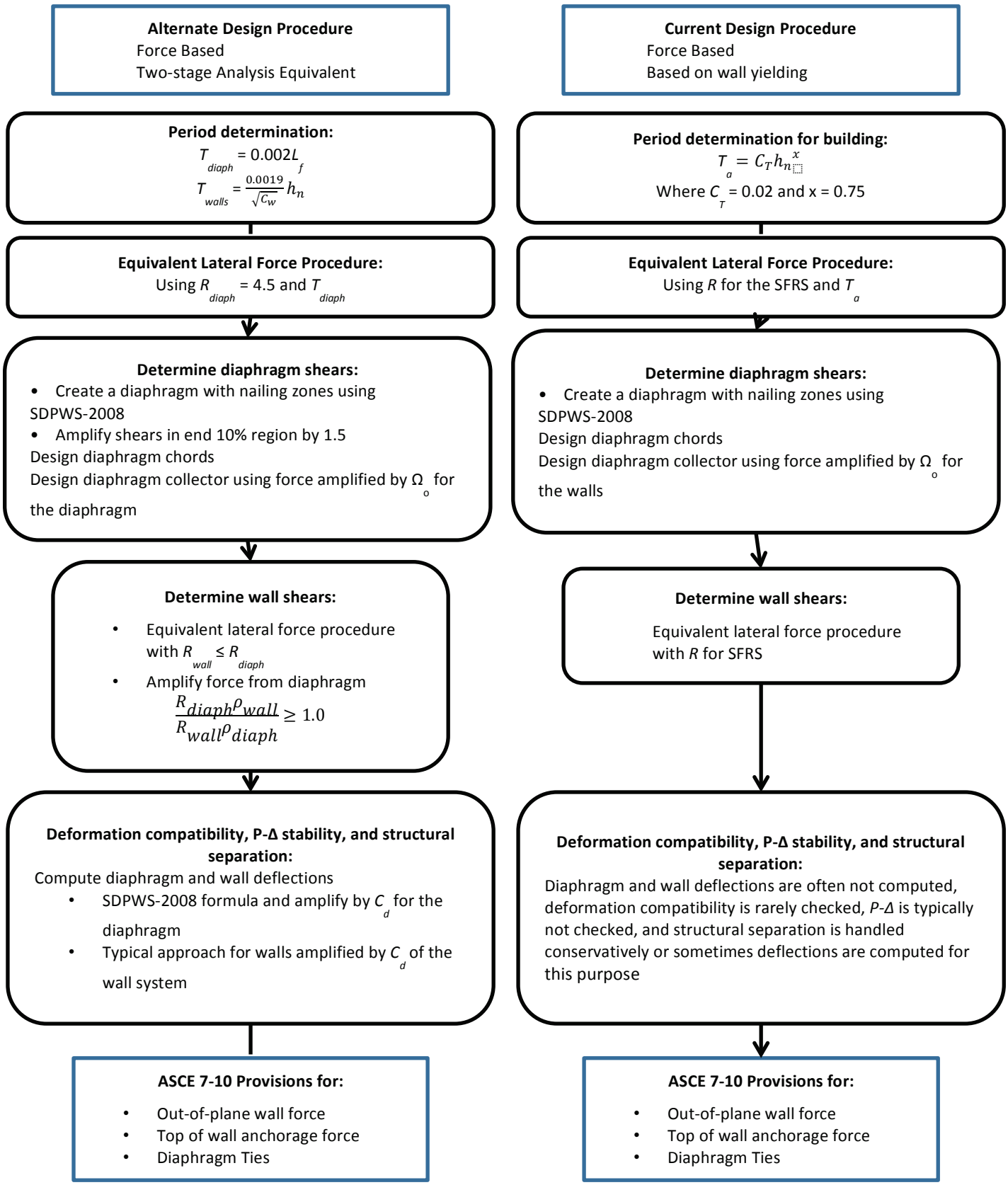

Figure 1.1 – Comparison of design steps for the alternate and current procedures

1.4 Implementation of the Alternate Design Procedure

The alternative procedure has yet to be considered for adoption by building code or standard writing organizations. As such, it is not adopted by any building code at this time. Use of the alternate procedure for new construction could be permitted by the building official on a case by case basis, as allowed for in Section 11.1.4 Alternate Materials and Methods of Construction and the last paragraph of Section 12.2.1 of ASCE 7-10. Use of the alternate procedure for voluntary seismic strengthening of RWFD buildings should be permissible under current building code provisions.

Although designs using the alternate procedure will likely not meet current code requirements, some of the principles can be implemented within current design requirements of ASCE 7-10. For example, the concept of having a stronger diaphragm end region that will be introduced in this report can be implemented by using current diaphragm required strength, while increasing the end regions of the diaphragm above current diaphragm strength requirements.

The principles of the alternate procedure can also be implemented as part of voluntary seismic strengthening projects. For example, rather than strengthening an entire existing diaphragm that is too weak by today's standards, increasing the nailing only in the end regions may move the location of first yielding away from the ends of the diaphragm and improve the overall behavior when subjected to strong earthquake shaking. Doing so would also require strengthening diaphragm-to-ledger and ledger-to-wall connections as well, but it would limit the strengthening to the perimeter regions of the diaphragm rather than the entire diaphragm. Also, the use of the two-stage procedure with a period of the diaphragm will reduce the design forces on large span diaphragms. Note that it would be more difficult to apply this procedure to existing building code upgrades in accordance with *Seismic Evaluation and Retrofit of Existing Buildings* (ASCE 41-13) [ASCE, 2013].

1.5 Scope and Limitations of the Alternate Procedure

The alternate design procedure presented in this report is applicable to the design of new and the retrofit of existing RWFD buildings with wood structural panel diaphragms in which diaphragm yielding is expected. The diaphragm must be rectangular in shape or consist of a multi-span diaphragm able to be separated into rectangular portions laterally supported on all four edges of each rectangular segment. The wood structural panels must be nailed to wood framing members or wood nailers. It does not apply to buildings in which the vertical wall elements are anticipated to experience significant yielding under the design earthquake.

At this time the alternate design procedure is not intended to apply to RWFD buildings with steel deck diaphragms. There are several reasons for not recommending its use even though use of the procedure for steel deck diaphragms has been studied (Koliou, 2014). Reasons include (1) tests results of a large

scale diaphragm showed significantly less distribution of yielding than the analyses show when loaded parallel to deck edges (Massarelli, et al., 2012), (2) steel deck diaphragms have not been envisioned to be yielding elements, and as such design strengths are based on monotonic tests, (3) data for reverse cyclically loaded connections is sparse and missing for many commonly used deck gages, (4) the post-yield stiffness of connectors is positive for only a small deformation, 1 to 2 mm, (5) few reverse cyclically loaded diaphragm tests have been performed while FEMA P695 requires comprehensive test data, and (6) many diaphragms in high seismic regions are designed using proprietary sidelaps for which no test data was available to include in the study. Additionally, end lap connectors that are expected to resist diaphragm shears in a ductile manner, while at the same time resisting out-of-plane wall anchorage forces in an elastic manner must be further studied and understood. This issue will likely require design limitations that have yet to be identified. These limitations demonstrate the high priority for further research on the seismic capabilities of steel deck diaphragms.

The building examples presented and the supporting analytical modeling use a SFRS consisting of concrete shear walls. It is believed that the alternate design procedure is equally suited for masonry shear wall systems. At this time the procedure presented in this report is not expressly intended to apply to braced frame buildings with flexible roof diaphragms; however, many of the concepts are expected to be relevant to this building type. In contrast to RWFD buildings, structures with a perimeter braced frame SFRS often do not have heavy walls, and the proposed period equation presented in this report and the buildings modeled behavior may not be applicable. Large RWFD buildings that use interior braced frames to reduce the roof diaphragm spans to manageable distances are a possible exception; the alternate procedure and its period assumptions are likely applicable.

1.6 Overview of Report Contents

The following is an overview of the contents of this report.

Chapter 2 provides a description of RWFD buildings and the performance of these buildings in past earthquakes.

Chapter 3 describes current design practice through the use of a design example and finishes with a discussion of the shortcomings of current design practice. The current code design procedure is presented before the alternate procedure, so that shortcomings of current practice can be brought to light and addressed with the alternate procedure.

Chapter 4 describes the basis for development of an alternate procedure to the design of RWFD buildings. It presents an estimated period formula applicable to a flexible diaphragm and discusses computation of the overall building fundamental period. It recommends the use of a diaphragm response modification coefficient and provides values for a diaphragm deflection amplification factor and a diaphragm overstrength factor. It also demonstrates that increasing the diaphragm strength in the

end regions of the diaphragm results in better distribution of diaphragm yielding. The final section of this chapter summarizes the steps required to implement the alternate design procedure.

Chapter 5 describes in detail implementation of the alternate design procedure. It describes a two-stage equivalent lateral force procedure in which the diaphragm is designed using the diaphragm's response modification coefficient and the diaphragm's period, and then the walls are designed using the response modification coefficient and period applicable the vertical elements of the SFRS. It uses the same building considered in Chapter 3 for current practice and redesigns it with the alternate procedure.

Chapter 6 demonstrates computation of the diaphragms deflection. It then describes use of the diaphragm deflection to check for deformation compatibility, second order effects and P-Δ instability, and building separation or setback.

Chapter 7 provides a comparison of key design results from current practice relative to the alternate design procedure. This includes a comparison of the required diaphragm nailing for each procedure.

Chapter 8 provides a list of future studies recommended on this topic in order to extend the use of the alternate procedure and develop a comprehensive set of seismic design provisions for RWFD buildings.

Chapter 9 provides conclusions.

The appendices provide background information on the analyses performed on archetypes designed using current practice. The analyses demonstrate the need for modified design requirements and the improvement in performance of archetypes designed with the alternate procedure. Appendix A provides commentary, discussion, and limitations of the alternate design procedure. Appendix B describes use of the FEMA P695 [FEMA, 2009] methodology to evaluate RWFD buildings for acceptable seismic performance. Appendix C includes a list of connectors used for flexible diaphragms that have been cyclically tested.

Evaluation of the current design procedure for RWFD buildings is described and the results presented in Appendices D to F. Appendix D describes how the current design approach was evaluated and provides summary results for archetype performance groups. It also provides information of how the period formulas were determined for RWFD buildings and diaphragms. Appendix E describes the archetypes, and Appendix F includes detailed FEMA P695 analysis results.

Evaluation of the alternate design procedure for RWFD buildings is described and the results presented in Appendices G to I. Appendix G includes summary results for the archetype performance groups, period information, and overstrength and deflection amplification factors. Appendix H describes the archetypes, and Appendix I includes detailed analysis results.

Appendix J includes information of a study on out-of-plane wall anchorage forces, and Appendix K includes analysis results of archetypes with uniform nailing over the entire span to determine the sensitivity to the spread of yielding if the shear amplification factor is applied over the entire diaphragm span.

THIS PAGE INTENTIONALLY LEFT BLANK

Chapter 2 Description of RWFD Buildings and Their Performance in Earthquakes

RWFD buildings have been a common building type for many decades, particularly in the western U.S. where seismic hazards are greatest. The performance of and damage to these buildings during major earthquakes have been recorded or documented in many reports and papers. Past performance indicates that special vulnerabilities have existed in this building type; however. Recent code changes implemented to address these vulnerabilities have not yet been tested by a major earthquake.

2.1 Description of Typical RWFD Structures

Structures containing rigid walls with flexible diaphragms are ubiquitous across our urban environment. Often labeled as "big-box" buildings, these structures are the mainstay for retail, storage and distribution facilities for North America's large companies. These buildings are favored by developers and owners for providing the most cost effective approach to enclosing large floor spaces while providing durable and secure perimeters.

RWFD buildings incorporate concrete or masonry walls, which are considered rigid in-plane, with flexible horizontal in-plane wood or steel roof diaphragm systems. These rigid walls act as shear walls to provide seismic shear resistance. Concrete wall systems are most often site-cast precast panels, usually referred to as tilt-up or tilt-wall panels [ACI 551, 2010]. These highly cost-efficient and versatile enclosures are common in many markets across North America, including in high seismic zones. Plant-cast precast concrete walls and concrete block masonry are also very popular perimeter shear wall systems enclosing these structures; the relative popularity varies significantly from one regional market to another. These rigid wall systems inherently contain large perimeter seismic masses relative to the roof diaphragm seismic mass. Details of how these buildings are constructed can be found in *Engineering Tilt-Up* [Mays and Steinbicker, 2013].

Roof diaphragms in these buildings consist either of a wood structural panel diaphragm or a steel deck diaphragm depending upon the regional preferences. Wood structural panel diaphragms are very common in the Western and Southwestern United States, especially in high seismic regions. Plywood, or more recently oriented strand board (OSB), is fastened with nails to wood framing to provide a structural diaphragm as well as a roofing substrate. More commonly encountered today, these wood structural panels are fastened to wood nailer plates that are factory installed on top of steel joist and joist-girder roof support structure. The speed and cost-efficiency of combining the wood-based diaphragm with a steel support structure make this "hybrid" system very popular in RWFD buildings in California, Nevada, Arizona, Oregon and Washington. The in-plane shear strength and stiffness of these diaphragms are a function of the wood structural panel thickness and grade, as well as nail size and spacing. The wood structural panel diaphragms are relatively flexible, weak, and lightweight compared with the surrounding stiff, strong, and heavy walls.

Steel deck diaphragms are more popular in Canada, Mexico, as well as the United States outside of the West and Pacific Northwest. The steel decking is fastened to supporting open web steel joists and adjacent deck panels with welds or screws, and sometimes with an assortment of proprietary fasteners. The in-plane shear strength and stiffness of these diaphragms are a function of the steel deck gage, deck profile, joist spacing, and fastener type and spacing [SDI, 2004]. Unlike composite steel decking topped with concrete, a popular floor and roof system in multistory buildings, untopped steel deck diaphragms are relatively lightweight, weak, and flexible in-plane compared with the surrounding walls.

A similar seismic response is also possible from buildings that incorporate rigid braced frames instead of concrete or masonry walls as the vertical elements of the SFRS. In very large distribution warehouses, interior braced frames are commonly used to reduce the horizontal roof diaphragm spans. The design methodology presented herein is believed to be equally applicable to these situations. The principal difference is that, unlike concrete or masonry walls, the braced frames often are not much stronger than the diaphragm. The reason is that the proportions of the walls are driven more by the need for functional enclosure of the space than for adequate out-of-plane strength. These reasons usually drive the design to a solution that has in-plane strength far in excess of code demands. The same is generally not true for steel braced frames.

Potentially, some metal building structures could also be included in a broader definition of RWFD buildings. The important factor to consider is the relative horizontal stiffness or period of vibration of the roof diaphragm compared to the vertical elements of the SFRS. Metal buildings with X-braced perimeter systems and a large steel deck diaphragm will possibly also have seismic behavior dominated by the diaphragm; however, metal buildings with repetitive steel frames and/or X-braced roof diaphragms likely will not be dominated by diaphragm behavior to the extent assumed in this alternate design methodology.

2.2 Seismic Performance History

The seismic performance of RWFD buildings in the past has often been poor. The first documented failures of a RWFD building due to seismic ground motions were warehouses at Elmendorf Air Force Base near Anchorage, Alaska in 1964. Designed in 1951 for a lateral force of only 8-percent of gravity under an allowable stress design approach [NRC, 1973], a partial steel rod X-braced diaphragm below a wood roof structure failed at the diaphragm boundaries due to inadequate shear transfer, causing two buildings to completely collapse (Figure 2.1). A few years later, the 1971 San Fernando earthquake tested this building type again with strong seismic ground motions. Because of the high density of RWFD buildings in the region, coupled with poor out-of-plane wall anchorage practices, significant failures caught the attention of the engineering community and quickly resulted in new code provisions.

Figure 2.1: Collapse of RWFD Buildings at Elmendorf Air Force Base, 1964 (Source: U.S. Air Force)

Thus far, the performance history of RWFD buildings has largely been dominated by the poor performance of the out-of-plane anchorage attaching the heavy walls to the lightweight roof diaphragms [SEAONC, 2001]. Wall-to-roof separations and partial collapses have been documented in the 1971 San Fernando earthquake [NOAA, 1973], 1984 Morgan Hill earthquake [EERI, 1985], 1987 Whittier Narrows earthquake [EERI, 1988], 1989 Loma Prieta earthquake [Phipps M, et. al., 1990], 1992 Landers/Big Bear earthquakes (Figure 2.2) [Shipp, 2010], and the 1994 Northridge earthquake (Figure 2.3) [SSC, 1995]. Because the earthquakes in which wall anchorage failures have been observed have occurred in California, and because the RWFD building roof systems in California are predominately wood structural panel, observed wall anchorage failures have historically been in wood diaphragms. The smaller number of steel deck diaphragm failures [Shipp, 2010; Brandow, 2010] observed to date could simply be associated with the limited inventory of this roof system where strong ground motions have occurred to date.

Figure 2.2: Partial Collapse of a RWFD Building with a steel deck diaphragm in Yucca Valley, 1992 (Source: Gregg Brandow)

Figure 2.3: Partial Collapse of a RWFD Building in the Northridge Earthquake, 1994 (Source: EERI)

In reaction to the repeated failures of the wall anchorage system in these buildings in the western United States, the Uniform Building Code (UBC) provisions have, multiple times, become more stringent and required higher design forces for out-of-plane wall anchorage (Figure 2.4). Based on observations following the Northridge earthquake, the current wall anchorage provisions referenced by the 2012 International Building Code (IBC) [ICC, 2012] are contained in ASCE 7-10 Section 12.11.2 [ASCE, 2010] and prescribe maximum expected design forces without relying upon connection ductility [SEAOC, 1999]. These design force levels and detailing requirements for out-of-plane wall anchorage have remained largely unchanged since they were introduced into the 1997 Uniform Building Code [ICBO, 1997]. Since that time, the current practice and force levels of anchoring heavy walls to the flexible diaphragms have not been tested by a strong earthquake event.

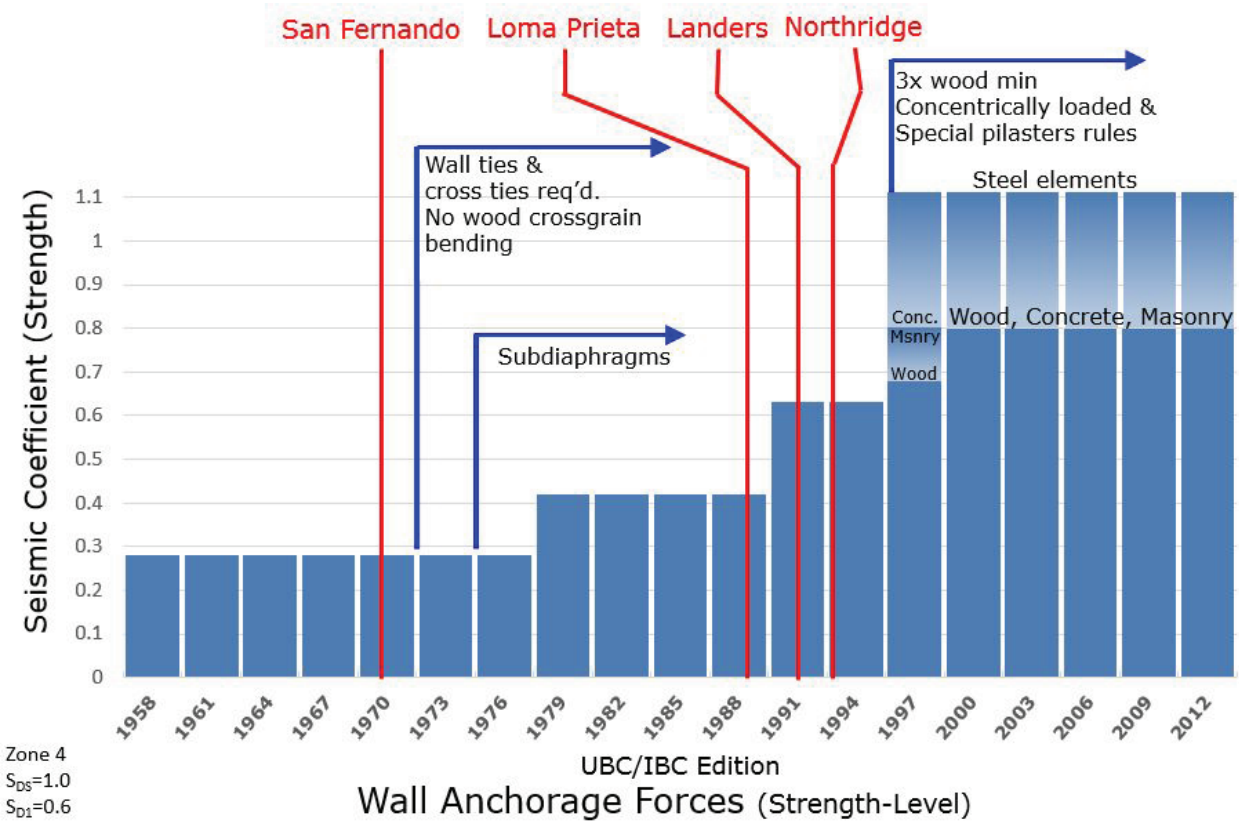

Figure 2.4: Evolution of Wall Anchorage Code Provisions (Source: John Lawson SE)

Observation of earthquake damage to the in-plane rigid shear walls or the main flexible roof diaphragm has been rare, except for collateral damage from the out-of-plane wall anchorage issues. The perimeter shear walls often consist of largely solid wall portions with relatively few penetrations, resulting in in-plane lateral strength significantly in excess of that required for seismic forces. This inherent overstrength of the shear walls transfers the inelastic building behavior into the diaphragm. It is important to consider that the out-of-plane detachment of the heavy walls from the diaphragm in the past may have protected the diaphragm from experiencing in-plane seismic forces which could have led to global failure. The overstrength of the walls, combined with the code required higher wall anchorage and collector force levels, could potentially make diaphragm yielding, foundation rocking or sliding, and global response more critical for RWFD buildings in future earthquakes.

Chapter 3 Current Design Practice Example

While the out-of-plane wall anchorage provisions have dramatically evolved after each damaging earthquake, code-based seismic design methodologies for the diaphragm and vertical elements of the SFRS have remained fairly consistent. For RWFD buildings, the past and current practices are to engineer the SFRS using the equivalent lateral force (ELF) procedure of ASCE 7-10 Section 12.8. This procedure assumes the predominant structural response is closely associated with the vertical elements of the SFRS. Under the ELF procedure, seismic forces are based on the assumption of lumped masses at story levels, supported on flexible elements that represent the lateral stiffness of shear walls or frames traditionally defining the SFRS. The period of the SFRS is key to determine the code-based seismic forces. Additionally, overstrength factor, Ω_o, and deflection amplification factor, C_d, are currently both determined based on the vertical elements of the SFRS.

3.1 Example Building Description (current practice)

To illustrate the concepts presented in this report, design of an example building is presented. The example building represents a common concrete tilt-up wall building with a low-sloped wood structural panel roof diaphragm. See Figure 3.1.

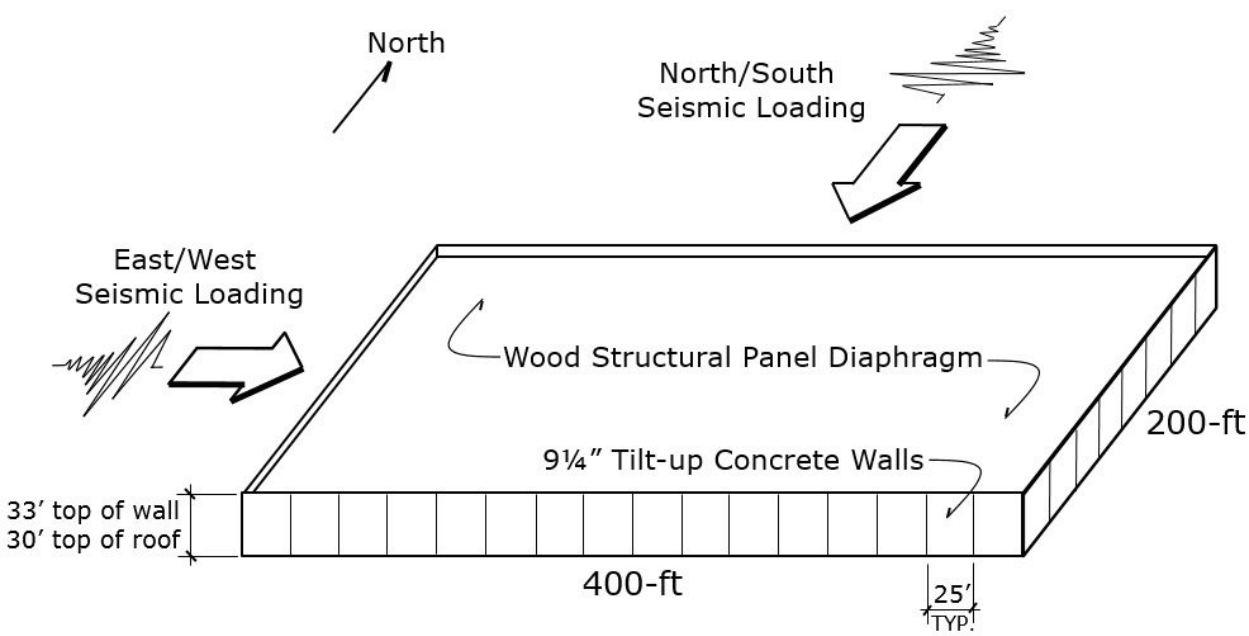

Figure 3.1: Example RWFD Building

Codes and Standards

2012 International Building Code (IBC)

Minimum Design Loads for Buildings and Other Structures (ASCE 7-10)

2008 Special Design Provisions for Wind and Seismic (SDPWS-2008)

Seismic-force-resisting system
Bearing-wall system consisting of intermediate precast concrete shear walls supporting a flexible diaphragm of wood structural panel construction.

Seismic and site data
Mapped spectral accelerations for the site $S_S = 1.5$ and $S_1 = 0.6$
Site Class = D
Risk Category = II (ASCE 7-10 Table 1.5-1)
Redundancy Factor $\rho = 1.0$ (computed for the walls and given for the diaphragm in accordance with ASCE 7-10 Section 12.3.4.1)

Wind: Assumed not to govern the design

Perimeter Walls
Wall Thickness = 9.25 inches of concrete (150 pcf, $f'_c = 4000$ psi)
Height = 30 feet to roof with another 3-foot for the parapet

Roof Structure
Panelized hybrid roof structure [Lawson J, 2013]
Structural-I sheathing (15/32" OSB wood structural panel)
Pre-engineered/pre-manufactured open-web steel joists and joist-girders with full-width wood nailers (popular hybrid system).
All wood is Douglas-fir/Larch (DF/L), S-Dry
Roof Dead Load = 12 psf assumed as a design load

Following common practice, the equivalent lateral force (ELF) procedure and the provisions of the 2012 IBC and ASCE 7-10 will be utilized for this design example unless otherwise noted.

Typically, the building inventory comprising RWFD buildings consists of concrete or masonry shear walls. In SDC C and higher, the permitted types of concrete and masonry shear wall systems are: intermediate precast concrete shear walls, special reinforced concrete shear walls, and special reinforced masonry shear walls. While special reinforced concrete and special masonry shear walls benefit from higher response modification coefficients, additional detailing and analysis provisions are applicable, so they are less frequently used. As a result, in one-story tilt-up concrete buildings, intermediate precast shear wall systems are most common. In SDC D and above, this lateral-force-resisting system has a height limitation of 40 feet, except in single-story storage warehouses where the limitation extends to 45 feet, per ASCE 7-10 Table 12.2-1. The use of the intermediate precast shear wall system will be illustrated for this building example.

3.2 Determine Design Spectral Response Accelerations S_{DS} and S_{D1} (current practice)

The short and long period site coefficients F_a and F_v are used to modify the mapped spectral accelerations S_S and S_1 to determine the design spectral response accelerations. Using the given mapped spectral accelerations $S_S = 1.5$ and $S_1 = 0.6$ and site class D, the following site coefficients are determined from IBC Tables 1613.3.1 (1) and (2). ASCE 7-10 Tables 11.4-1 and 11.4-2 may also be consulted.

$F_a = 1$ (short period)
$F_v = 1.5$ (1-second period)

Using these site coefficients, the site-adjusted spectral accelerations are determined:

$$S_{MS} = F_a S_S = 1.0(1.5) = 1.5 \text{ (short period)} \qquad \text{IBC Eq. 16-37}$$

$$S_{M1} = F_v S_1 = 1.5(0.6) = 0.9 \text{ (1-second period)} \qquad \text{IBC Eq. 16-38}$$

The design spectral response accelerations are obtained as follows:

$$S_{DS} = \frac{2}{3} S_{MS} = 1.0 \text{ (short period)} \qquad \text{IBC Eq. 16-39}$$

$$S_{D1} = \frac{2}{3} S_{M1} = 0.6 \text{ (1-second period)} \qquad \text{IBC Eq. 16-40}$$

Using the design spectral response accelerations and the risk category, the next step is to determine the appropriate Seismic Design Category from IBC Tables 1613.3.5 (1) and (2). With S_1 less than 0.75, both the short-period and 1-second-period design categories are level D; thus, SDC D governs.

Short-period category = D — IBC T 1613.3.5(1)
1-second-period category = D — IBC T 1613.3.5(2)
Governing SDC = D

Using ASCE 7-10 Section 12.6 in conjunction with Table 12.6-1, the equivalent lateral-force (ELF) procedure of Section 12.8 is most commonly used to determine the seismic base shear coefficient.

3.3 Determine Fundamental Building Period (current practice)

For a concrete shear wall building, the approximate fundamental period, T_a, under current practice is obtained using ASCE 7-10 Equation 12.8-7 with $C_T = 0.020$ and $x = 0.75$. For this building, the average roof height, h_n, is 30 feet.

$T_a = C_T h_n^{3/4} = (0.02)30^{0.75} = 0.26$ seconds ASCE 7-10 Eq. 12.8-7

Alternatively, Equation 12.8-9 could have been used.

Because this example involves a regular structure five stories or fewer in height having a period, T_a, less than 0.5 seconds, the base shear coefficient, C_s, can be based on an S_{DS} that need not exceed the value calculated using a value of 1.5 for S_S (Section 12.8.1.3). However, in our example S_S already does not exceed 1.5, thus the design spectral response accelerations and SDC remain as originally calculated.

$S_{DS\ design} = 1.0$ (short period)
$S_{D1\ design} = 0.6$ (1-second period)
SDC = D

3.4 Base Shear Using the ELF Procedure (current practice)

ASCE 7-10 Section 12.8.1 defines the seismic base shear as

$V = C_s W$ ASCE 7-10 Eq. 12.8-1

where

$C_s = \frac{S_{DS}}{R/I_e}$ ASCE 7-10 Eq. 12.8-2

Because these tilt-up concrete walls will be considered load-bearing, intermediate precast shear walls, the following seismic performance factors are applicable to the building:

$R = 4$	Response modification coefficient	ASCE 7-10 T 12.2-1
$\Omega_o = 2½$	Overstrength factor	
$C_d = 4$	Deflection amplification factor	

In addition, the importance factor described in ASCE Section 11.5 is obtained from Table 1.5-2 based on the building's given Risk Category II:

$I_e = 1.0$ ASCE 7-10 T 1.5-2

Therefore, per Eq. 12.8-2

$$C_s = \frac{S_{DS}}{R/I_e} = \frac{1.0}{4/1.0} = 0.25$$

Checking the maximum limit for C_s with Eq. 12.8-3 where $T \leq T_L$

$$C_{s\,max} = \frac{S_{D1}}{T\left(R/I_e\right)} = \frac{0.6}{0.26\left(4/1.0\right)} = 0.58 > 0.25 \quad \text{OK}$$

Checking the minimum allowed value for C_s, ASCE 7-10 Equations 12.8-5 and 12.8-6 are applicable. In this example, S_1 is equal to 0.6*g*: therefore, Equation 12.8-6 is also required to check the minimum allowed C_s.

$$C_{s\,min} = 0.044 S_{DS} I_e = 0.044(1.0)(1.0) = 0.044 < 0.25 \quad \text{OK} \qquad \text{ASCE 7-10 Eq. 12.8-5}$$

$$C_{s\,min} = 0.01 < 0.25 \quad \text{OK} \qquad \text{ASCE 7-10 Eq. 12.8-5}$$

$$C_{s\,min} = \frac{0.5 S_1}{R/I_e} = \frac{0.5(0.6)}{4/1.0} = 0.075 < 0.25 \quad \text{OK} \qquad \text{ASCE 7-10 Eq. 12.8-6}$$

The calculated value for $C_s = 0.25$ is between the maximum and minimum allowed values.

$$C_{s\ \text{governs}} = 0.25$$

Substituting into Equation 12.8-1, we obtain the base shear equation for the building for each orthogonal axis direction of the structure, which is used to determine the design forces in the shear walls.

$$V = C_s W = 0.25W$$

3.5 Diaphragm Design Forces Using the ELF Procedure (current practice)

Because the current code practice is based on a classical vibration model using lumped masses (at the diaphragm) elevated on a flexible column (frames or shear walls), the diaphragm's forces are assumed to be closely associated with the response of the vertical elements of the SFRS.

The following formula is used in current practice to determine the total seismic force F_{px} on the diaphragm at a given level of a building in each direction.

$$F_{px} = \frac{\sum_{i=x}^{n} F_i}{\sum_{i=x}^{n} w_i} w_{px}$$ ASCE 7-10 Eq. 12.10-1

As determined, the base shear for this building is $V = 0.25W$. Because it is a one-story building, Equation 12.10-1 simply becomes the following

$$F_{px} = 0.25 w_{px}$$

F_{px} shall not be less than

$$0.2 S_{DS} I_e w_{px} = 0.2(1.0)(1.0) w_{px} = 0.2 w_{px}$$ ASCE 7-10 Eq. 12.10-2

But need not exceed

$$0.4 S_{DS} I_e w_{px} = 0.4(1.0)(1.0) w_{px} = 0.4 w_{px}$$ ASCE 7-10 Eq. 12.10-3

Based on the criteria given in Section 12.10.1.1, $F_{px} = 0.25 w_{px.}$

Therefore, current practice dictates for diaphragm design in each direction to use $F_p = 0.25 w_{p.}$

Using a flat-beam analogy, where the diaphragm is idealized as a simply-supported beam spanning between supporting walls, north/south seismic forces are resisted by shear walls on grid lines A and J, and east/west seismic forces are resisted by shear walls on grid lines 1 and 5. For this building, it is not required to combine both orthogonal directions based on ASCE 7-10 Sections 12.5.3 and 12.5.4. Each orthogonal uniform load across this flat-beam model is illustrated in Figure 3.2.

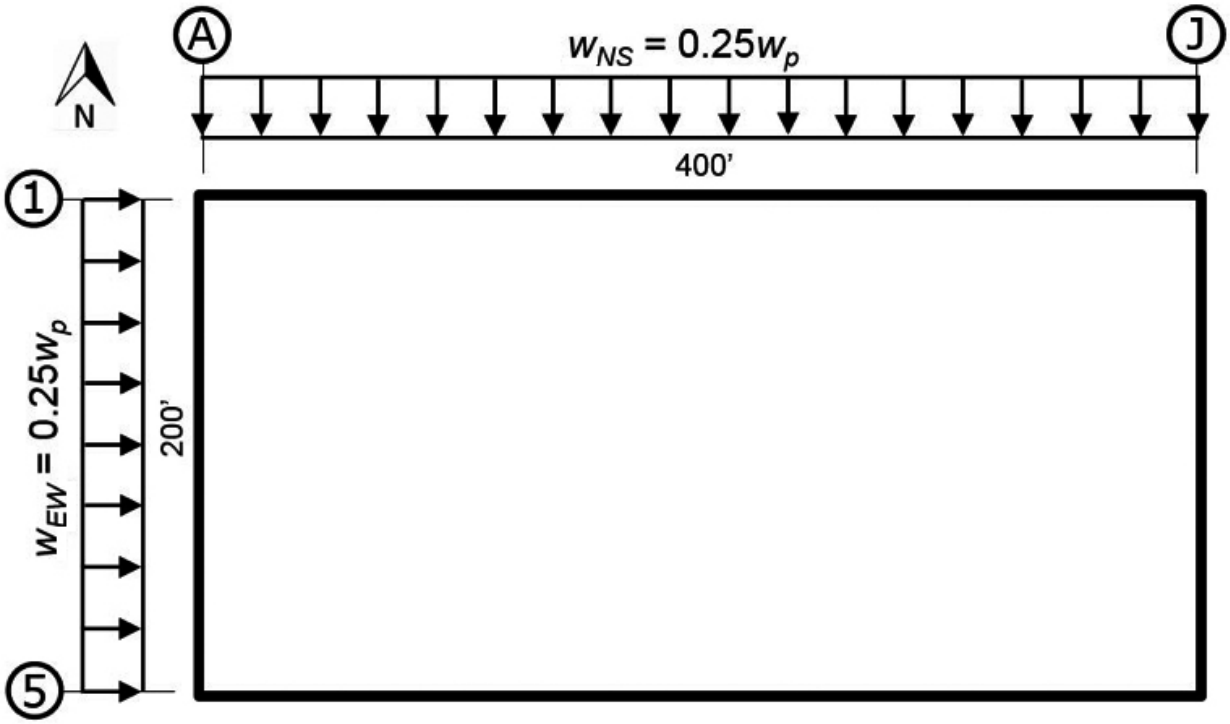

Figure 3.2: Diaphragm Loading Model (both orthogonal directions shown)

The uniformly distributed loads w_{NS} and w_{EW} applied laterally to the diaphragm are computed using the diaphragm lengths and unit weights and the tributary wall heights and unit weights:

Roof dead load = 12 psf

Wall dead load = 116 psf (9¼" thick at 150 pcf)

Roof height = 30'-0" (above floor)

Top of wall = 33'-0" (above floor)

$$w_{NS} = 0.25(12psf)(200') + 2\left[0.25(116psf)33'\left(\frac{33'}{2}\right)\left(\frac{1}{30'}\right)\right] = 1653plf$$

$$w_{EW} = 0.25(12psf)(400') + 2\left[0.25(116psf)33'\left(\frac{33'}{2}\right)\left(\frac{1}{30'}\right)\right] = 2253plf$$

The maximum design shears are now computed using simple statics on the uniformly loaded flat beam model. Because of the building's regular shape and uniformly distributed mass, the loading diagram will be uniform and the reactions V_{NS} at grid lines A and J will be equal. See Figure 3.3.

North-south diaphragm shear:

$$V_{NS} = w_{NS}\frac{400\text{ ft}}{2} = 1653\frac{400\text{ ft}}{2} = 330{,}600\ lbs, maximum$$

North-south unit shear:

$$v_{NS} = \frac{V_{NS}}{200\text{ ft}} = \frac{330{,}600}{200\text{ ft}} = 1653\ plf, maximum$$

East-west diaphragm shear:

$$V_{EW} = w_{EW}\frac{200\ ft}{2} = 2253\ plf\frac{200\ ft}{2} = 225{,}300\ lbs, maximum$$

East-west unit shear:

$$v_{EW} = \frac{V_{EW}}{400\text{ ft}} = \frac{225{,}300}{400\text{ ft}} = 563\ plf, maximum$$

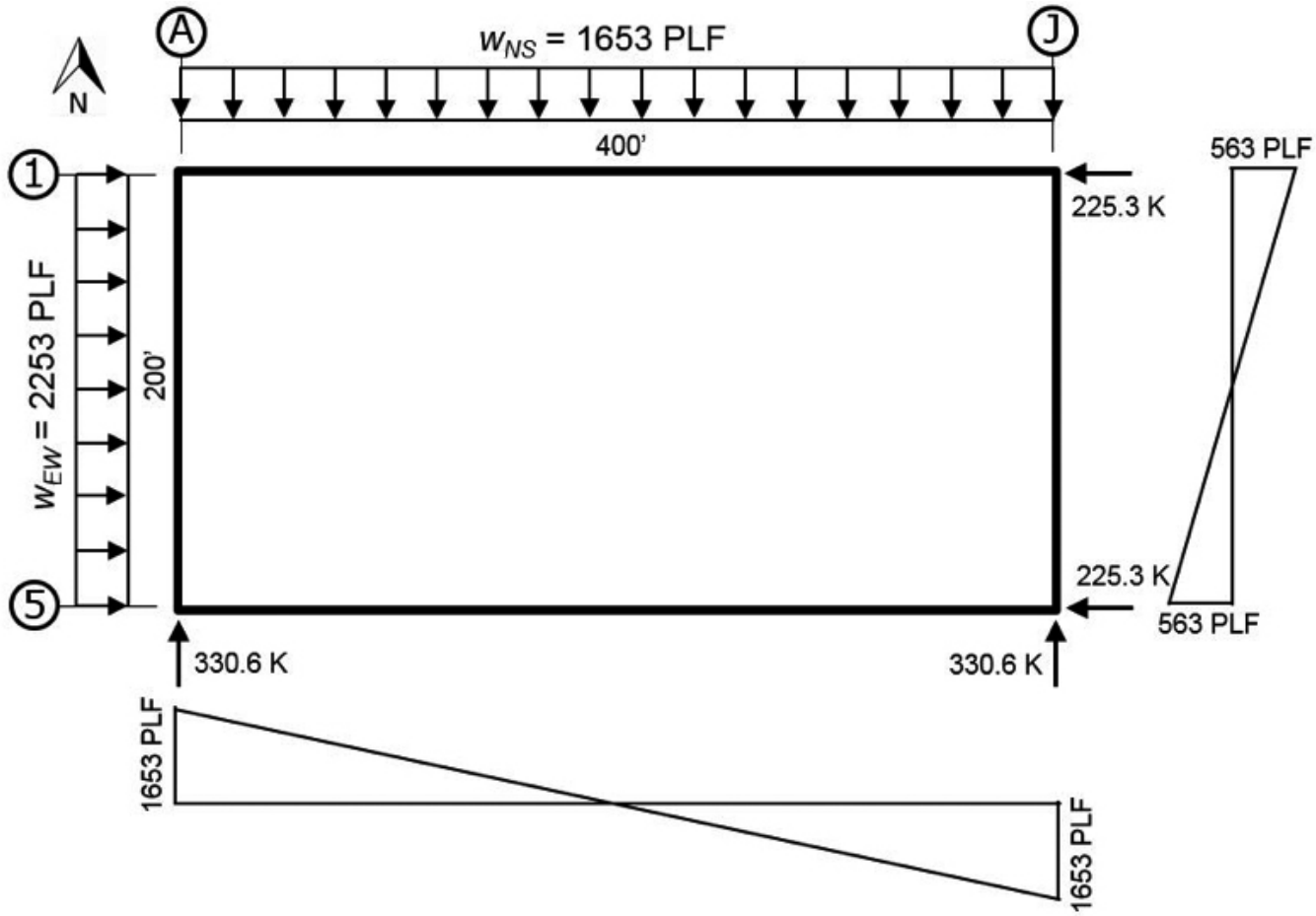

Figure 3.3: Diaphragm Shear Distribution in both Orthogonal Directions

3.6 North/South Diaphragm Shear Design (current practice)

In Section 3.5, the maximum diaphragm shears were determined for each orthogonal direction. ASCE 7-10 Section 12.5 does not require simultaneous load from two directions in this building. The highest unit shear demand is in the north/south direction with v_{NS} = 1653 plf (unfactored). The nominal diaphragm shear capacities are provided in Special Design Provisions for Wind and Seismic (SDPWS-2008) [AWC, 2008] Tables 4.2A and 4.2B for a wide range of blocked diaphragm conditions. Panelized roof systems are commonly blocked based on their modular arrangement. Many engineers still use the Allowable Stress Design (ASD) format for timber design, even though the published nominal resistance values for diaphragms can be easily converted to strength format. This example will follow ASD convention for the timber diaphragm design.

The basic loading combinations are given in IBC Section 1605.3.1 and those involving earthquake loading have been simplified in ASCE 7-10 Section 12.4.2.3, where load combination (5) will govern the design.

$(1.0 + 0.14S_{DS})D + H + F + 0.7\rho Q_E$ ASCE 7-10 Sec. 12.4.2.3

When considering horizontal wind or seismic loads on a structural diaphragm, the vertical loading is not considered when evaluating the lateral diaphragm unit shear stress. Thus, the applicable load combination is simplified using $D = 0$, $H = 0$, $F = 0$ and $L = 0$. Additionally, the redundancy factor ρ is set to 1.0 for typical diaphragms per ASCE 7-10 Section 12.3.4.1. Therefore, the applicable basic load combination reduces to $0.7Q_E$.

$$v_{NS\,(ASD)} = 0.7v_{NS} = 0.7(1653) = 1157 \text{ plf}$$

$$v_{EW\,(ASD)} = 0.7v_{EW} = 0.7(563) = 394 \text{ plf}$$

Using these unit shear values, the designer may enter either SDPWS-2008 Table 4.2A or 4.2B to select a diaphragm assembly with an appropriate shear capacity. 15/32-inch Structural I sheathing is traditionally used as a minimum thickness in panelized construction [Lawson J, 2013]. The panelized sheathing system is inherently fully blocked and typically follows layout Case 2 (east/west loading) and 4 (north/south loading) illustrated in SDPWS-2008 Tables 4.2A and 4.2B. SDPWS-2008 Tables 4.2A and 4.2B are at a nominal strength level, and ASD design values are obtained by dividing by a factor of two in accordance with SDPWS-2008 Section 4.2.3.

In the north/south direction, the ASD unit shear demand is greater than the maximum ASD capacities obtained from SDPWS-2008 Table 4.2A, thus reference to the high-load diaphragm shears in Table 4.2B will be necessary. The on-center (o.c.) nail spacing shown here requires thicker framing to prevent splitting. The capacity is reduced from the table nominal strength value to allowable stress design value by dividing in half per SDPWS-2008 Section 4.2.3.

15/32”-thick Structural I sheathing
10d nails in *2 lines* at
2 ½” (o.c.) boundaries and continuous north/south edges
3” o.c. other edges
10d nails in 1 line at
12” o.c. intermediate (field)
4x framing width at adjoining edges CAPACITY = 2580/2 = 1290 plf (ASD)

$$v_{NS\,(ASD)} = 0.7v_{NS} = 0.7(1653) = 1157 \text{ plf} < 1290 \text{ plf} \quad \text{OK}$$

The construction of this diaphragm system is illustrated in Figure 3.4.

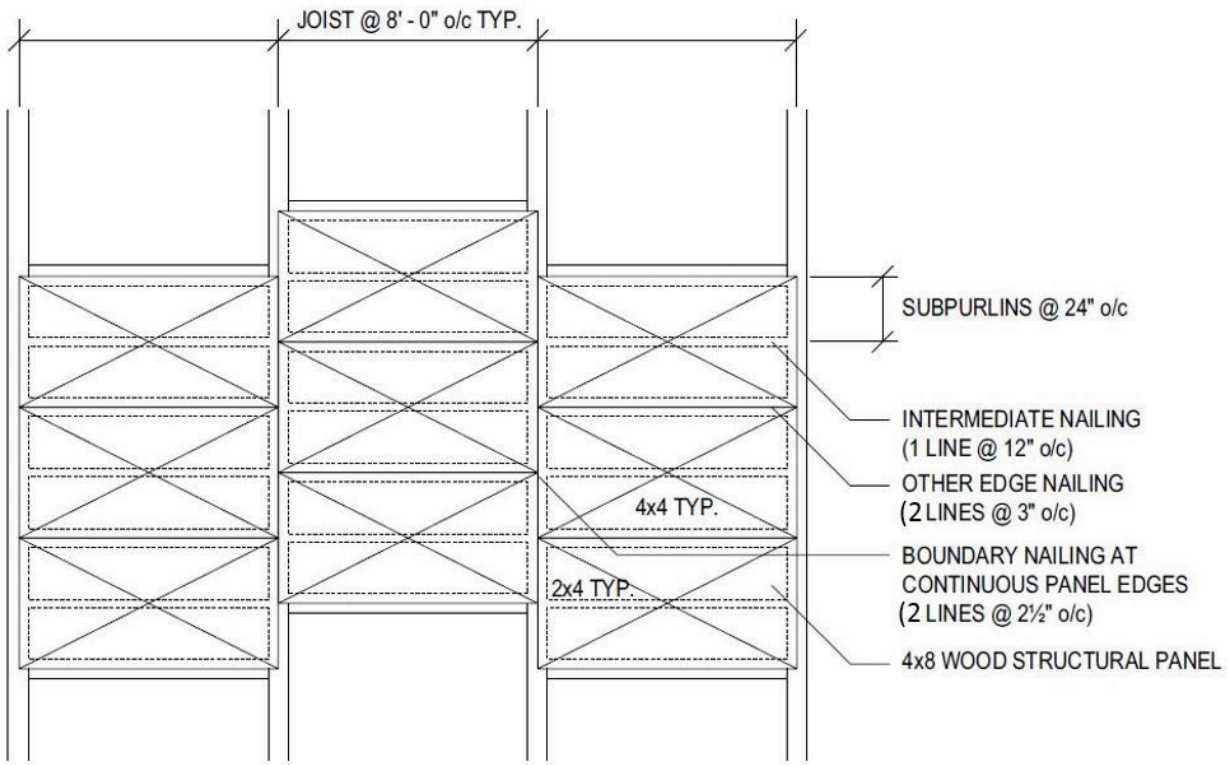

Figure 3.4: Sheathing Layout and Nailing for a Panelized Roof System [Lawson J, 2013]

For a building this size, it is not efficient to install the heavy diaphragm nailing required at the boundary over the entire roof structure. Because the shear demands diminish towards the center of the diaphragm span, it is permitted to reduce the nailing and subpurlin widths as the corresponding unit shears also reduce. For this example, Table 3.1 identifies various diaphragm nailing configurations from the SDPWS-2008 that will be utilized at different portions of this building. The ASD shear values are simply the nominal strengths listed in SDPWS-2008 Tables 4.2A and 4.2B divided by a factor of two per Section 4.2.3. For a panelized roof structure, layout case 2 and 4 are applicable.

Table 3.1 – Diaphragm Nailing Schedule (Cases 2 and 4)

15/32" Structural I OSB Sheathing (DOC PS 2 [NIST, 2004]) with 10d nails (0.148" dia x 2" long minimum)					
Zone	Framing Width at Adjoining Edges	Lines of Nails	Nailing per line at Boundary & Continuous Edges	Nailing per line at Other Edges	ASD Allowable Shear (plf)
1	2x	1	6" o.c.	6" o.c.	320
2	2x	1	4" o.c.	6" o.c.	425
3	2x	1	2½" o.c.	4" o.c.	640
4	3x	1	2" o.c.	3" o.c.	820
5	4x	2	2½" o.c.	4" o.c.	1005
6	4x	2	2½" o.c.	3" o.c.	1290

At the diaphragm boundaries (grid lines A and J), Nailing Zone 6 was determined to be acceptable. At some location inward as the diaphragm shears diminish, Nailing Zone 5 will become acceptable. The transition from Nailing Zone 6 to Nailing Zone 5 may be solved using statics as follows:

Shear Demand (ASD) = Shear Capacity (ASD)

$0.7[330{,}600 \text{ lbs} - (1653 \text{ plf})x] = 1005 \text{ plf } (200 \text{ ft})$

where

x = the demarcation distance from the diaphragm boundary.

Solving for x obtains

$x = 26.3$ ft

Because a panelized roof system typically consists of 8-foot wide wood structural panels, the joist spacing module is also 8 feet, and the transition should be increased to the next 8-foot increment. In this case, it is increased to x = 32 feet.

The transition locations between Zones 5 and 4, Zones 4 and 3, Zones 3 and 2, and Zones 2 and 1 for the north-south loading direction are found using the same process resulting in Table 3.2.

Table 3.2 – Diaphragm Nailing Zone Shear Checks

Nailing Zone	Distance from Boundary	Strength Level Unit Shear	ASD Unit Shear	Allowable Shear Capacity
6	0 feet	v_{max} = 1653 plf	v_{ASD} = 1157 plf	1290 plf
5	32 feet	v_{max} = 1389 plf	v_{ASD} = 972 plf	1005 plf
4	64 feet	v_{max} = 1124 plf	v_{ASD} = 787 plf	820 plf
3	96 feet	v_{max} = 860 plf	v_{ASD} = 602 plf	640 plf
2	128 feet	v_{max} = 595 plf	v_{ASD} = 417 plf	425 plf
1	152 feet	v_{max} = 397 plf	v_{ASD} = 278 plf	320 plf

The resulting nailing zone layout for the north/south loading is shown in Figure 3.5.

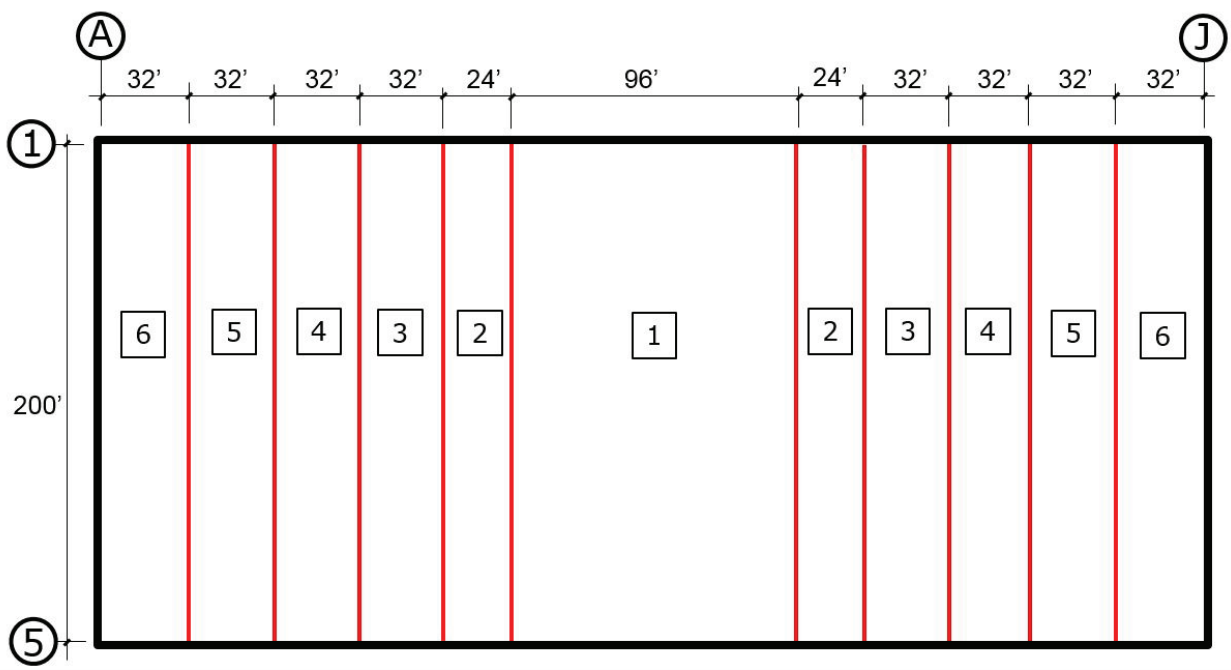

Figure 3.5: North/South Nailing Zone Layout

An additional check when designing wood diaphragms is to check their plan aspect ratios against the limitations in the SDPWS-2008 Table 4.2.4. For blocked diaphragms such as those that occur in panelized construction, the maximum aspect ratio is L/W = 4:1. In this example, the north/south loading direction is the critical L/W ratio.

$$L/W = 400/200 = 2.0 < 4 \quad \textit{Okay}$$

3.7 North/South Diaphragm Chord Design (current practice)

Recall that a flexible diaphragm may be thought of as a flat horizontal beam where the shear resistance is obtained by the wood structural panel sheathing across the roof surface. However, tensile forces from horizontal bending are not considered to be resisted by the sheathing, but by perimeter chords acting in tension and compression instead.

To resist bending efficiently, the diaphragm chords are traditionally placed at the extreme sides of the diaphragm. In buildings with masonry or concrete perimeter walls, these chords are often steel ledger angles or channels at the roof line. Chord forces are determined using simple statics as illustrated in Figure 3.6. Maximum chord forces will occur at the center of the diaphragm's span where the maximum moment occurs.

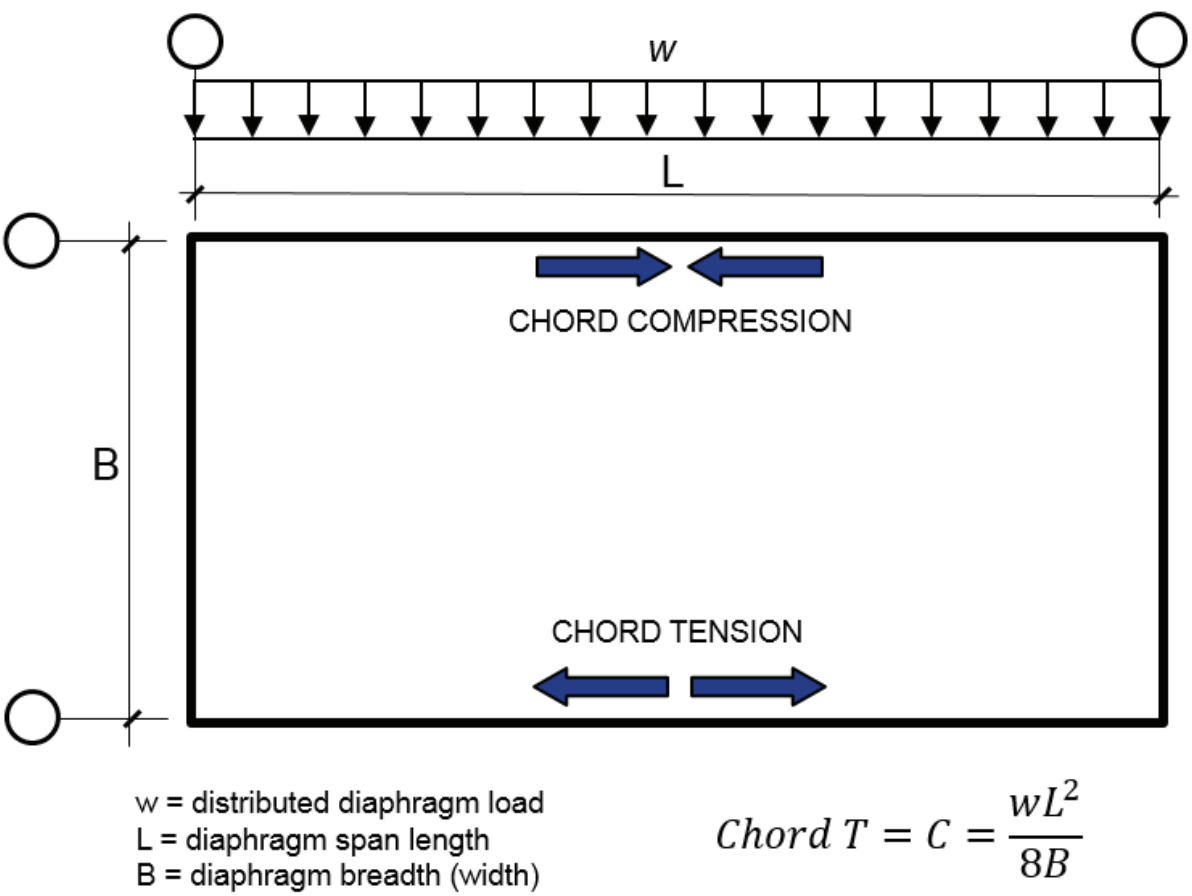

$$Chord\ T = C = \frac{wL^2}{8B}$$

Figure 3.6: Diaphragm Chord Forces

Using the equations in Figure 3.6, the maximum tensile chord force for our building example is determined:

$$T = \frac{M}{B} = \frac{w_{NS}L^2}{8B} = \frac{1653\ plf(400)^2}{8(200)} = 165{,}300\ lbs$$

The chord is designed here using strength design with ASTM A36 Steel (F_y = 36 ksi). Consulting IBC Section 1605.2, the applicable load factor for seismic forces is 1.0. The area of steel required is:

$$A_S = \frac{T}{\emptyset F_y} = \frac{(165.3)}{0.9(36)} = 5.10\ in^2$$

Using a L5x5x5/8 rolled steel angle satisfies this chord demand.

L5x5x5/8 Steel Area A_S = 5.90 in^2 > 5.10 in^2

3.8 East/West Diaphragm Shear Design (current practice)

Similar to the north/south loaded direction, the orthogonal east/west direction will also require consideration using the same sequential process. In Section 3.6, the maximum diaphragm shear in the east/west direction was determined to be v_{EW} = 563 plf (unfactored); and converting to allowable stress design (ASD), the maximum diaphragm shear is as follows:

$$v_{EW(ASD)} = 0.7v_{EW} = 0.7(563) = 394 \text{ plf}$$

As before, SDPWS-2008 Table 4.2A is used to select diaphragm nailing with an appropriate shear capacity. In the north/south loaded direction, Case 4 is the loading configuration, but for the east/west direction this becomes a Case 2 configuration. The applicable Case determines the nail spacing along the continuous adjoining panel edges in the direction parallel to load. Comparing the diaphragm's shear demand with Table 1 of Section 3.6, Nailing Zone 2 is selected:

$$v_{EW(ASD)} = 394\ plf < 425\ plf\ (Nailing\ Zone\ 2)$$

At some distance away from the diaphragm boundary (walls at grid lines 1 and 5), Nailing Zone 1 in Table 1 will be acceptable due to the diminishing unit diaphragm shears. Using the same approach as done in the north/south direction, the location of the nailing zone transition from Zone 2 to 1 is found and Table 3.3 is developed.

Table 3.3 – Diaphragm Nailing Zone Shear Checks

Nailing Zone	Distance from Boundary	Strength Level Unit Shear	ASD Unit Shear	Allowable Shear Capacity
2	0 feet	v_{max} = 563 plf	v_{ASD} = 394 plf	425 plf
1	20 feet	v_{max} = 451 plf	v_{ASD} = 315 plf	320 plf

Combining the nailing requirements for the north/south loading with the east/west loading results in Figure 3.7.

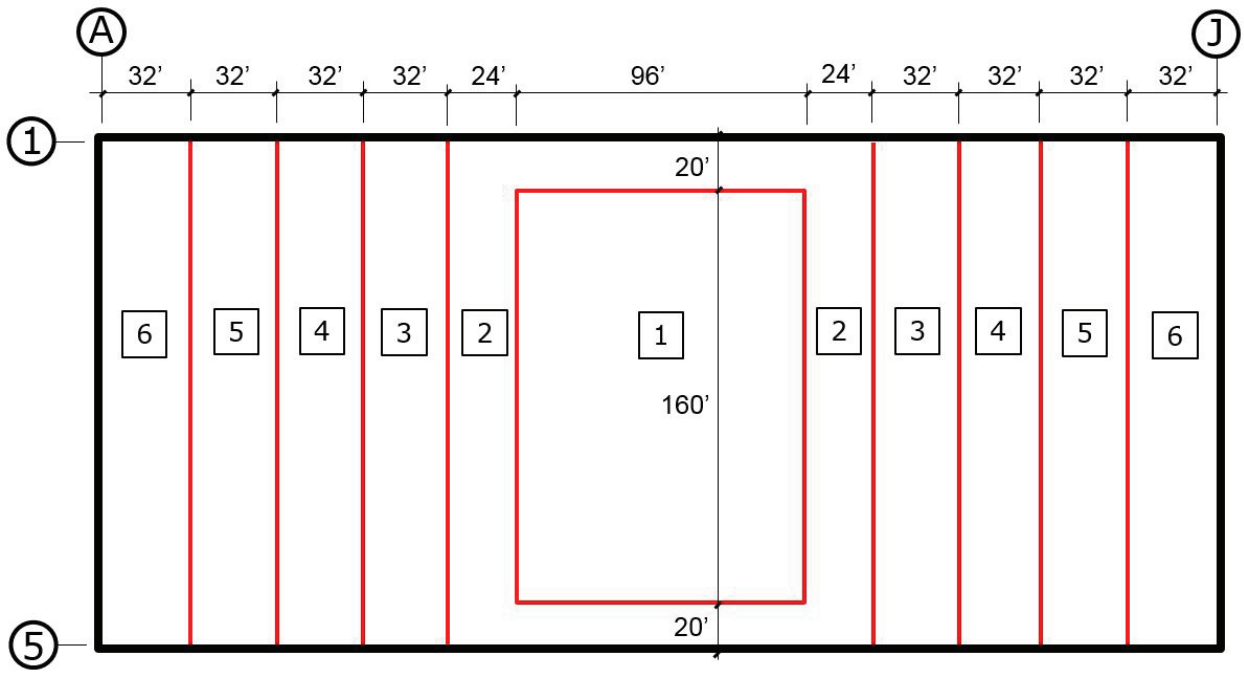

Figure 3.7: North/South and East/West Nailing Zones Combined

3.9 East/West Diaphragm Chord Design (current practice)

With the diaphragm chords placed at the extreme sides of the diaphragm, the maximum chord forces in the east/west loaded direction are computed as follows:

$$T = \frac{M}{B} = \frac{w_{EW}L^2}{8B} = \frac{2253\ plf(200)^2}{8(400)} = 28{,}100\ lbs$$

The required area of the steel chord is:

$$A_S = \frac{T}{\emptyset F_y} = \frac{(28.1)}{0.9(36)} = 0.87\ in^2$$

Using an L4x4x1/4 rolled steel angle as a practical minimum size satisfies this chord demand.

L4x4x1/4 Steel Area $A_S = 1.93\ in^2 > 0.87\ in^2$

3.10 Shear Wall Force Using the ELF Procedure (current practice)

For a single-story building, the diaphragm's support reactions are the basis of the applied loads to the shear wall lines. The flexible diaphragm with its tributary mass will generate a lateral force near the top of the wall, F_{v1}. Additionally, the rigid concrete in-plane walls have significant self-weight that will also generate lateral forces near their center of mass, F_{v2}. See Figures 3.8 and 3.9.

As determined previously in Section 3.5, the diaphragm reactions to the shear walls based on $\rho_{diaph} = 1.0$ are as follows:

North/South Diaphragm Reactions

$$F_p = V_{NS} = 330{,}600\ lbs$$

East/West Diaphragm Reactions

$$F_p = V_{EW} = 225{,}300\ lbs$$

These diaphragm reaction forces need to be amplified to an appropriate shear wall design force if the redundancy factor for the SFRS is greater than 1.0.

$$F_{v1} = F_p \times \left(\frac{\rho_{wall}}{\rho_{diaph}}\right)$$

where for this example $\rho_{wall} = 1.0$ (computed) and $\rho_{diaph} = 1.0$ (ASCE 7-10 Section 12.3.4.1)

Therefore, the shear wall design force from the diaphragm in each orthogonal direction are as follows:

North/South

$F_{v1} = 330{,}600\ lbs$

East/West

$F_{v1} = 225{,}300\ lbs$

Next, the lateral seismic force generated from the walls' self-weight must be included for design. Because this is a single-story building, the self-weight seismic force F_{v2} is simply the wall line's self-weight multiplied by the base shear coefficient C_s and any applicable redundancy factor ρ for the building. The base shear coefficient C_s for both axes of the building was determined in Section 3.4.

$F_{v2} = C_s W = 0.25 W_{p\text{-}wall}$

For the north/south direction, the wall's self-weight $W_{p\text{-}wall}$ is computed as

$$W_{p-wall} = 116\ psf \times 200\ ft \times 33\ ft = 765{,}600\ lbs$$

Therefore

$F_{v2} = 0.25 W_{p\text{-}wall} = 0.25(765{,}600) = 191{,}400$ lbs

Therefore, the total shear wall design force F_v for the north/south direction is

$F_v = F_{v1} + F_{v2} = 330{,}600 + 191{,}400$

$F_v = 522{,}000$ lbs or 522 kips

For the east/west direction, the wall's self-weight $W_{p\text{-}wall}$ is computed as

$$W_{p-wall} = 116\ psf \times 400\ ft \times 33\ ft = 1{,}531{,}200\ lbs$$

Therefore

$F_{v2} = 0.25 W_{p\text{-}wall} = 0.25(1{,}531{,}200) = 382{,}800$ lbs

Therefore, the total shear wall design force F_v for the east/west direction is

$$F_v = F_{v1} + F_{v2} = 225{,}300 + 382{,}800$$

$$F_v = 608{,}100 \text{ lbs or } 608 \text{ kips}$$

Figures 3.8 and 3.9 illustrate the forces acting on the shear walls providing lateral resistance in the north/south and east/west directions respectfully. The design forces at the base of the shear walls are 552 kips north/south and 608 kips east/west. These forces include the entire weight of the walls and are appropriate for the design of shear forces that transfer to the slab on ground or foundation. In-plane shear design considerations for tilt-up concrete shear walls may be found in other sources [Mays and Steinbicker, 2013].

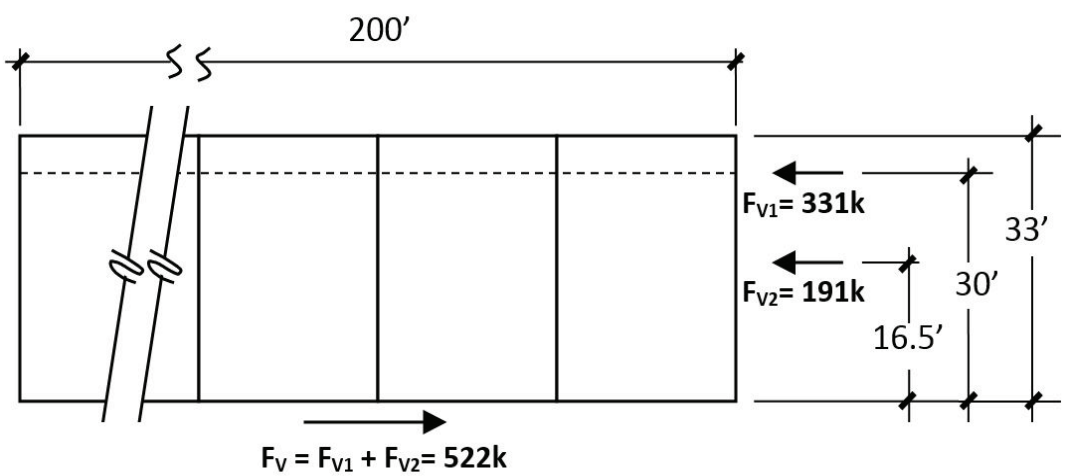

Figure 3.8: North/South Lateral Design Forces acting on the Shear Walls (Lines A & J)

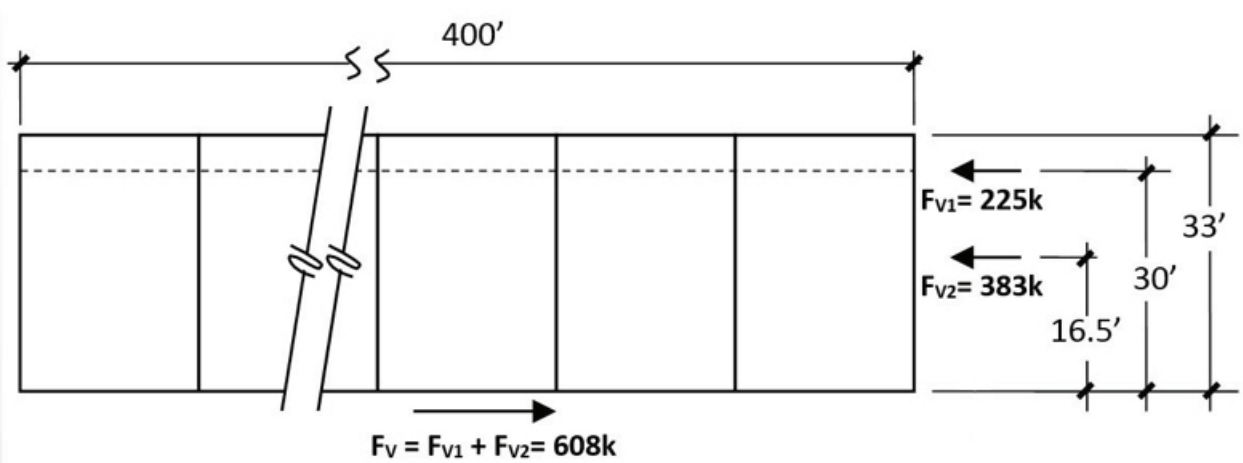

Figure 3.9: East/West Lateral Design Forces acting on the Shear Walls (Lines 1 & 5)

3.11 Shortcomings of Current Practice

The simplistic model assumed by the ELF procedure fails to capture the actual behavior of RWFD buildings. The ELF procedure assumes that the seismic response consists primarily of deforming vertical elements and that the horizontal diaphragm is rigid, i.e. deformation of the diaphragm is not considered. However, for most RWFD structures the primary seismic response is dominated by the deformation of the horizontal flexible diaphragm. A more accurate structural model is needed to capture the flexible diaphragm potentially dominating the response.

The ELF procedure also inappropriately assumes that the primary inelastic behavior is in the vertical wall or frame system, instead of the roof diaphragm. The seismic response modification coefficient, R, the overstrength factor Ω_o, and the deflection amplification factor C_d in ASCE 7-10 Table 12.2-1 are utilized to estimate the strength demands, capacities and deflections on systems that are designed using linear methods while responding in the nonlinear range. Currently, the selection of R, Ω_o and C_d for design is solely based on the performance characteristics of the SFRS's vertical elements. In reality, the inelastic behavior is likely to be in the horizontal diaphragm and the current ELF procedure fails to characterize this diaphragm response adequately. Currently, wood and steel flexible diaphragms and rigid concrete diaphragms are all designed as if they have the same seismic response and performance.

In current practice the seismic diaphragm shears used for design are directly related to the type of vertical elements used in the SFRS. In fact, some engineers routinely select special reinforced concrete shear walls (R=5) in their design (instead of intermediate precast, R=4) to reduce the diaphragm design shears and allow the diaphragm to span farther. The same motive drives some engineers to place girder support columns adjacent to the intermediate precast shear walls, converting the bearing wall system (R=4) to a building frame system (R=5) in one direction. The selection of the SFRS solely driven by a desired diaphragm load outcome is not a desirable practice, because it fails to recognize the likely building behavior. Current seismic design provisions in ASCE 7-10 may unintentionally encourage this practice.

Because RWFD buildings typically have excessive strength in the shear walls as compared with the diaphragm, it is unrealistic to expect the yielding to be in the walls instead of the diaphragm; despite the fact that the response modification coefficient R is selected based on that assumption. Past failures have typically been out-of-plane wall detachments, and building codes have responded to these failures by increasing the out-of-plane wall anchorage design force. Assuming that failure of out-of-plane wall anchorage is prevented, diaphragm yielding and potential failure may become the critical behavior. The ELF procedure of ASCE 7-10 as currently applied to RWFD buildings does not account for this diaphragm behavior.

Chapter 4 Development of an Alternate Seismic Design Procedure

With seismic response dominated by the horizontal diaphragm in RWFD structures, it is more realistic that design forces be developed around the diaphragm's behavior. Furthermore, because the inelastic behavior in a RWFD building is typically located in the diaphragm, it is more realistic that the seismic system capacity be developed around the overstrength and ductility of the diaphragm, rather than of the vertical elements of the SFRS. An alternate procedure based on the diaphragm's response would be more realistic and has the potential to better permit evaluation of a structure's margin against collapse.

A more accurate method of establishing seismic design loads for buildings dominated by diaphragm response is to consider the diaphragm's period relative to the design spectral acceleration. As an example, ASCE 41-13 [ASCE, 2013] provides the *Linear Static Procedure* to rehabilitate existing one-story RWFD buildings by estimating the diaphragm-dominated building period and then establishing a pseudo-lateral force on the system. A number of other sources have proposed other methods of estimating flexible diaphragm periods and their corresponding pseudo-lateral force [Freeman et. al., 2002; PEER, 2004; SEAONC, 2001]. With a more accurate period of the dominating response, the force-based procedures of ASCE 7 can be used more appropriately. Furthermore, the use of an ELF approach with a response modification coefficient R, an overstrength factor Ω_o, and a deflection amplification factor C_d, related to the diaphragm's design, construction and detailing, is expected to produce more rational results.

Both the inelastically acting horizontal diaphragm and the SFRS's vertical elements need a unified design methodology. The fact that RWFD buildings have a flexible upper portion (the diaphragm) supported in series with a rigid lower portion (the walls) make them ideally suited to be designed similar to the two-staged ELF procedure that currently exists within ASCE 7-10 Section 12.2.3.2. This approach is often used for residential podium type structures where three or four story wood shear wall buildings are supported on masonry or concrete shear wall parking structures. This approach encourages the two portions to be analyzed for seismic loading independently, and then combined as appropriate. As the seismic forces are handed off from one portion to another, they are adjusted to reflect the next portion's expected seismic performance influenced by its period and stipulated R-coefficient.

Chapter 4 provides background on key parameters incorporated into the alternate procedure for RWFD buildings. For simplicity, it is reasonable to develop a methodology for RWFD structures that can fit within the existing code framework already familiar to practitioners, yet providing a more rational approach than currently exists.

4.1 Determination of Building and Diaphragm Period

As mentioned previously, a primary objective of an alternate design methodology is a design considering seismic response and seismic performance factors uniquely associated with a building dominated by the flexible diaphragm instead of the vertical portion of the SFRS. The diaphragm period T_{diaph} is a very important parameter in determining a more realistic seismic response.

A number of approaches have been proposed in the past to more accurately estimate the periods of various flexible diaphragm dominated buildings [Koliou, 2014]. One approach in current use for seismic evaluation is the fundamental period equation within ASCE 41-13 for one-story buildings with flexible diaphragms.

$$T_a = \sqrt{0.1\Delta_w + 0.078\Delta_d} \qquad \text{ASCE 41-13 Eq. 7-19}$$

where

T_a= fundamental period in sec. in the direction of consideration.
Δ_w = maximum in-plane wall displacement in inches at 1.0g
Δ_d = maximum diaphragm displacement in inches at 1.0g

While this equation has credibility from the fact that it is formally adopted in an ASCE standard, it has been criticized as being derived from an improper flexural beam idealization for the diaphragm instead of a more realistic shear beam idealization. Wilson et. al.[Wilson, 2013] derived an equation based on shear beam behavior and recommends that the diaphragm component $(0.078\Delta_d)^{0.5}$ be revised to $(0.066\Delta_d)^{0.5}$ within the ASCE 41-13 procedure. With this modification, the following equation for the fundamental period of one-story buildings with flexible diaphragms becomes:

$$T_a = \sqrt{0.1\Delta_w + 0.066\Delta_d} \qquad \text{Equation (1)}$$

Equation (1) is mathematically derived and provides a valuable approach provided that accurate wall and diaphragm displacements can be computed. However, this equation is better suited for analyzing existing structures than it is for design because it requires one to compute the wall and diaphragm deflections. For design, an estimate of the period is needed to establish wall and diaphragm design forces. One cannot compute the deflections of the walls and diaphragm until after these elements have been designed, which is typical of most design problems

To meet the objective of developing a design methodology that is simple to implement and accounts for diaphragm flexibility, a simple period approximation, T_a, was desired. The research conducted in conjunction with this report developed simple separate period formulas, T_a, for RWFD buildings with wood or steel deck diaphragms based on a semi-empirical analysis using a special numerical model of 23 archetypes designed under ASCE 7-10.The design seismic demand was based on the upper bound of

design spectral response accelerations for Seismic Design Category D, designated as SDC D_{max}. For the purposes of creating archetypes for evaluation under FEMA P695, this period T_a was selected to be the algebraic sum of T_{diaph} and T_{walls}. In the case of the wood diaphragm, the period formula $T_a = T_{diaph} + T_{walls}$ tracks very closely with the formula, Equation (1), developed by Wilson et. al [Wilson, 2013] for diaphragms less than 250-ft long. For lengths over 250 feet, the proposed formulas provide a smaller period than Wilson's equation [Koliou, 2014]. The approximate period equations represent the elastic building period at an applied load approximately equal to code level forces prior to a shift in the period due to inelastic behavior. More information on the development of these formulas is provided in Appendix D Section D.2 and Appendix G Section G.1.2.

The following equations were developed empirically from the results obtained from 23 archetype building configurations involving 33-ft high concrete tilt-up walls 9¼" thick in a high seismic hazard region. Generally speaking, situations with more or less mass will have a corresponding diaphragm design with more or less stiffness, thus directly offsetting the mass variation. Therefore, the proposed period formulas are independent of mass. Additionally, because the diaphragm deformations were found to be overwhelmingly shear dominated, the diaphragm's aspect ratio does not significantly affect the period. T_{diaph} is simply based on the diaphragm's span L_f, and T_{walls} is based on current ASCE 7-10 provisions for concrete or masonry shear wall buildings. The reader is cautioned that the equation for T_{walls} was developed for shear wall buildings of various heights and with heavy floor and roof masses, and will probably overestimate the period for this type of building, but it serves a useful purpose for this discussion.

For wood structural panel diaphragms [Koliou, 2014]:

$$T_{diaph} = 0.002L_f \qquad \text{Equation (2)}$$

$$T_{walls} = \frac{0.0019}{\sqrt{C_w}} h_n \qquad \text{ASCE 7-10 Eq. 12.8-9}$$

For steel deck diaphragm [Koliou, 2014]:

$$T_{diaph} = 0.001L_f \qquad \text{Equation (3)}$$

$$T_{walls} = \frac{0.0019}{\sqrt{C_w}} h_n \qquad \text{ASCE 7-10 Eq. 12.8-9}$$

where

L_f = The span, in feet, of the horizontal flexible diaphragm being considered; the span is measured between vertical elements that provide lateral support to the diaphragm in the direction considered.

h_n = The structural height defined in ASCE 7-10 Section 11.2.
C_w = Shear wall coefficient for concrete and masonry walls per ASCE 7-10 Equation 12.8-10.

$$C_w = \frac{100}{A_B}\sum_{i=1}^{x}\left(\frac{h_n}{h_x}\right)^2 \frac{A_i}{\left[1 + 0.83\left(\frac{h_i}{D_i}\right)^2\right]}$$

A_B = area of base of structure, ft^2
A_i = web area of shear wall i in ft^2
D_i = length of shear wall i in ft
h_i = height of shear wall i in ft
x = number of shear walls in the building effective in resisting lateral forces in the direction under consideration

For our example wood diaphragm building, Equation 2 will be used to estimate the diaphragm's approximate period, T_{diaph}, and ASCE 7-10 Eq. 12.8-9 will be used to estimate the walls' approximate period, T_{walls}; however, the two periods will not be combined to estimate a building period, T_a, out of concern that this will overestimate the building period and underestimate the seismic load effect.

$$T_{diaph} = 0.002L_f$$
$$T_{walls} = \frac{0.0019}{\sqrt{C_w}}h_n$$

Compute building area A_B

$$A_B = 200ft \times 400ft = 80{,}000ft^2$$

This building is comprised of a series of equal 25-ft long concrete tilt-up wall panels acting as shear walls around the building perimeter. Thus all parameters for each wall i are the same.

$$A_i = 25ft \times \frac{9.25in}{12} = 19.3ft^2/wall$$
$$D_i = 25ft$$
$$h_i = 30ft$$

In the transverse direction (north/south) there are eight wall panels along each line of resistance, or a total of sixteen panels in the considered direction (x = 16). Similarly, in the longitudinal direction (east/west) there are thirty-two panels total in the considered direction (x = 32). Thus the shear wall coefficient C_w is different in each orthogonal direction.

North/South:

$$C_w = \frac{100}{80{,}000}(16)\left(\frac{30}{30}\right)^2 \frac{19.3}{\left[1 + 0.83\left(\frac{30}{25}\right)^2\right]} = 0.176$$

$$T_{diaph} = 0.002(400ft) = 0.800\ sec$$

$$T_{walls} = \frac{0.0019}{\sqrt{0.176}}30ft = 0.136\ sec$$

Using this alternative approach, the diaphragm period alone is estimated at 0.800 seconds compared with the code's current approximate period of 0.26 seconds for the building using ASCE 7-10 Equation 12.8-7 or 0.136 seconds using Equation 12.8-9.

East/West:

$$C_w = \frac{100}{80{,}000}(32)\left(\frac{30}{30}\right)^2 \frac{19.3}{\left[1 + 0.83\left(\frac{30}{25}\right)^2\right]} = 0.352$$

$$T_{diaph} = 0.002(200ft) = 0.400\ sec$$

$$T_{walls} = \frac{0.0019}{\sqrt{0.352}}30ft = 0.096\ sec$$

Using this alternative approach, the diaphragm period is estimated at 0.400 seconds compared with the code's current approximation for the building of 0.26 seconds using ASCE 7-10 Equation 12.8-7 or 0.096 seconds using Equation 12.8-9. Determination of periods used when implementing the alternate RWFD procedure is further discussed in Chapter 5 of this report.

4.2 Response Modification Coefficient, *R*, Selection

As previously stated, a primary objective is to identify seismic response and seismic performance factors considering response dominated by the flexible diaphragm instead of the vertical elements of the SFRS. The structural response modification coefficient, *R,* is an important parameter to estimate strength demands on systems that are designed using linear methods, such as the ELF procedure, but may respond in the nonlinear range when subject to strong ground motions. *R* coefficients currently in ASCE

7 are largely based on judgment. Historically, validation of seismic performance factors was simply based on observations following major earthquakes.

While learning from earthquakes is invaluable when validating current design factors, a more systematic form of validation is needed when proposing new R coefficients and new design procedures. The methodology contained in FEMA P695 [FEMA, 2009] was developed specifically to provide a means to evaluate a SFRS proposed for adoption into building codes, but can be used to evaluate proposed design procedures as well. The primary objectives of a FEMA P695 study are to obtain an acceptably low probability of collapse of the SFRS under maximum considered earthquake (MCE) ground motions and to provide a uniform protection against collapse across various structural systems. An appropriate P695 evaluation must develop a representative nonlinear model that includes both detailed design information of the system as well as comprehensive test data on the post-yield performance of system components and subassemblies. The procedure evaluates the probability of collapse during strong earthquake shaking while accounting for a variety of possible ground motions, uncertainties, and a range of building configurations representing the design space. The building example being illustrated in this report is an example of just one of the archetypes evaluated as part of the RWFD study introduced in Section 1.0.

An appropriate response modification coefficient unique to the diaphragm, R_{diaph}, was determined using a trial-and-error process using FEMA P695. The first trial evaluated existing ASCE 7-10 designs using intermediate precast (tilt-up) concrete shear walls (R = 4) with both wood and steel deck diaphragms for their acceptability. As expected, the results showed the inelastic behavior was clearly in the diaphragms instead of the in-plane walls, confirming the need for a diaphragm-based approach. Even though the diaphragm design capacity was intentionally stepped down to efficiently follow the shear demand reduction towards the diaphragm interior as is often done in practice, the analysis results indicate that the inelastic response of the diaphragm is concentrated adjacent to the supporting shear walls.

Because the inelastic behavior was not well distributed across the diaphragm, the localized inelastic response near the shear wall supports was quickly overwhelmed by the limited ability of the connectors to dissipate large amounts of energy, and led to global building failure. This phenomenon was observed in both the steel and wood deck diaphragm analyses. The FEMA P695 analysis results for archetypes using R equal to 4 for the intermediate precast wall system did not meet the required margin against collapse required by the FEMA P695 methodology, thus indicating revised R-coefficients are necessary. A detailed description of the implementation of FEMA P695 evaluations for use on this project and the numerical computer model are contained in Appendix B.

A direct approach to resolve the deficient margin against collapse identified for RWFD buildings designed using existing practice is to design the flexible diaphragms using a response modification coefficient, R_{diaph}, that represents the ductility and overstrength of the diaphragm instead of the

walls. Two approaches could be taken to assigning a value or values to R_{diaph}, either (1) assign a single value and design the diaphragm assuming a linear distribution of design shear along the diaphragm's span length or (2) assign a value to R_{diaph} but amplify the design shear in targeted zones within the diaphragm, to encourage the spread of yielding across more of the diaphragm' length. Based on the P695 results for the current design procedure, approach (1) requires an R_{diaph} value significantly less than 4 to obtain acceptable performance during a maximum considered earthquake (MCE) event if design shear is assumed to be distributed linearly along the diaphrag span length. Approach (2) in which the inelastic diaphragm behavior is spread away from the diaphragm boundaries by designing for amplified shear in targeted zones has the potential of requiring a less punitive R_{diaph} over much of a diaphragm's span length. Such an approach is discussed in the following subsection.

4.2.1 Encouraging Distributed Inelastic Behavior

Analytical studies have demonstrated that the performance of a diaphragm during strong earthquake shaking can be improved if yielding is spread over a large portion of a diaphragm's span instead of focused at the boundary. The spread of diaphragm yielding is improved if the location of initial yielding is shifted away from the boundaries of the diaphragm. Surprisingly, this can be achieved either by intentionally weakening a portion the diaphragm's interior areas below current building code levels, or by increasing the strength-to-demand ratio of the diaphragm near its boundaries.

Distributing the inelastic behavior deeper into the diaphragm also requires that the diaphragm connectors that yield first exhibit sufficient positive post-yield stiffness behavior. In other words, once the critical connectors begin to yield, they need to resist increasing load rather than maintaining the initial yield load so connectors elsewhere in the diaphragm also reach their yield load. The connectors that yield must also have sufficient post-yield deformability so the diaphragm as a whole has adequate post-yield deformability to provide the required collapse resistance. The overall diaphragm deformability increases if connector yielding spreads over a large portion of the diaphragm. Also, the spread of yielding reduces the deformation demand on individual connectors. The hysteretic responses of the nail connectors in the wood structural panel diaphragms have sufficient positive post-yield stiffness to effectively move the location of first yield away from the diaphragm boundaries and spread the yielding over a large portion of the diaphragm's span. In the case of steel deck diaphragms, insufficient data is available to make that determination. Thus, the recommendations for spreading diaphragm yielding are limited to wood structural panel diaphragms at this time. An alternative for steel deck diaphragms could involve simply using a smaller R_{diaph} until sufficient data is obtained to justify an approach that distributes inelastic behavior. An appropriate R_{diaph} for steel deck diaphragms where the spreading of inelastic behavior is beyond the scope of this report.

Using the numerical model developed for the FEMA P695 evaluation, several archetypes were designed with varying degrees of weakening below current code level design forces at interior diaphragm span locations. A series of incremental dynamic analyses were conducted and the results were promising. It was observed that indeed relative weakening of the diaphragm interior assists in protecting the perimeter boundary areas from excessive inelastic demand, and increases the overall margin against building collapse. Additional information on these studies is contained in Koliou [2014]. Similar results were obtained using a combination of weakening interior portions of the diaphragm below current code level forces and amplifying the design shear forces in the end regions of the diaphragm, which is the approach used for the alternate design procedure proposed in this report.

In the development of the alternate design procedure, it was recognized that often in smaller buildings with low shear demands a minimum fastener size at maximum spacing is provided uniformly across the entire diaphragm, thus not permitting intentional weakening. Partially to address this situation, a shear amplification factor is applied to increase the design shear of the diaphragm's boundary areas to improve the spread of diaphragm yielding away from diaphragm boundaries. In this approach, the diaphragm boundary areas are designed the same as the diaphragm interior but with an applied shear amplification factor. In diaphragms where a designer simply elects to apply the boundary's shear amplification factor across the entire wood diaphragm, acceptable performance will still be achieved but the performance will be reduced as discussed in Appendix K.

One potential concern with the spread of diaphragm yielding is its impact on the cost of repair. If diaphragm yielding occurs over a larger percentage of the roof area, a larger area of the diaphragm may require repair following an earthquake. A potential tradeoff between improved collapse resistance and cost of repairs may exist. For buildings in which higher potential repair costs are a concern, designing the diaphragm for higher forces or trying to force the yielding into the vertical wall elements may be desirable.

4.2.2 Diaphragm Response Modification Coefficient and Shear Amplification

As discussed above in Section 4.2, an assumed linear distribution of design shear along the diaphragm span requires R_{diaph} to be less than 4, but as discussed in Section 4.2.1, R_{diaph} could potentially be increased if design shear is increased in targeted areas near the diaphragm supports to spread yielding within the diaphragm.

Based on this premise, a FEMA P695 study was conducted on a set of archetype buildings with weakened interior portions of a diaphragm; trial and error was used to evaluate different values of R_{diaph} with different nonlinear shear distribution along the length of the diaphragm span. From this study the alternative procedure was developed for one-story RWFD buildings. The FEMA P695 evaluation included a set of buildings of various sizes, shapes and seismic exposures, designed by incorporating a new approximate building period (Equations 2, 4, 6), reducing the strength of the interior diaphragm portions with a response modification coefficient $R_{diaph} = 4.5$ (instead of 4), and strengthening the

diaphragm boundary regions (a minimum width of 10% of the diaphragm span at each end) with 50% more capacity. With this alternate design procedure, the FEMA P695 evaluation showed a significant improvement in the collapse capacity and met all collapse margin targets required to show equivalency to the seismic performance intent of the current building code.

4.3 Deflection Amplification Factor, C_d, Selection

Deflections are used in design to check for deformation compatibility, second order effects, P-Δ stability, property line setbacks, and separation at seismic joints. These are required to be checked at the design earthquake force level. Diaphragms in RWFD buildings are expected to go into the inelastic range during a design earthquake; however, the design forces used to compute diaphragm deflections are based on elastic behavior. Thus the computed elastic deformations must be amplified to get realistic values. Essentially, this amplification is reversing the process that the response modification coefficient, R, provided to the design level forces.

The value of C_d computed in accordance FEMA P695 assuming 2% damping, is equal to 1.25 times the value of response modification coefficient, R. See Appendix Section G.3. However, the ratio of mean diaphragm deflection for design earthquake shaking to the diaphragm deflection due to design forces reduced by R computed for the archetypes as part of this study indicate that a deflection amplification factor, C_d, equal to the response modification coefficient, R, for the corresponding structural system is appropriate. The basis for $C_{d\ diaph}$ is presented in Appendix G Section G.3.

The diaphragm deflection for design earthquake shaking can be obtained by first computing the elastic deflection for design earthquake forces using the equations of the *Special Design Provisions for Wind and Seismic with Commentary* (SDPWS-2008) [AWC, 2009] and then multiplying this value by C_d.

4.4 Overstrength Factor, Ω_o, Selection

For design of a limited number of critical elements, the building code dictates using special load combinations with overstrength to prevent these critical elements from being the weak link. The overstrength factor, Ω_o, is used to increase the design forces to appropriate design levels for this purpose. When conducting a study under FEMA P695 to evaluate a proposed response modification coefficient, R, a suitable overstrength factor, Ω_o, can be determined for the proposed structural system being considered.

Because the diaphragm is expected to be where the inelastic behavior occurs, the use of a unique overstrength factor, Ω_o, tied to the diaphragm is more appropriate for the design of diaphragm collectors and their connections than the current procedure which uses the shear wall system's Ω_o. For this study a diaphragm overstrength value of 2 was computed in accordance with FEMA P695.

4.5 Overview of the Alternate Seismic Design Procedure

The alternate design procedure can be thought of as a two-stage approach to designing a RWFD building: first, the diaphragm is designed using its own response modification coefficient, period and detailing rules, and second, the vertical elements of the SFRS are designed using the existing design provisions of ASCE 7-10 with minor modifications.

The alternate design procedure is only permitted to be used when all of the following conditions apply:

- The building is single-story,
- The perimeter walls are concrete or masonry,
- The diaphragm is wood structural panel, nailed to wood framing or wood nailers,
- The diaphragm is rectangular or can be divided into rectangular plan areas that are laterally supported on each edge,
- The value of T_{diaph} is greater than or equal to 3 times the value of period of the walls, T_{walls}, computed using ASCE 7-10 Eq. 12.8-9 as indicated in Step 8, and
- The approximate period, T_a, computed using ASCE 7-10 Equation 12.8-9 for the shear walls is small enough to be in the constant acceleration portion of the design spectrum.

The following provides an overview of the steps required to implement the alternate procedure:

1. A response modification coefficient of the diaphragm, R_{diaph} equal to 4.5 is assigned.

2. The wood diaphragm period is determined using Equation (3):

$$T_{diaph} = 0.002L_f$$

where

L_f = the span, in feet, of the horizontal flexible diaphragm being considered; the span is measured between vertical elements that provide lateral support to the diaphragm in the direction being considered.

The value of T_{diaph} shall be greater than or equal to 3 times the value of period of the walls, T_{walls}, computed using ASCE 7-10 Eq. 12.8-9 as indicated in Step 8. Although it is believed that the equation for T_{walls} will overestimate the actual period, this limitation is to remain consistent with the comparative range of building responses investigated in this study.

3. C_s is determined in accordance with the equivalent lateral force procedure in Section 12.8.1 of ASCE 7-10 but using R_{diaph} in place of R and T_{diaph} in place of T_a computed in accordance ASCE 7-10 Eq. 12.8-7 or Eq. 12.8-9.

4. Diaphragm design shears are computed using the following force acting on the diaphragm

$$F_p = C_s w_p$$

where

F_p= the force acting on the diaphragm per unit length.

w_p= the tributary seismic weight applicable per unit length of diaphragm including the tributary weight of the walls acting out-of-plane.

5. The diaphragm design shears are increased by a shear amplification factor of 1.5 for the end 10% of the diaphragm span length at each end of the diaphragm span.

6. Diaphragm chords are designed for the diaphragm flexure resulting from diaphragm loads computed using F_p in Step 4 without the amplification in Step 5.

7. Collectors and their connections are designed for the forces computed from the design diaphragm shears collected and amplified by a diaphragm overstrength factor, $\Omega_{o\ diaph}$, equal to 2.

8. The vertical elements of the SFRS, i.e., shear walls, are designed for in-plane forces using the equivalent lateral force procedure of ASCE 7-10 Section 12.8 but with the force from the diaphragm as computed in Step 4 amplified by $(R_{diaph}/\rho_{diaph})/(R_{wall}/\rho_{wall})$ but not less than 1.0. The response modification coefficient, R_{wall}, is assigned the value for the type of vertical system being engineered but not greater than R_{diaph}. The approximate period, T_a, is computed using ASCE 7-10 Equation 12.8-9 for the shear walls. This period, for the type of building envisioned, should always be small enough to be in the constant acceleration portion of the design spectrum. Acceleration computed using R_{wall} and T_a is applied to the seismic mass of the in-plane walls. The detailing requirements and system limitations of ASCE 7-10 Table 12.2-1 apply even though the R_{wall} may have been reduced to be less than or equal to R_{diaph}.

9. Deflections are computed for the diaphragm and the wall system. Elastic diaphragm deflection, $\delta_{e\ diaph}$, is computed using the force level, F_p, in Step 4 and Equation 4.2-1 in SDPWS-2008 Section 4.2.2. The elastic diaphragm deflection should be amplified by a deflection amplification factor for the diaphragm, $C_{d\ diaph}$, equal to 4.5 and a formula similar to ASCE 7-10 Equation 12.8-15.

$$\delta_{diaph} = \frac{C_{d\ diaph}\delta_{e\ diaph}}{I_e}$$

Deflection of the wall system should be computed for design level forces and amplified by C_d for the wall system.

$$\delta_{wall} = \frac{C_{d\ wall}\delta_{e\ wall}}{I_e}$$

The computed deflection is used to check that the interconnection of structural wall elements and connections to supporting framing systems have sufficient ductility and rotational capacity in accordance with ASCE 7-10 Section 12.11.1. For SDC D to F, the computed deflection is also used to check that the permissible deflection of attached elements is not exceeded in accordance with ASCE 7-10 Section 12.12.2. If appropriate, the computed deflections are used to determine required seismic separations or property setbacks in accordance with ASCE 7-10 Section 12.12.3.

10. Second order/P-Δ effects for the building are checked in accordance with ASCE 7-10 Section 12.8.7 but both diaphragm and wall deflections should be included. The diaphragm deflection component can be reduced to approximately two-thirds of the maximum diaphragm deflection because the diaphragm tributary seismic weight on average moves approximately two-thirds of the diaphragm deflection plus the deflection of the in-plane walls.

11. Out-of-plane wall forces and out-of-plane top-of-wall anchorage forces and detailing requirements are designed in accordance with Sections 12.11.1 and 12.11.2 of ASCE 7-10 except that k_a is set equal to 2 for all diaphragm spans in Equation 12.11-1. Appendix J provides addition information regarding this.

Information on the study that demonstrates the adequacy of this alternate seismic design procedure is provided in Appendices A and G to I. A more specific description of this design method in code-based language is also provided in Appendix A to this report.

Chapter 5 Implementation of the Alternate Seismic Design Procedure

Explanation of how to implement the alternate design procedure listed in Section 4.5 is provided in this chapter. Redesign of the example building introduced in Chapter 3 is used to demonstrate and explain the procedure.

5.1 A Two-Stage ELF Procedure

Conceptually, a RWFD building is simply a flexible diaphragm structure supported by a more rigid wall structure below. In regards to the seismic load path, the flexible diaphragm is in series with the rigid walls, and could conceivably be viewed in part as a vertical combination of SFRS under ASCE 7-10 Section 12.2.3.1. If viewed as an upper flexible diaphragm supported by a lower rigid shear wall system, this is similar to today's common podium buildings with a flexible SFRS at the upper floors supported on a rigid SFRS at the lower floors.

The two-stage ELF procedure of ASCE 7-10 Section 12.2.3.2, first introduced into the 1988 Uniform Building Code [ICBO, 1988], is commonly used in practice today for podium structures. This philosophy is adapted for use in the alternate procedure for RWFD buildings. When an upper flexible portion is supported by a lower rigid portion, a two-stage procedure encourages the use of two different periods T and two different response modification coefficients R in series within the same building to determine the applied seismic design forces to each portion. Furthermore, two separate overstrength factors, Ω_o, and deflection amplification factors, C_d, may be utilized when appropriate, one pair of Ω_o and C_d values for the diaphragm and another for the walls.

Currently, the two-stage analysis procedure within ASCE 7-10 Section 12.2.3.2 limits its applicability to situations where the period of the entire structure is not greater than 1.1 times the period of the upper portion considered as a separate structure. Additionally, applicability is also limited to situations where the lower portion is at least ten times stiffer than the upper portion. These limitations were placed to account for the uncertainty of the structure's behavior when the differences in the stiffnesses or periods are small. However, these limitations are deemed to not be necessary to the alternate design methodology presented here, because this procedure was validated through FEMA P695 with a wide range of diaphragm and wall stiffnesses as well as diaphragm and building periods that often fell significantly below the stiffness ratio thresholds. Thus, some influence or interaction between the walls and diaphragm due to stiffnesses or periods that begin to approach each other is already reflected in the FEMA P695 validation. The alternate procedure should be valid as long as the approximate period of the diaphragm computed in accordance with Equation (2) is at least three times the approximate period of the walls computed using ASCE 7-10 Equation 12.8-9.

5.2 First Stage – Diaphragm Design

The first stage of the analysis involves design of the diaphragm as a separate structure using an ELF procedure in each direction. As previously discussed, special seismic response modification coefficients, overstrength factors and deflection amplification factors have been established for the flexible diaphragm comprised of wood structural panels. Additionally, a comparison of the periods for the diaphragm and the in-plane shear walls is necessary to verify that the alternative design procedure is valid.

$$T_{diaph} = 0.002L_f \qquad \text{Equation (2)}$$

$$T_{walls} = \frac{0.0019}{\sqrt{C_w}} h_n \qquad \text{ASCE 7-10 Equation 12.8-9}$$

where

C_w and h_n are per ASCE 7-10 Section 12.8.2.1

Seismic Performance Factors:

R_{diaph} = 4.5 provided an amplified shear boundary zone is incorporated into the diaphragm
$\Omega_{o\ diaph}$ = 2.0 for the design of collectors, etc. (See Section 4.4)
$C_{d\ diaph}$ = 4.5 for the calculation of diaphragm deflections (See Section 4.3)
ρ = 1.0 (ASCE 7-10 Section 12.3.4.1)

The design spectral accelerations will be the same as current practice. As previously determined:

$S_{DS\ design}$ = 1.0 (short period)
$S_{D1\ design}$ = 0.6 (1-second period)
SDC = D

5.3 Diaphragm Design Coefficient C_s Using the ELF Procedure

ASCE 7-10 Section 12.8.1 defines the seismic base shear as

$$V = C_s W \qquad \text{ASCE 7-10 Eq. 12.8-1}$$

where

$$C_s = \frac{S_{DS}}{R/I_e}$$ ASCE 7-10 Eq. 12.8-2

Because the flexible diaphragm is supported by the significantly stiffer rigid shear walls, the diaphragm will be viewed as a separate structure with its base at the roof-to-wall interface. Thus using Equation 12.8-1 the diaphragm force F_p will be represented as

$$F_p = C_s w_p$$

Now with the ability to differentiate between the wall's and diaphragm's response modification coefficients, a unique C_S is initially obtained for the diaphragm. Per Equation 12.8-2

$$C_s = \frac{S_{DS}}{R_{Diaph}/I_e} = \frac{1.0}{4.5/1.0} = 0.222$$

With the greater flexibility of the diaphragm compared to the walls, it is now possible that the upper bound for C_s using Equation 12.8-3 may govern, indicating that the seismic response is off the plateau of the design spectrum.

Before the upper bound for C_s can be computed, the approximate fundamental period of the diaphragm in each orthogonal axis direction must be considered. The north/south (transverse) loading direction will be considered first, followed by the east/west (longitudinal) loading direction.

<u>North/South Direction:</u>

As previously determined in Section 4.1:

$$T_{diaph} = 0.800\ sec$$

$$T_{wall} = 0.136\ sec$$

For engineers using ASCE 41-13 to evaluate RWFD buildings, standard practice has been to use the building's period T_a from ASCE 41-13 Eq. 7-19 to develop pseudo forces for the diaphragm. However, engineers using ASCE 7-10's two-stage procedure typically design the upper flexible portion considering its own isolated period. There is some inconsistency between how the period is selected between these two approaches.

In this study, the numerical model analyzed 54 building archetypes whose diaphragms were designed using the building's full period $T_a = T_{diaph} + T_{walls}$, similar to the ASCE 41-13 approach; and the results were found to be acceptable under the FEMA P695 validation. However, situations where the walls may behave more like frames could cause the design forces to become unconservative due to the longer design period utilized. It is recommended and will be illustrated in this example to design the diaphragm for its own approximate period using Equations (2) and (3), instead of including the walls' contribution. This will result in a smaller period causing the diaphragm design forces to potentially increase for very large buildings whose spectral design acceleration is off the constant acceleration plateau.

At this point it is also necessary to compare the ratio of diaphragm period (0.800 sec) to wall period (0.136 sec). By definition, RWFD buildings require the vertical portions of the SFRS to be relatively stiffer than the horizontal diaphragm. This study investigated archetypes with ratios that got within 3 when considering ASCE 7-10 Equation 12.8-9, and thus recommend that this alternative procedure be limited to those situations where diaphragm-to-wall period ratio exceeds 3. For the north/south direction, this ratio is equal to 5.9, thus acceptable.

Returning back to the computation of C_s for the purposes of determining the diaphragm's design force, a check of the upper limit for C_s is necessary where $T \leq T_L$. Using the building period $T_{diaph} = 0.800$ seconds, the following is determined:

$$C_{s\,max} = \frac{S_{D1}}{T\left(R/I_e\right)} = \frac{0.6}{0.800\left(4.5/1.0\right)} = 0.167 < 0.222 \qquad \text{ASCE 7-10 Eq. 12.8-3}$$

The fundamental period is longer than the transition period, T_s, equal to 0.6 seconds so the fundamental period is off the design spectrum's constant acceleration plateau and in the $1/T$ region of the spectrum. Thus, preliminarily C_s equals 0.167. Checking the minimum allowed value for C_s, ASCE 7-10 Equations 12.8-5 and 12.8-6 are applicable. In this example, S_1 is equal to 0.6*g*: therefore, Equation 12.8-6 is valid to check the minimum allowed C_s.

$$C_{s\,min} = 0.044 S_{DS} I_e = 0.044(1.0)(1.0) = 0.044 < 0.167 \quad \text{OK} \qquad \text{ASCE 7-10 Eq. 12.8-5}$$

$$C_{s\,min} = 0.01 < 0.167 \quad \text{OK} \qquad \text{ASCE 7-10 Eq. 12.8-5}$$

$$C_{s\,min} = \frac{0.5 S_1}{R/I_e} = \frac{0.5(0.6)}{4.5/1.0} = 0.067 < 0.167 \quad \text{OK} \qquad \text{ASCE 7-10 Eq. 12.8-6}$$

The calculated value of $C_s = 0.167$ is above all the minimum allowed values.

$$C_{s\ \text{governs}} = 0.167$$

Substituting into Equation 12.8-1, we obtain the diaphragm force equation for the north/south direction of the structure, which is used to determine the design forces acting on the diaphragm.

$$F_p = V_{N/S} = C_s W$$

$$F_p = 0.167 w_p$$

<u>East/West Direction:</u>

As previously determined in Section 4.1:

$$T_{diaph} = 0.400\ sec$$

$$T_{wall} = 0.096\ sec$$

By definition, RWFD buildings require the vertical portions of the SFRS to be relatively stiffer than the horizontal diaphragm, and a limitation of this procedure is that the ratio of diaphragm period to wall period be at least equal to 3, when T_{walls} is evaluated using ASCE 7-10 Equation 12.8-9. For this example building, the diaphragm period (0.400 sec) to wall period (0.096 sec) ratio is equal to 4.2, thus acceptable.

Checking the upper limit for C_s where $T \leq T_L$

$$C_{s\ max} = \frac{S_{D1}}{T\left(R/_{I_e}\right)} = \frac{0.6}{0.400\left(4.5/_{1.0}\right)} = 0.333 > 0.222 \qquad \text{ASCE 7-10 Eq. 12.8-3}$$

The fundamental period is short enough to be on the design spectrum's plateau, thus preliminarily C_s = 0.222. Checking the minimum allowed value for C_s, ASCE 7-10 Equations 12.8-5 and 12.8-6 are applicable. In this example, S_1 is equal to 0.6*g*: therefore, Equation 12.8-6 is valid to check the minimum allowed C_s.

$$C_{s\ min} = 0.044 S_{DS} I_e = 0.044(1.0)(1.0) = 0.044 < 0.222 \quad \text{OK} \qquad \text{ASCE 7-10 Eq. 12.8-5}$$

$C_{s\,min} = 0.01 < 0.222$ OK ASCE 7-10 Eq. 12.8-5

$C_{s\,min} = \frac{0.5S_1}{R/I_e} = \frac{0.5(0.6)}{4.5/1.0} = 0.067 < 0.222$ OK ASCE 7-10 Eq. 12.8-6

The calculated value of $C_s = 0.222$ is above all the minimum allowed values.

$C_{s\ \text{governs}} = 0.222$

Substituting into Equation 12.8-1, we obtain the diaphragm force equation for the north/south direction of the structure, which is used to determine the design forces in the diaphragm.

$F_p = V_{E/W} = C_s W$

$F_p = 0.222 w_p$

Each of the uniformly distributed diaphragm design loads $0.167w_p$ and $0.222w_p$ in the north/south and east/west directions respectfully are different than the current practice value of $0.25w_p$. These differences are attributed to recognition of the longer period of the long spanning diaphragm in the north/south direction and better distribution of yielding along the diaphragm spans reflected in the response modification coefficient (R=4.5 instead of 4). However, this increase in R also requires an amplification of design shear in the end regions of the diaphragm that will be explained in Section 5.5. This amplification of the diaphragm design shears is effectively a local reduction of R_{diaph} relative to a value of 4.5 in the diaphragm end regions.

5.4 Diaphragm Forces Using the ELF Procedure

Using our flat-beam analogy, north/south seismic forces are resisted by shear walls on grid lines A and J, and east/west seismic forces are resisted by shear walls on grid lines 1 and 5. A uniformly distributed load across this flat-beam is illustrated in Figure 5.1.

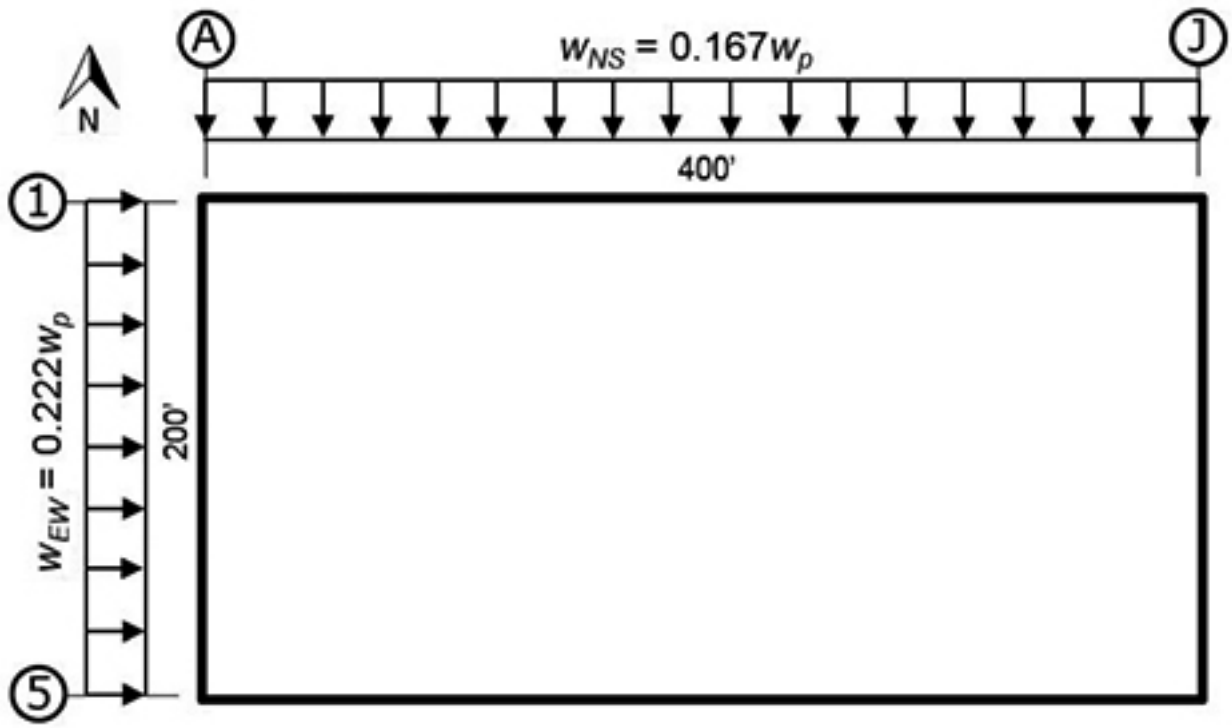

Figure 5.1: Diaphragm Loading Model (Alternate Procedure)

The uniform loads w_{NS} and w_{EW} applied laterally to the diaphragm are computed using the diaphragm lengths and unit weights and the tributary wall heights and unit weights:

Roof dead load = 12 psf

Wall dead load = 116 psf (9¼" thick at 150 pcf)

Roof height = 30'-0"

Top of wall = 33'-0" (above floor)

$$w_{NS} = 0.167(12psf)(200') + 2\left[0.167(116psf)33'\left(\frac{33'}{2}\right)\left(\frac{1}{30'}\right)\right] = 1104plf$$

$$w_{EW} = 0.222(12psf)(400') + 2\left[0.222(116psf)33'\left(\frac{33'}{2}\right)\left(\frac{1}{30'}\right)\right] = 2000plf$$

The maximum design shears are now computed using simple statics on the uniformly loaded flat beam model. Because of the building's symmetry, V_{NS} at grid lines A and J will be equal. See Figure 5.2.

North-south diaphragm shear:

$$V_{NS} = w_{NS}\frac{L}{2} = 1104\frac{(400\text{ ft})}{2} = 220{,}800\ lbs$$

North-south unit shear:

$$v_{NS} = \frac{V_{NS}}{200\text{ ft}} = \frac{220{,}800}{200\text{ ft}} = 1104\ plf\ maximum$$

East-west diaphragm shear:

$$V_{EW} = w_{EW}\frac{L}{2} = 2000\frac{(200\text{ ft})}{2} = 200{,}000\ lbs$$

East-west unit shear:

$$v_{EW} = \frac{V_{EW}}{400\text{ ft}} = \frac{200{,}000}{400\text{ ft}} = 500\ plf, maximum$$

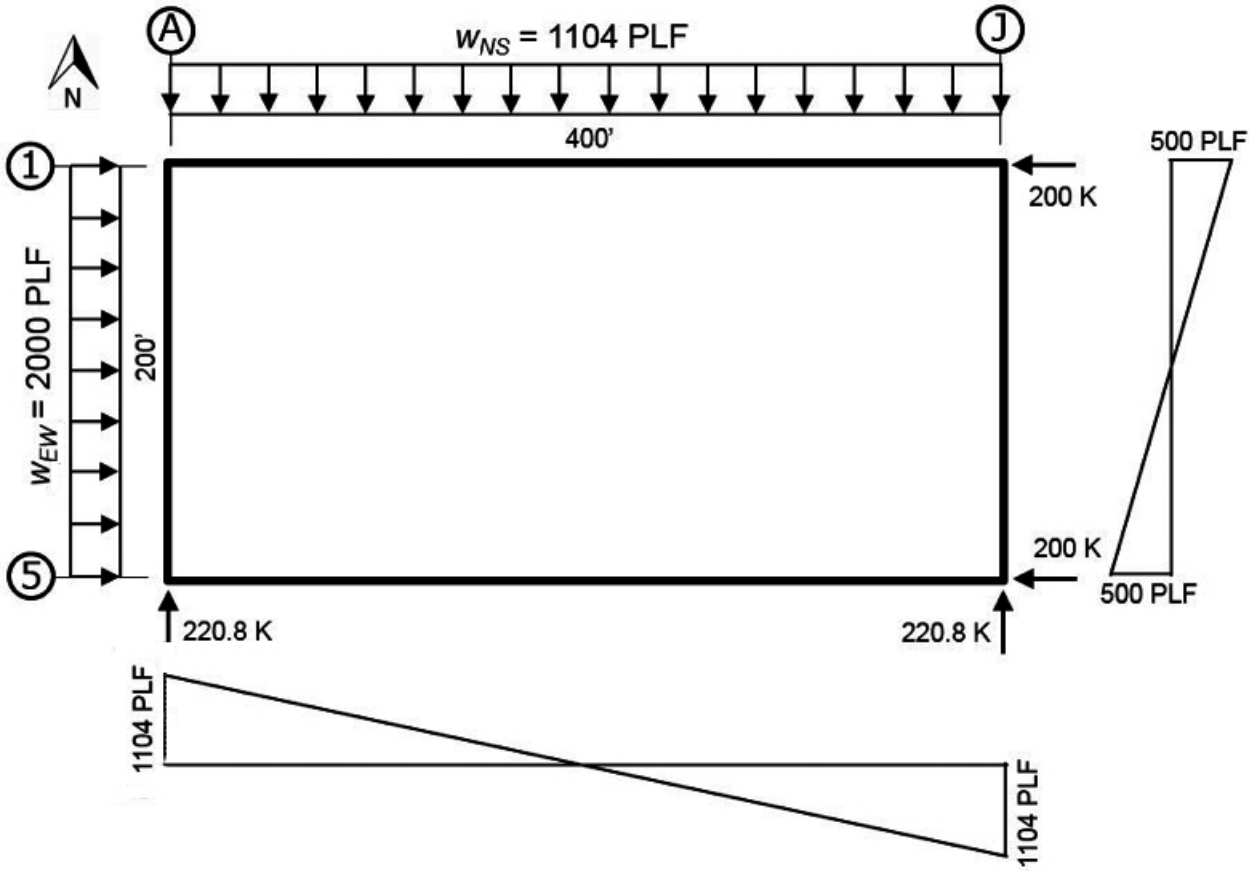

Figure 5.2: Diaphragm Shear Distribution

5.5 North/South Diaphragm Shear Design

The diaphragm design for the shears follows a similar approach as that outlined in Section 3.6, which illustrates current practice. In Section 5.4 above, the maximum diaphragm shears were determined for each orthogonal direction; but as mentioned earlier, performance was found to improve in the computer model's FEMA P695 analyses when inelastic behavior was better distributed, and this was accomplished in part by providing overstrength in the amplified shear boundary zones of the diaphragm. More specifically, the ten-percent of the diaphragm's length $0.10L$ at each end is designed for 1.5 times more diaphragm shear than otherwise would have been computed. Figure 5.3 illustrates the design shear distribution across the diaphragm in each direction.

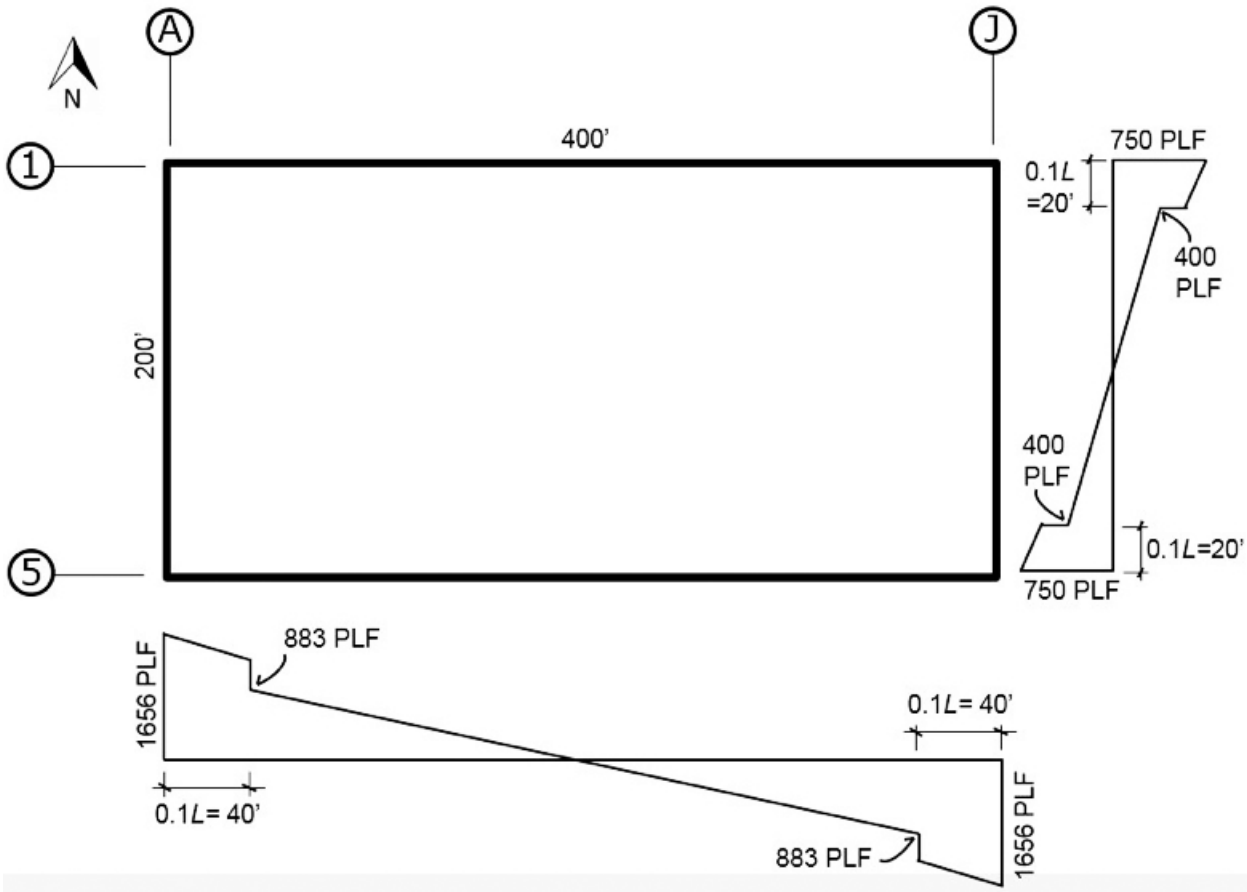

Figure 5.3 – Shear Diagrams for the Diaphragm Design with the 1.5x Factor.

As observed in Figure 5.3, the worst unit shear demand is in the north/south direction with v_{NS} = 1104x1.5 = 1656 plf (unfactored). The nominal diaphragm shear capacities are provided in SDPWS-2008 Tables 4.2A and 4.2B for a wide range of blocked diaphragm conditions. As done in Section 3.6 for current design, an ASD approach using the blocked panelized roof system will be followed.

$$v_{NS\,(ASD)} = 0.7v_{NS} = 0.7(1656) = 1159 \text{ plf}$$

$$v_{EW\,(ASD)} = 0.7v_{EW} = 0.7(750) = 525 \text{ plf}$$

Using these unit shear values, the designer enters either SDPWS-2008 Table 4.2A or 4.2B to select a diaphragm assembly with an appropriate shear capacity for 15/32-inch Structural I sheathing with 10d nails.

In the north/south direction, the ASD unit shear demand is greater than the maximum ASD capacities obtained from SDPWS-2008 Table 4.2A, thus reference to the high-load diaphragm shears in Table 4.2B will be necessary. The on-center (o.c.) nail spacing shown here requires thicker framing to prevent splitting. The capacity has been reduced from the table nominal strength value to an allowable stress design value by dividing in half per SDPWS-2008 Section 4.2.3.

15/32"-thick Structural I sheathing
10d nails in *2 lines* at
2 ½" (o.c.) boundaries and continuous north/south edges
3" o.c. other edges
10d nails in 1 line at
12" o.c. intermediate (field)
4x framing width at adjoining edges CAPACITY = 2580/2 = 1290 plf (ASD)

$$v_{NS\,(ASD)} = 0.7v_{NS} = 0.7(1656) = 1159 \text{ plf} < 1290 \text{ plf} \quad \text{OK}$$

The construction of this diaphragm system is illustrated in Figure 3.4:

The nailing and subpurlin widths may be reduced as the corresponding unit shears also reduce. For this example, Table 5.1 identifies various diaphragm nailing configurations from the SDPWS-2008 that will be utilized at different portions of this building. The ASD shear values are simply the nominal strengths listed in SDPWS-2008 Tables 4.2A and 4.2B divided by a factor of two per Section 4.2.3. Note that the framing and nailing listed for Zones 1 to 6 in Table 5.1 are the same as those listed for Zones 1 to 6 in Table 3.1 for the current practice design example in Chapter 3.

Table 5.1 – Diaphragm Nailing Schedule (Cases 2 and 4)

15/32" Structural I OSB Sheathing (DOC PS 2 [NIST, 2004]) with 10d nails (0.148" dia x 2" long minimum)					
Zone	Framing Width at Adjoining Edges	Lines of Nails	Nailing per line at Boundary & Continuous Edges	Nailing per line at Other Edges	ASD Allowable Shear (plf)
1	2x	1	6" o.c.	6" o.c.	320
2	2x	1	4" o.c.	6" o.c.	425
3	2x	1	2½" o.c.	4" o.c.	640
4	3x	1	2" o.c.	3" o.c.	820
5	4x	2	2½" o.c.	4" o.c.	1005
6	4x	2	2½" o.c.	3" o.c.	1290

At the diaphragm boundaries (grid lines A and J), Nailing Zone 6 was determined to be acceptable. At some location inward as the diaphragm shears diminish, Nailing Zone 5 will become acceptable. The transition from Nailing Zone 6 to Nailing Zone 5 may be located using statics as follows:

Shear Demand (ASD) = Shear Capacity (ASD)

$$0.7[V_{NS} - (w_{NS})x](1.5) = (1005 \text{ plf})B \qquad \text{Equation (7)}$$

$$0.7[220{,}800 \text{ lbs} - (1104 \text{ plf})x](1.5) = 1005 \text{ plf } (200 \text{ ft})$$

where

x = the demarcation distance from the diaphragm boundary.

Solving for x obtains

$x = 26.6$ ft

Because a panelized roof system typically consists of 8-foot wide wood structural panels, the joist spacing module is also 8 feet, and the transition should be increased to the next 8-foot increment. In this case, it is increased to x =32 feet; however, this leaves only 8 feet more until the shear demand dramatically reduces at $0.1L$ = 40-ft from the boundary as seen in Figure 5.3. Therefore it is elected to provide Nailing Zone 6 across the entire amplified shear boundary zone of the diaphragm.

It is important to observe that the potential transition location from nailing Zone 6 to Zone 5 selected occurs within the $0.1L$ or 40-ft wide boundary strip, thus Equation 7 is still valid with the 1.5 factor included. For the first nailing zone transition at or past $0.1L$ from the boundary shear element, the 1.5 shear amplification factor in Equation (7) may be omitted.

Latitude in the locating potential nailing zone transitions further away from the diaphragm boundary is possible within the end regions where shear is amplified, at the transition between amplified and non-amplified shear, and within the interior portions of the diaphragm where shear is not amplified. The basis for this latitude is the results of analyses of archetypes in which the nailing pattern at the boundary is used for the entire diaphragm span. Although these archetypes did not perform as well as the archetypes with multiple nailing zones, they met the acceptable performance criteria.

After 0.1L, the shear demand drops dramatically and some nailing zone assemblies may be skipped entirely. The transition locations between Zones 5 and 4, Zones 4 and 3, Zones 3 and 2, and Zones 2 and 1 for the north-south loading direction are found using the same process resulting in the following Table; however, it is important to recognize that the 1.5 shear amplification factor is only on the outer 0.1L portions.

Because the shear diagram (Figure 5.3) has a large stepped reduction in the design shear at 0.1L, nailing zones 5 and 4 are not utilized. This significant transition in nailing from zone 3 to 6 may catch framers by surprise; or worse it could be confusing and lead to field errors. As such, engineers should consider this construction aspect in their structural observation program.

Table 5.2 – Diaphragm Nailing Zone Shear Checks

Nailing Zone	Distance from Boundary	Maximum Unit Shear	ASD Unit Shear	Allowable Shear Capacity
6	0 feet	v_{max} = 1656 plf	v_{ASD} = 1159 plf	1290 plf
5	---	---	---	1005 plf
4	---	---	---	820 plf
3	40 feet	v_{max} = 883 plf	v_{ASD} = 618 plf	640 plf
2	96 feet	v_{max} = 574 plf	v_{ASD} = 401 plf	425 plf
1	120 feet	v_{max} = 442 plf	v_{ASD} = 309 plf	320 plf

The resulting nailing zone layout for the north/south loading is shown in Figure 5.4.

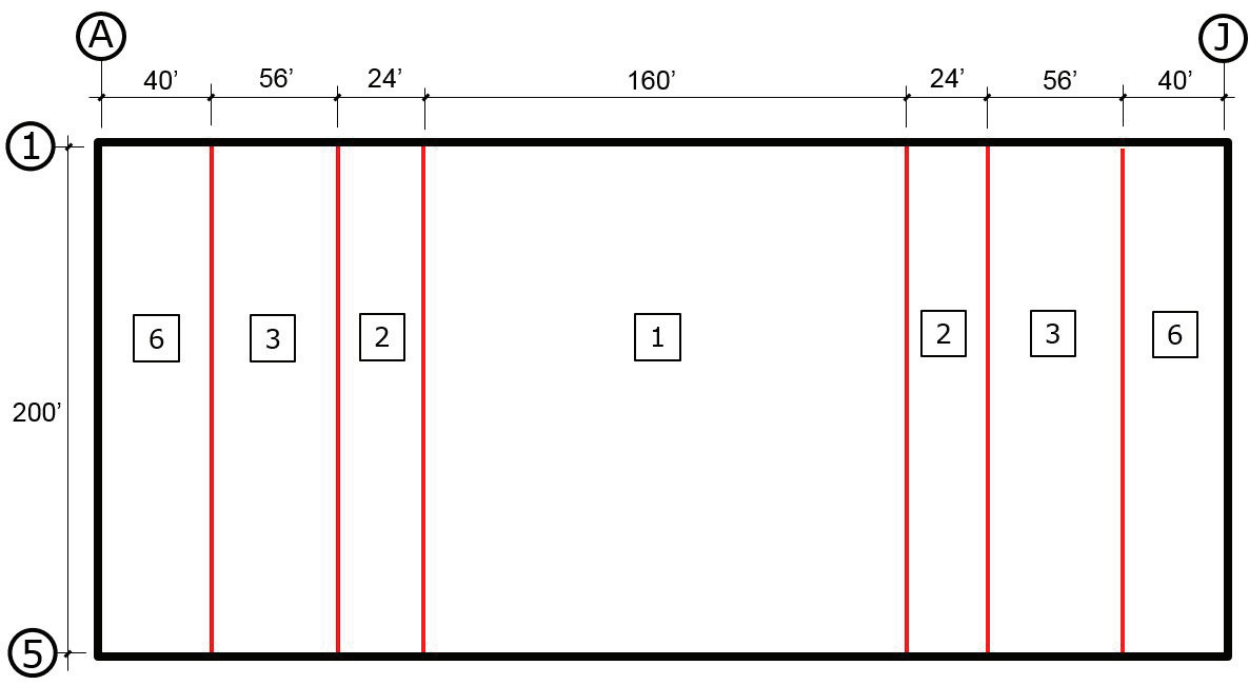

Figure 5.4: North/South Nailing Zone Layout

When designing wood diaphragms, the diaphragm aspect ratio must also be checked against the limitations in the SDPWS-2008 Table 4.2.4. For blocked diaphragms such as those that occur in panelized construction, the maximum aspect ratio is $L/W = 4:1$. In this example, the north/south loading direction is the critical L/W ratio.

$$L/W = 400/200 = 2.0 < 4 \quad \textit{Okay}$$

5.6 North/South Diaphragm Shear Transfer to Walls

As the diaphragm shears reach the diaphragm boundary, this seismic force must be transferred to the vertical SFRS, or as in this example the concrete shear walls. Traditionally, this transfer has been through a wood ledger at the inside face of wall. Occasionally, no parapets are utilized in the architectural design and a wood nailer is provided at the top of wall in place of a ledger. With the alternate design procedure, the diaphragm boundary nailing to the wood ledger/nailer and the ledger/nailer's bolting to the shear walls are designed using the diaphragm shear force with the 1.5 shear amplification factor to encourage the spreading of yielding within the diaphragm.

This example utilizes steel ledgers as discussed in Section 3.7. Steel ledgers have become very popular in large RWFD buildings, utilizing steel angles or channels bolted to the inside face of the shear walls. When these steel ledgers are combined with wood nailers on the top flange at the diaphragm interface, the provisions mentioned above for wood ledgers/nailers still apply. However, it has also become popular to omit the wood nailer and directly fasten the wood structural panel to the steel ledger with pneumatically driven steel pins. These proprietary pins typically have an ICC ES approval and can usually be driven through 3/8" thick steel, however there is no cyclic test data available to evaluate the post-yield behavior. Therefore, the pin design forces are designed with an overstrength factor, Ω_o, associated with the diaphragm.

Ledger bolting capacities into the concrete or masonry shear walls shall comply with ACI 318-11 or TMS 402-13 provisions respectfully.

5.7 North/South Diaphragm Chord Design

Recall that a flexible diaphragm may be thought of as a flat horizontal beam where the shear resistance is obtained by the wood structural panel sheathing across the roof surface and the flexural resistance is obtained from perimeter chords. As illustrated in the current-practice design of Section 3.7, these chords are steel ledger angles at the roof line. Chord forces are determined using simple statics as shown in Figure 3.6, and the design force is a uniformly distributed load without the 1.5 shear amplification

design factor. Maximum chord forces will occur at the center of the diaphragm's span where the maximum moment occurs.

The maximum tensile chord force for our building example is determined as follows:

$$T = \frac{M}{B} = \frac{w_{NS}L^2}{8B} = \frac{1104\ plf(400)^2}{8(200)} = 110{,}400\ lbs$$

The chord is designed here using strength design with ASTM A36 Steel (F_y = 36 ksi). Consulting IBC Section 1605.2, the applicable LRFD load factor for seismic forces is 1.0. The area of steel required is:

$$A_S = \frac{T}{\emptyset F_y} = \frac{(110.4)}{0.9(36)} = 3.41\ in^2$$

Using an L5x5x3/8 rolled steel angle satisfies this chord demand.

L5x5x3/8 Steel Area $A_S = 3.65\ in^2 > 3.41\ in^2$

5.8 East/West Diaphragm Shear Design

Similar to the north/south loaded direction, the orthogonal east/west direction will also require consideration using the same sequential process. In Section 5.5, the maximum diaphragm shear in the east/west direction was determined to be v_{EW} = 750 plf (unfactored) including the 1.5 shear amplification factor; and converting to allowable stress design (ASD), the maximum diaphragm shear is as follows:

$$v_{EW(ASD)} = 0.7v_{EW} = 0.7(750) = 525\ \text{plf}$$

As before, SDPWS-2008 Table 4.2A is used to select diaphragm nailing with an appropriate shear capacity. In the north/south loaded direction, Case 4 is the loading configuration, but for the east/west direction this becomes a Case 2 configuration. The applicable Case determines the nail spacing along the continuous adjoining panel edges in the direction parallel to load. Comparing the diaphragm's shear demand with the capacities of Section 5.5's Table 5.1, Nailing Zone 3 is selected:

$$v_{EW(ASD)} = 525\ plf < 640\ plf\ (Nailing\ Zone\ 3)$$

At some distance away from the diaphragm boundary (walls at grid lines 1 and 5), Nailing Zone 2 in Table 5.1 will be acceptable due to the diminishing unit diaphragm shears. With the dramatic drop in design shear at 0.1L = 20-ft, Nailing Zone 2 can be skipped altogether. Using the same approach as done

in the north/south direction, the locations of the nailing zone transition from Zone 3 to 2, and Zone 2 to 1 are found and shown in Table 5.3.

Table 5.3 – Diaphragm Nailing Zone Shear Checks

Nailing Zone	Distance from Boundary	Maximum Unit Shear	ASD Unit Shear	Allowable Shear Capacity
3	0 feet	v_{max} = 750 plf	v_{ASD} = 525 plf	640 plf
2	---	---	---	425 plf
1	20 feet	v_{max} = 400 plf	v_{ASD} = 280 plf	320 plf

Combining the nailing requirements for the north/south loading with the east/west loading results in Figure 5.5.

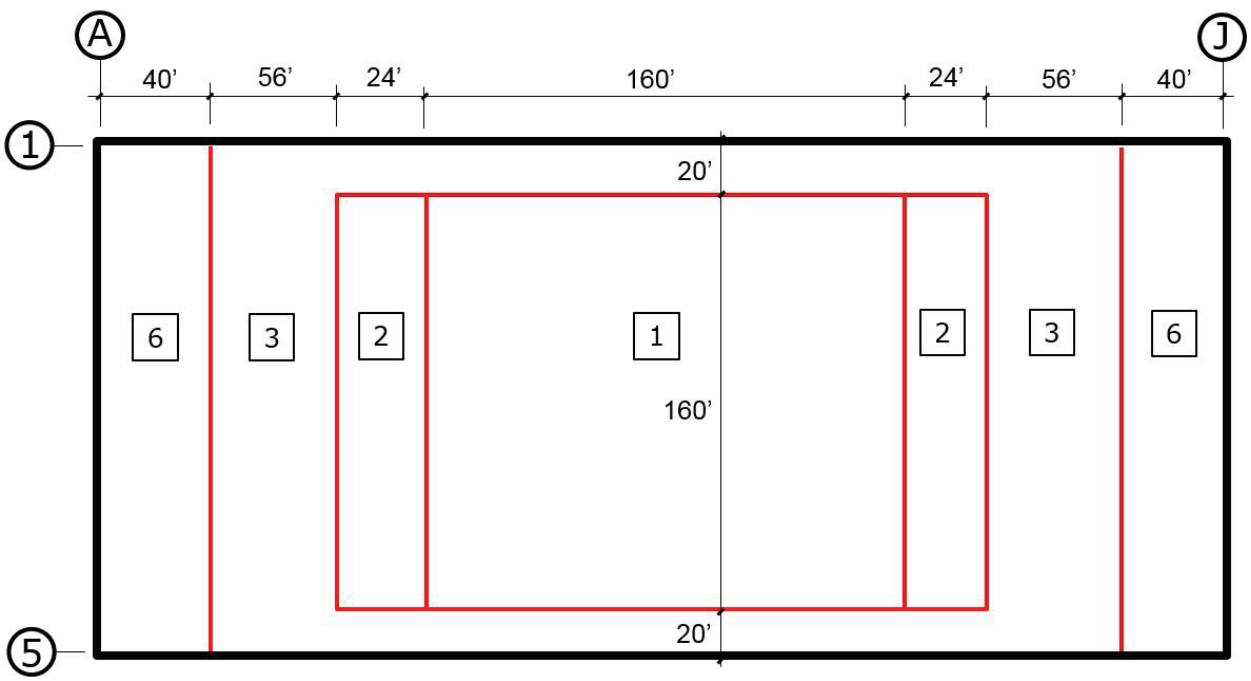

Figure 5.5: North/South and East/West Nailing Zones Combined Layout

5.9 East/West Diaphragm Shear Transfer to Walls

Similar to the north/south diaphragm force design, the seismic diaphragm shears must be transferred to the vertical concrete shear walls. As discussed in Section 5.6, the shear transfer is designed with the 1.5 shear amplification factor, with an additional diaphragm overstrength factor Ω_o at locations where proprietary pin fasteners are used at steel ledgers.

Unlike the north/south force direction, the diaphragm boundaries resisting east/west seismic forces along grid lines 1 and 5 do not have uniform boundary nailing. While most of the length contains nailing zone 3 requirements, the first and last 40-ft of this wall line contain nailing zone 6 requirements, whose stiffness may attract more load. In this example, there is a belief that the shear transfer to the steel ledger is non-uniform; however, the steel ledger was designed as the diaphragm chord in Section 5.7 and contains sufficient capacity to drag and redistribute the shear load appropriately to the shear wall elements. This is especially true when the diaphragm chord design is based on the maximum force at midspan, yet the chord design remains consistent along the entire shear wall line.

5.10 East/West Diaphragm Chord Design

With the diaphragm chords placed at the extreme sides of the diaphragm, the maximum chord forces in the east/west loaded direction are computed in a similar fashion as the north/south direction:

$$T = \frac{M}{B} = \frac{w_{EW}L^2}{8B} = \frac{2000\ plf(200)^2}{8(400)} = 25{,}000\ lbs$$

The required area of the steel chord is:

$$A_S = \frac{T}{\emptyset F_y} = \frac{(25.0)}{0.9(36)} = 0.77\ in^2$$

Using an L4x4x1/4 rolled steel angle as a practical minimum size satisfies this chord demand.

L4x4x1/4 Steel Area $A_S = 1.93\ in^2 > 0.77\ in^2$

5.11 Second Stage – Shear Wall Design

The second stage of the analysis involves the design of the heavy in-plane shear walls, whose period does not involve the diaphragm component, and is thus comparatively small. However, it does include the diaphragm mass as well as a portion of the perpendicular out-of-plane walls and in-plane walls. Additionally, the response modification coefficient R and redundancy factor ρ for the design of the in-plane walls will be as currently specified within ASCE 7-10 for that specific shear wall system.

Determining the lateral design forces for the in-plane shear walls involves a conversion of the diaphragm design forces based on R_{diaph} and ρ_{diaph} (ρ_{diaph} equal to 1.0) into the shear wall design forces based on R_{wall} and ρ_{wall}, where the determination of ρ remains unchanged from ASCE 7-10 Section 12.3.4. This conversion design philosophy is also found in ASCE's two-stage analysis procedure of Section 12.2.3.2.

It should be noted that the current design philosophy embedded within the code is that when two different SFRS's are in a vertical combination (Section 12.2.3.1), the lower system's response modification coefficient R is not to rise above that of the upper system's. In other words, the lower SFRS's design force shall not be reduced more than the upper system's design force, due to system ductility and overstrength. This philosophy is additionally included in ASCE's two-stage analysis procedure in Section 12.2.3.2 which also includes consideration of different redundancy factors that may occur in the upper and lower systems. Thus the diaphragm design force conversion to the shear wall design force is always an amplification, and this design philosophy will be maintained in this report. In summary, R_{wall} /ρ_{wall} used in the shear wall design shall always be less than or equal to R_{diaph}/ρ_{diaph}. Note that the 1.5 shear amplification factor applied to the design of the diaphragm end regions is not included in the conversion to wall forces.

The following sections illustrate this design procedure in each orthogonal direction on the example building:

5.12 Shear Wall Force Using the ELF Procedure

Because the building is being evaluated as two different seismically behaving portions, the force to the in-plane shear walls will have two significant components. The flexible diaphragm with its tributary mass will generate a lateral force near the top of the wall, F_{v1}. Additionally, the rigid concrete in-plane walls have significant self-weight that will also generate lateral forces near their center of mass, F_{v2}.

First, diaphragm forces imparted into the shear walls will be converted to be consistent with the expected seismic performance of an intermediate precast shear wall system. The diaphragm forces used for the design of the shear walls below will not include the 1.5 amplification factor used to design the diaphragm end regions.

As determined previously in Section 5.4, the diaphragm reactions to the shear walls based on $R_{diaph} = 4.5$ and $\rho_{diaph} = 1.0$ are as follows:

North/South Diaphragm Reactions

$$F_p = V_{NS} = 220{,}800 \ lbs$$

East/West Diaphragm Reactions

$$F_p = V_{EW} = 200{,}000 \ lbs$$

These diaphragm reaction forces need to be amplified to an appropriate shear wall design force.

North/South

$$F_{v1} = F_p \times \left(\frac{R_{diaph}/\rho_{diaph}}{R_{wall}/\rho_{wall}} \right)$$

where

$$\left(\frac{R_{diaph}/\rho_{diaph}}{R_{wall}/\rho_{wall}} \right) = \left(\frac{4.5/1.0}{4/1.0} \right) = 1.125 > 1.0 \ldots . OK$$

$$F_{v1} = 220{,}800 \times 1.125$$

$$F_{v1} = 248{,}400\ lbs$$

East/West

$$F_{v1} = F_p \times \left(\frac{R_{diaph}/\rho_{diaph}}{R_{wall}/\rho_{wall}} \right)$$

where

$$\left(\frac{R_{diaph}/\rho_{diaph}}{R_{wall}/\rho_{wall}} \right) = \left(\frac{4.5/1.0}{4/1.0} \right) = 1.125 > 1.0 \ldots . OK$$

$$F_{v1} = 200{,}000 \times 1.125$$

$$F_{v1} = 225{,}000\ lbs$$

Second, the lateral seismic force generated from the walls' self-weight must be included for design. The walls' self-weight will have a seismic response unique to its period of vibration, therefore the ELF procedure's base shear equation will be revisited.

ASCE 7-10 Section 12.8.1 defines the seismic base shear as

$$V = C_s W \qquad \text{ASCE 7-10 Eq. 12.8-1}$$

where

$$C_s = \frac{S_{DS}}{R/I_e} \qquad \text{ASCE 7-10 Eq. 12.8-2}$$

Now working with the intermediate precast concrete shear walls (R = 4) instead of the diaphragm (R_{diaph} = 4.5), a unique C_S is obtained for the shear wall design. Per Equation 12.8-2

$$C_s = \frac{S_{DS}}{R/I_e} = \frac{1.0}{4/1.0} = 0.25$$

An upper bound for C_s must now be computed using the approximate period of the rigid shear walls using Equation 12.8-3. As previously determined, the approximate T_{walls} is different in each orthogonal direction when using Equation 12.8-9. The north/south (transverse) loading direction will be considered first, followed by the east/west (longitudinal) loading direction.

<u>North/South Direction:</u>

$$T_a = T_{walls} = 0.136\ sec$$

Checking the upper limit for C_s where $T \leq T_L$

$$C_{s\,max} = \frac{S_{D1}}{T\left(R/I_e\right)} = \frac{0.6}{0.136\left(4/1.0\right)} = 1.10 > 0.25 \qquad \text{ASCE 7-10 Eq. 12.8-3}$$

As expected for rigid shear walls, the fundamental period is short enough to be on the design spectrum's constant acceleration plateau, thus preliminarily C_s equals 0.25. Checking the minimum allowed value for C_s, ASCE 7-10 Equations 12.8-5 and 12.8-6 are applicable. In this example, S_1 is equal to 0.6g: therefore, Equation 12.8-6 is valid to check the minimum allowed C_s.

$$C_{s\,min} = 0.044 S_{DS} I_e = 0.044(1.0)(1.0) = 0.044 < 0.25 \quad \text{OK} \qquad \text{ASCE 7-10 Eq. 12.8-5}$$

$$C_{s\,min} = \frac{0.5S_1}{R/I_e} = \frac{0.5(0.6)}{4/1.0} = 0.075 < 0.25 \quad \text{OK}$$ ASCE 7-10 Eq. 12.8-6

The calculated value of $C_s = 0.25$ is above all the minimum allowed values.

$C_{s\ \text{governs}} = 0.25$

Substituting into Equation 12.8-1, we obtain the lateral force F_{v2} equation for the shear wall's self-weight, $W_{p\text{-}wall}$, for the north/south direction of the structure.

$F_{v2} = C_s W = 0.25 W_{p\text{-}wall}$

The wall self-weight $W_{p\text{-}wall}$ is computed as

$$W_{p-wall} = 116psf \times 200ft \times 33ft = 765{,}600\ lbs$$

Therefore

$F_{v2} = 0.25 W_{p\text{-}wall} = 0.25(765{,}600) = 191{,}400$ lbs

Therefore, the total shear wall design force F_v for the north/south direction is

$F_v = F_{v1} + F_{v2} = 248{,}400 + 191{,}400$

$F_v = 439{,}800$ lbs or 440 kips

<u>East/West Direction</u>

Because the east/west load direction has the same R_{wall}, ρ_{wall}, and because T_a is smaller than in the north/south direction, the seismic response coefficient, C_s, is still on the constant acceleration plateau, $F_{v2} = 0.25 W_{p\text{-}wall}$.

$F_v = F_{v1} + F_{v2} = 225{,}000 + 0.25 W_{p\text{-}wall}$

The wall self-weight $W_{p\text{-}wall}$ is computed as

$$W_{p-wall} = 116psf \times 400ft \times 33ft = 1{,}531{,}200\ lbs$$

Therefore

$$F_{v2} = 0.25W_{p\text{-}wall} = 0.25(1{,}531{,}200) = 382{,}800 \text{ lbs}$$

Therefore, the total shear wall design force F_v for the east/west direction is

$$F_v = F_{v1} + F_{v2} = 225{,}000 + 382{,}800$$

$$F_v = 607{,}800 \text{ lbs or } 608 \text{ kips}$$

Figures 5.6 and 5.7 illustrate the forces acting on the shear walls providing lateral resistance in the north/south and east/west directions respectfully. The design forces at the base of the shear walls are 440 kips north/south and 608 kips east/west. These forces include the entire weight of the walls and are appropriate for the design of shear forces that transfer to the slab on ground or foundation.

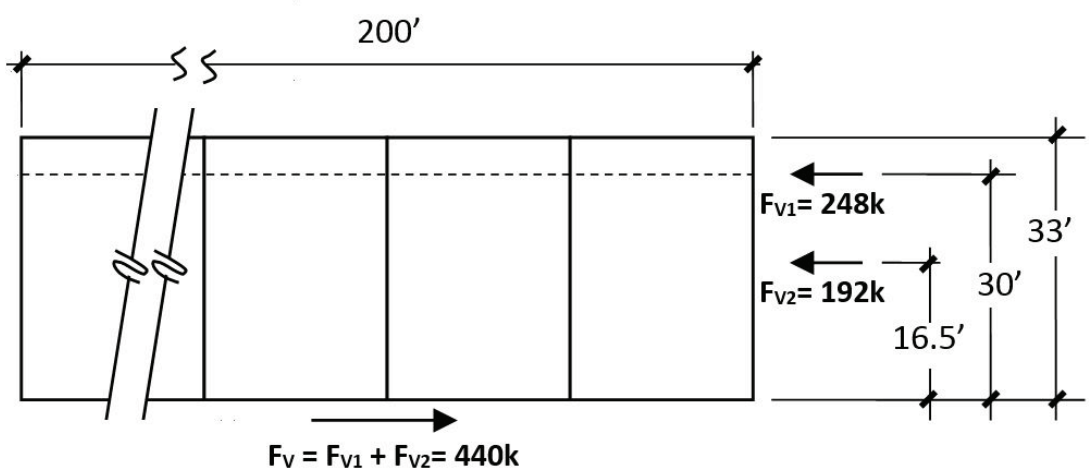

Figure 5.6: North/South Lateral Design Forces acting on the Shear Walls (Lines A & J)

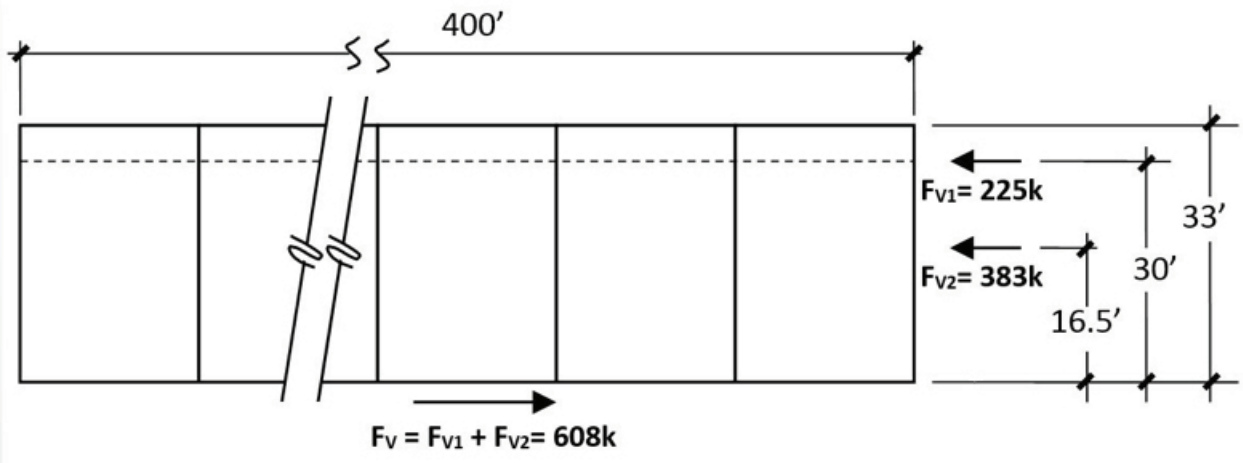

Figure 5.7: East/West Lateral Design Forces acting on the Shear Walls (Lines 1 & 5)

5.13 Limitations and Adaptations of the Alternate Design Procedure

The alternate design methodology was presented for a very basic single story, rectangular building with solid walls and no interior vertical SFRS elements. Often the design of much larger buildings is necessary, and these situations often require interior shear walls or braced frames to keep the diaphragm shears manageable. For these one-story buildings with multiple-span diaphragm, each diaphragm span can be evaluated separately, and appropriately combined and adjusted as the design load is brought to the shear walls.

Situations involving two or more stories, non-rectangular plans, diaphragm materials outside the typical nailed wood structural panel, and vertical SFRS other than concrete or masonry have not been properly evaluated to determine whether the alternate design procedure is applicable. Caution is needed before this design procedure is applied to situations that fall outside of the archetype inventory created for this project. Some areas of further study are listed in Section 8 of this report.

THIS PAGE INTENTIONALLY LEFT BLANK

Chapter 6 Diaphragm Deflection Check

Seismic ground motion typically causes more lateral deformation in the diaphragm than in the walls of RWFD buildings. The magnitude of the diaphragm deflections can be large enough to impact the building's structural integrity, compromise the attached non-structural elements, or cause the building to pound against adjacent structures. Large diaphragm deflections may also result in excessive second-order loading P-delta effects, causing instability that leads to collapse.

ASCE 7-10 Section 12.12.2 limits diaphragm deflections to the amount that will permit the attached elements to maintain their structural integrity and to continue supporting their prescribed loads. The intent is to prevent substantial damage to structural elements and their connections, the failure of which can lead to local structural collapse. This requirement is also intended to prevent excessive $P\Delta$ effects that could lead to a sidesway collapse. For non-structural elements, the intent is to prevent failure of connections or to compromise the self-integrity that could result in a localized falling hazard. In order to evaluate these aspects of structural design, the engineer needs to compute the approximate building deformation as a combination of the deflection of the diaphragm and vertical elements of the SFRS.

6.1 Deflection of North/South Diaphragm

For the building example, the diaphragm deflection in the north/south direction will be greater than that in the east/west direction, and thus only the north/south direction will be checked. Procedures for computing horizontal diaphragm deflections under lateral loading are found in SDPWS-2008 Section 4.2.2. Equation 4.2-1 provides a simplified method of computing deflections of wood structural panel diaphragms by considering the contribution of flexural bending, shear deformation, nail slip and chord slip.

$$\delta_{dia} = \frac{5vL^3}{8EAW} + \frac{0.25vL}{1000G_a} + \frac{\sum(x\Delta_c)}{2W} \qquad \text{SDPWS Eq. 4.2-1}$$

where

δ_{dia} = maximum mid-span diaphragm deflection determined by elastic analysis, in
v = Maximum diaphragm shear, ft (assuming a uniformly loaded rectangular diaphragm)
L = horizontal span of diaphragm, ft
W = diaphragm span depth, ft
E = chord's modulus of elasticity, psi
A = cross sectional area of chord, in^2
G_a = apparent diaphragm shear stiffness, kips/in
Δ_c = chord slip at each connection, in
x = distance from chord splice to nearest support, ft

For our diaphragm example, the following parameters are determined below:

v = 1104 plf (Section 5.4)
L = 400 ft
W = 200 ft
E = 29,000,000 psi
A = L5x5x5x3/8 = 3.65 in^2 (Section 5.6)
G_a = 24 kips/in Zone 1 (SDPWS-2008 Table 4.2A)
= 15 kips/in Zone 2 (SDPWS-2008 Table 4.2A)
= 20 kips/in Zone 3 (SDPWS-2008 Table 4.2A)
= 51 kips/in Zone 6 (SDPWS-2008 Table 4.2B)
Δ_c = 0 (Welded chord connections assumed, and have no slip)

The contribution from flexural deformation $\frac{5vL^3}{8EAW}$ is derived from a horizontal beam with a uniformly applied distributed load. The term EA will represent in this example the steel chord stiffness; however, the concrete walls themselves will also provide significant flexural stiffness to the diaphragm. Therefore, this equation generally overestimates the flexural contribution to diaphragm displacement.

$$\delta_{dia\ flexure} = \frac{5vL^3}{8EAW} = \frac{5(1104plf)(400ft)^3}{8(29{,}000{,}000psi)(3.65in^2)200ft} = 2.09\ in$$

The shear deformation and nail slip contribution $\frac{0.25vL}{1000G_a}$ is derived from a horizontal beam with a uniformly applied distributed load, uniform shear stiffness and uniform diaphragm nailing. In general, the shear deformation between two points, L_i apart, under constant shear, v, is simply vL_i/G_a. In a simply supported beam with a uniformly distributed load, the shear is not constant but decreases linearly and thus the average shear, v_{ave}, between the two points is applicable, $v_{ave}L_i/G_a$. Because the average shear is half the maximum shear

$$v_{ave} = 0.5v$$

and the distance to the maximum deformation at midspan, L_i, is half the total span L

$$L_i = 0.5L$$

With the apparent shear stiffness G_a in kips/inch, the shear deformation contribution becomes

$$\delta_{dia\ shear} = \frac{v_{ave}L_i}{1000G_a} = \frac{0.5v(0.5L)}{1000G_a} = \frac{0.25vL}{1000G_a}$$

and this matches the shear deformation term in SDPWS-2008 Eq. 4.2-1.

For efficiency reasons, large diaphragms seldom have uniform diaphragm nailing across the building and thus the shear deformation term needs to be modified. For a diaphragm with various strips of different nailing zones, there are several approaches to this modification. As previously discussed, the shear deformation between two points at distance L_i apart under an average shear of v_{ave} is

$$\delta_{dia\ shear} = \frac{v_{ave} L_i}{G_a}$$

With multiple nailing zone strips of width L_i, and apparent shear stiffness G_{ai} in kips/inch, and average shears $v_{i\ ave}$, the total shear deformation at midspan can be computed as the summation of each strip's contribution between the edge and the midspan of the diaphragm:

$$\delta_{dia\ shear} = \sum \frac{v_{i\ ave} L_i}{1000 G_{ai}}$$

where

$v_{i\ ave}$ = the average diaphragm shear within each shear stiffness (nailing) zone
L_i = the length of each shear stiffness zone measured perpendicular to loading
G_{ai} = the apparent shear stiffness of each shear stiffness zone being considered

This approach assumes the nailing zones are continuous strips oriented from north to south as illustrated in Figure 5.4; however, the east/west diaphragm design caused Nailing Zone 3 to wrap around Nailing Zone 1 as illustrated in Figure 5.5. To simplify the analysis, the additional nailing from Zone 3 (north and south of Zone 1) will be ignored which will result in an overestimate of diaphragm deformation (conservative). Table 6.1 provides an organized approach to the computation working from grid A to the midspan. This format allows each different nailing zone strip to be evaluated separately.

Table 6.1 – Shear Deformation and Nail Slip Computation Table

Zone	v_{left}	v_{right}	$v_{i\ ave}$	L_i	G_a	$\frac{v_{i\ ave} L_i}{1000 G_{ai}}$
6	1104	883	994	40	51	0.78 in
3	883	574	729	56	20	2.04 in
2	574	442	508	24	15	0.81 in
1	442	0	221	80	24	0.74 in
					∑ =	4.37 in

$$\delta_{dia\ shear} = \sum \frac{v_{i\ ave} L_i}{1000 G_{ai}} = 4.37\ in$$

The chord slip contribution to diaphragm deformation $\frac{\sum(x\Delta_c)}{2W}$ is assumed to be zero because of the use of welded chord splices ($\Delta_c = 0$).

$$\delta_{dia\ chord\ slip} = \frac{\sum(x\Delta_c)}{2W} = 0\ in$$

Considering all the diaphragm deflection contributions we obtain

$$\delta_{dia} = \delta_{dia\ flexure} + \delta_{dia\ shear} + \delta_{dia\ chord\ slip} = 2.09 + 4.37 + 0 = 6.48 \text{ in}$$

Because the applicable load combination involves 1.0*E*, this unfactored diaphragm deflection is also the deflection at strength-based design loads. But recall that the seismic coefficient C_s in Section 5.3 involves dividing the maximum expected building response by the diaphragm's response modification coefficient R_{diaph}. To properly estimate the diaphragm's maximum expected deflection, the earlier effects of dividing by *R* must be reversed, and this is accomplished with the use of the deflection amplification factor C_d. ASCE 7-10 Equation 12.12-1 (or 12.8-15) may be used to compute the maximum expected diaphragm deflection δ_{max}.

$$\delta_M = \frac{C_d \delta_{max}}{I_e}$$

$C_d = 4.5$ (Section 4.5)

$\delta_{max} = 6.48$ in (an elastic response under strength-level forces)

$I_e = 1.0$ (importance factor)

$$\delta_{M-diaph} = \frac{C_d \delta_{max}}{I_e} = \frac{4.5(6.48)}{1} = 29.2\ in$$

The computed elastic deflection (δ_{max}) of the diaphragm allows one to estimate the period of the diaphragm using Wilson's shear beam formula (Equation 1) as a guide. In this instance, the result can be approximated as $T_{diaph} = (0.066\delta_{max})^{0.5}$ where δ_{max} is based on 1.0g of acceleration, and results in a period significantly larger than the 0.800 seconds. At this time, this alternative design procedure is based upon using $T_{diaph} = 0.002L$ for wood structural panel diaphragms, and a larger period computed by other methods is not permitted for design.

6.2 Deflection of North/South Walls

It is anticipated that the diaphragm deflection will be the majority of the overall structural deformation; however, shear wall deflection should be added to the diaphragm deflection to obtain the total deformation used to evaluate its impact. The deflection of a cantilever shear wall has two components: a flexural component and a shear component from the following equation.

$$\delta_{wall} = \delta_{wall\ flexure} + \delta_{wall\ shear}$$

$$\delta_{wall} = \frac{Ph^3}{3EI} + \frac{1.2Ph}{GA}$$

The adjusted load onto the shear wall was computed in Section 5.10 as 440 kips, but a portion of this was from the diaphragm acting at the roof (F_{v1} = 248.4 kips), and a portion was from the wall's self-weight effectively acting at the mid-height (F_{v2} = 191.4 kips). One approach to approximate the combined effect of these two forces is to place half the wall force at the roof height with the diaphragm force.

$$P = 248.4 + \frac{191.4}{2} = 344\ kips$$

$$h = 30\ ft$$

The material properties and section properties are computed for the eight 25-ft long concrete shear walls (9¼" thick, f'_c = 4000 psi)

$$E = 57\sqrt{f_c'} = 57\sqrt{4000} = 3.6\times10^3\ ksi$$

$$G = \frac{E}{2(1+\nu)} = \frac{3.6\times10^3}{2(1+0.2)} = 1.50\times10^3\ ksi$$

$$I_g = \frac{bh^3}{12} = \frac{9.25(25\times12)^3}{12}\times8\ walls = 166.5\times10^6\ in^4$$

$$A_g = bL = 9.25\ in(25\ ft\times12)\times8\ walls = 22{,}200\ in^2$$

The section properties I_g and A_g are for the gross section, but it is possible that the concrete members will crack, which will reduce the effective stiffness of the shear walls. ACI 318-11 Section 8.8.2(b) [ACI, 2011] gives some guidance on approximating the reduced stiffness to determine lateral deflections

in concrete members. More specifically, without a more accurate analysis, half the stiffness obtained from the gross section properties may be considered.

$$\delta_{wall} = \frac{Ph^3}{3E(0.5I_g)} + \frac{1.2Ph}{G(0.5A_g)}$$

$$\delta_{wall} = \frac{344(30\times12)^3}{3(3.6\times10^3)(0.5\times166.5\times10^6)} + \frac{1.2(344)(30\times12)}{1.5\times10^3(0.5\times22{,}200)}$$

$$\delta_{wall} = 0.018 + 0.009 = 0.027\ in$$

To properly estimate the shear walls' maximum expected deflection, the earlier effects of dividing by response modification coefficient, *R,* must be reversed, and this is accomplished with the use of the deflection amplification factor C_d. ASCE 7-10 Equation 12.12-1 (or 12.8-15) may be used to compute the maximum expected wall deflection $\delta_{M\text{-}wall}$.

$$\delta_{M-wall} = \frac{C_d\delta_{wall}}{I_e}$$

C_d = 4.0 (ASCE 7-10 Table 12.2-1)

δ_{wall} = 0.027 in (an elastic response under strength-level forces)

I = 1.0 (importance factor)

$$\delta_{M-wall} = \frac{C_d\delta_{wall}}{I} = \frac{4.0(0.027)}{1} = 0.11\ in$$

The total system displacement is the sum of the two deflection components.

$$\delta_M = \delta_{M-diaph} + \delta_{M-wall} = 29.2 + 0.11 = 29.3\ in$$

This is the total anticipated inelastic deformation during the design seismic forces. It is observed that the contribution from the shear walls is very small, and could have been neglected in this situation. One of the prime characteristics of RWFD buildings is that the diaphragm dominates the response of the building, and this is surely evident here.

6.3 Limits on Diaphragm Deflection – Deformation Compatibility

In order to prevent damage to attached structural elements or any non-structural elements and their attachments, the engineer should be familiar with the expected building deflection and whether portions of the building are compatible with that deformation. ASCE 7-10 Section 12.12.2 and SDPWS-2008 Section 4.2.1 both state the following in terms of maintaining structural integrity during diaphragm deflections:

> *"Permissible deflection shall be that deflection that will permit the diaphragm and any attached elements to maintain their structural integrity and continue to support their prescribed loads as determined by the applicable building code or standard."*

No prescriptive limits on deformation compatibility are given in either the 2012 IBC or the ASCE 7-10, instead it is left to the structural engineer's judgment.

RWFD buildings typically occur in masonry or concrete shear wall buildings, and thus the diaphragm deflection results in the columns and perpendicular walls rotating about their bases due to diaphragm translation at the top. This rotation is likely acceptable if the columns and walls were modeled with pinned bases during their individual design, even if some unintentional fixity exists.

Perimeter walls that have significant fixity at the base, often because they are anchored to the floor slab and foundation, should be evaluated as to their ability to yield and rotate at their base. The governing building codes for concrete and masonry slender wall design (ACI 318 and TMS 402) require these slender walls to be tension-controlled flexural members. This allows the walls to better accommodate any out-of-plane localize yielding at the base while continuing to carry vertical loads. The assumption of plastic hinges forming at the base of various elements prior to reaching the maximum displacement, δ_M, is acceptable provided that these hinges do not result in an unstable structural mechanism or a loss of vertical support.

6.4 Limits on Diaphragm Deflection – Second Order Effects and *P*-Δ Instability

One potential safety concern with large flexible diaphragms that have large deflections is the rise in second order effects including *P*-Δ instability. As the roof translates, the tops of columns and walls also translate, resulting in a leaning gravity system that generates additional lateral forces further exacerbating the deflection.

One simple method to evaluate this concern is through the stability coefficient, θ, of ASCE 7-10 Section 12.8.7. Although this stability coefficient, θ, was not originally intended to be used to evaluate diaphragm deformations, with some simple adjustments it is a useful tool to investigate the diaphragm system stability under *P*-Δ effects.

$$\theta = \frac{P_x \Delta I_e}{V_x h_{sx} C_d}$$ ASCE 7-10 Eq. 12.8-16

where

P_x = the vertical gravity load acting on the translating system, kips
Δ = the weighted average horizontal translation, inches
I_e = importance factor
V_x = the seismic shear force acting on the translating system under consideration, kips
h_{sx} = the height of the translating system under consideration, inches
C_d = the dynamic amplification factor. Because the overwhelming majority of the horizontal translation is from the diaphragm, this factor may be based on the diaphragm's C_d.

This equation evaluates the relative magnitude of the horizontal load added to the lateral force resisting system at the system's maximum expected deformation. An increase of 10% or less ($\theta \leq 0.10$) is considered tolerable under ASCE 7-10 without a more detailed investigation.

The vertical gravity load acting on the translating system, P_x, has a component from the roof weight, $P_{x\ roof}$, and a component from the wall weight, $P_{x\ wall}$. As indicated by the applicable load combinations, the roof live load is excluded from the weight of the translating roof system. Because the wall's center of mass between the roof and slab on ground is only translating approximately half of the roof's translation, the $P_{x\ wall}$ may be computed as the upper half of the wall plus any parapet. The load factors are 1.0 for this investigation.

$P_{x\ roof}$ = 12 psf (400 ft)(200 ft) = 960 kips

$$P_{x\ wall} = \frac{9.25\ in}{12}(150\ pcf)\left(\frac{30ft}{2} + 3ft\right)400ft(2\ sides) = 1{,}665\ kips$$

$P_x = P_{x\ roof} + P_{x\ wall}$ = 960 + 1,665 = 2625 kips

Δ = the average horizontal translation. A deflecting flexible diaphragm will approximate a parabolic shape, and thus the average translation of the roof and perpendicular walls will be two-thirds the maximum translation.

$$\Delta = \frac{2}{3}\delta_M = \frac{2}{3}(29.3\ in) = 19.5\ in$$

V_x = the seismic shear force acting on the translating system under consideration

$$V_x = 1104\ plf\ (400\ ft) = 442\ kips$$

h_{sx} = the height of the translating system under consideration

$$h_{sx} = 30\ ft \times 12 = 360\ in$$

$C_d = 4.5$

$$\theta = \frac{P_x \Delta I_e}{V_x h_{sx} C_d} = \frac{2625(19.5)1.0}{442(360)4.5} = 0.071\ \leq 0.10 \quad okay$$

Because the stability coefficient is less than 10%, the *P*-Δ effects on story shears, moments, and drifts need not be considered further.

It is worth mentioning here that diaphragm deflection is not included when evaluating the story drift limits of ASCE 7-10 Section 12.12.1. These limitations on building drift were developed primarily for the classic flexible frame system with a rigid diaphragm to prevent excessive distortion within the plane of the frame or shear wall. In masonry and concrete tilt-up buildings, the vertical elements deflect very little in-plane, with the bulk of translation occurring in the diaphragm. The story drift limits of the building code do not apply to the diaphragm deflection.

6.5 Limits on Diaphragm Deflection – Building Separations and Setbacks

Another diaphragm deflection limitation that must be investigated is building setbacks from property lines or adjacent buildings per ASCE 7-10 Section 12.12.3. For this investigation, the total δ_M is computed as the sum of the shear walls' in-plane drift and the diaphragm's in-plane deflection. However, the in-plane drift of the stiff concrete or masonry shear walls is usually insignificant compared with the diaphragm, and so is often ignored.

At property lines, the required building setback is δ_M. When evaluating two buildings on the same property, the required separation between those two buildings may be evaluated as the square-root-of-the-sum-of-the-squares (SRSS) of the two independent δ_M's per ASCE 7-10 Equation 12.12-2.

THIS PAGE INTENTIONALLY LEFT BLANK

Chapter 7 Comparison of Designs Using Current Practice and Alternate Design Procedure

This chapter presents a comparison of key design computations and results of the Chapter 3 design in accordance with current practice, compared to equivalent computations and results of the alternate design procedure presented in Chapter 5. A list of common design features is provided in Table 7.1, a comparison of the diaphragm designs is provided in Table 7.2, and a comparison of the shear wall designs is provided in Table 7.3. Comparison of design forces in Table 7.2 indicates that in general the alternate design procedure requires the diaphragm to be designed for lower forces. The exceptions are that the shear amplification for the north-south direction (transverse loading) results in essentially equivalent design force at the diaphragm edge and end 10% regions and that the shear amplification in the east-west direction (longitudinal loading) results in higher diaphragm design forces along the edge and end 10% regions. These observations are reflected in the nailing patterns that show that the alternate design procedure has less stringent nailing requirements in the interior of the diaphragm, the same nailing requirement in the zone along the east and west edges, and more stringent nailing along the mid length of the north and south edges.

Table 7.1 Common Features for Example Buildings

Diaphragm:	Wood structural panel diaphragm
Plan dimensions:	200 ft north-south x 400 ft east-west
Wall thickness:	9-1/4 in.
Wall height:	30 ft from slab on ground to diaphragm plus 3 ft tall parapet
Roof design dead load:	12 psf
Spectral parameters	S_{DS} = 1.0 and S_{D1} = 0.6
Seismic Design Category	D

Table 7.2 Comparison of Diaphragm Designs Using Current Practice and Alternate Design Procedure

Current Practice Design	**Alternate Design Procedure**
$R = 4$, $\Omega_o = 2.5$, and $C_d = 4$	$R_{diaph} = 4.5$, $\Omega_{o\ diaph} = 2.0$, and $C_{d\ diaph} = 4.5$
$T_a = C_T h_n^{3/4} = (0.02)30^{0.75} = 0.26$ seconds ASCE 7-10 Eq. 12.8-7	$T_{diaph} \quad 0.002(400ft) \quad 0.800\ sec$ $T_{walls} = \frac{0.0019}{\sqrt{0.176}} 30ft = 0.136\ sec$
$C_s = \frac{S_D}{R/I_e} = \frac{1.0}{4/1.0} = 0.25$	North-South

Current Practice Design	Alternate Design Procedure
	$C_s = \frac{S_{D1}}{T_{diaph}\left(R/I_e\right)} = \frac{0.6}{0.800\left(4.5/1.0\right)} = 0.167$ East-West $C_s = \frac{S_{DS}}{R_{Diaph}/I_e} = \frac{1.0}{4.5/1.0} = 0.222$
$F_p = 0.25w_p$	North-South: $F_p = 0.167w_p$ East-West: $F_p = 0.222w_p$
w_{NS} $1653plf$ $w_{EW} = 2253plf$	w_{NS} $1104plf$ $w_{EW} = 2000plf$
Unit shear at diaphragm edge: $v_{NS} = 1653\ plf$ $v_{EW} = 563\ plf$	Unit shear at diaphragm edge (amplified x 1.5): $v_{NS} = 1104\ plf\ (1656\ plf)$ $v_{EW} = 500\ plf\ (750\ plf)$
Diaphragm nailing pattern current practice from Figure 3.7	Diaphragm nailing pattern alternate design from Figure 5.5
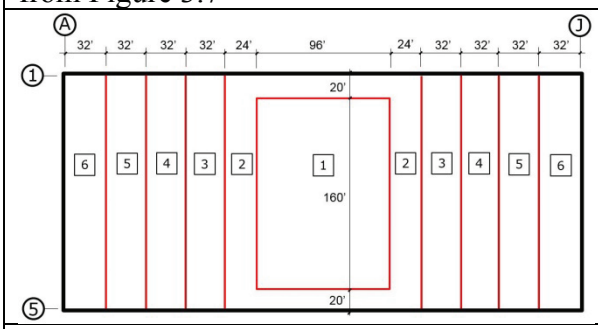	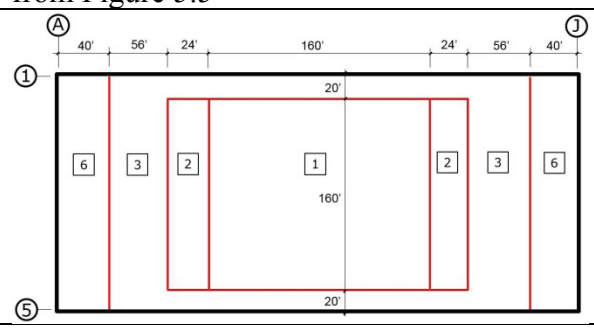
North-south diaphragm chords $A_{s\ required} = 5.10\ in^2$ L5x5x5/8 steel angle, As = 5.90 in^2 East-west diaphragm chords $A_{s\ required} = 0.87\ in^2$ L4x4x1/4 steel angle, As = 1.93 in^2	North-south diaphragm chords $A_{s\ required} = 3.41\ in^2$ L5x5x3/8 steel angle, As = 3.65 in^2 East-west diaphragm chords $A_{s\ required} = 0.77\ in^2$ L4x4x1/4 steel angle, As = 1.93 in^2

Table 7.3 Comparison of Shear Wall Design Forces Using Current Practice and Alternate Design Procedure

Current Practice Design	**Alternate Design Procedure**
$R = 4$, $\Omega_o = 2.5$, and $C_d = 4$	$R_{wall} = 4$, $\Omega_{o\ wall} = 2.5$, and $C_{d\ wall} = 4$
$T_a = C_T h_n^{3/4} = (0.02)30^{0.75} = 0.26$ seconds ASCE 7-10 Eq. 12.8-7	$T_{diaph} \quad 0.002(400ft) \quad 0.800\ sec$ $T_{walls} = \frac{0.0019}{\sqrt{0.176}} 30ft = 0.136\ sec$
$C_s = \frac{S_D}{R/I_e} = \frac{1.0}{4/1.0} = 0.25$	North-South $C_s = \frac{S_{DS}}{R_{wall}/I_e} = \frac{1.0}{(4/1.0)} = 0.25$ East-West $C_s = \frac{S_{DS}}{R_{wall}/I_e} = \frac{1.0}{4/1.0} = 0.25$
In-plane shear at base of shear walls: $V_{NS} = 552\ kips$ $V_{EW} = 608\ kips$	In-plane shear at base of shear walls: $V_{NS} = 440\ kips$ $V_{EW} = 608\ kips$

THIS PAGE INTENTIONALLY LEFT BLANK

Chapter 8 Future Studies for Design of RWFD Buildings

The investigation and modeling performed to develop the alternate design procedure assumed a rectangular building with solid walls. Additional studies would be valuable for bringing the design procedure described in this report into ASCE 7. The following discussion describes some additional work that would give greater insight into the design of these buildings.

8.1 Steel Deck Diaphragms

The design example provided in this report illustrated design of a wood structural panel diaphragm nailed to wood member. A similar approach might be applicable to a steel deck diaphragm; however, additional studies are needed to develop an appropriate response modification coefficient R, considering connector ductility and the system behavior in each orthogonal direction relative to the deck orientation.

In addition, the encouragement of spreading the inelastic behavior across greater portions of the diaphragm to improve margins against collapse needs additional study for the steel deck. This concept of spreading ductility needs a sufficient positive post-yield slope in the assembly behavior, and further studies are necessary to determine whether steel decking can satisfy this.

8.2 Out-of-Plane Top of Wall Anchorage Forces

The results of an out-of-plane wall study [Koliou 2014] indicate that the current wall anchorage provisions in ASCE 7-10 are likely adequate except the k_a term applicable to shorter diaphragm spans should be eliminated and the factor of 0.4 should become 0.8. The study also showed that there are corner affects that can occur. Additional studies should focus on the following:

1. Determine whether the out-of-plane design forces are large enough in situations where the diaphragm might remain elastic due to excess diaphragm strength provided to meet strength demands in the orthogonal direction.
2. Determine the forces on parapets, particularly taller parapets that are common at the front of big-box retail stores,
3. Determine whether top of wall anchorage near building corners needs to be designed for higher forces as discussed in Appendix J,
4. Determine whether there is a need to combine the design for out-of-plane wall forces with in-plane diaphragm shears,
5. Determine whether shears in a subdiaphragm should be combined with the main diaphragm shears.
6. Determine the effect of non-parallel (skewed) walls on out-of-plane wall forces.

Items 1, 2, and portions of 4 and 5 can be studied with the simplified numerical model developed for this project. Items 3, portions of 4 and 5, and 6 are best studied using three-dimensional nonlinear models. The portion of 4 that is best studied with a three dimensional nonlinear diaphragm model is determining how to combine the connector forces from out-of-plane wall anchorage for which the connection is expected to remain elastic and main diaphragm shears for which the connection is expected to become inelastic.

8.3 In-Plane Wall Yielding/Rocking

In this report, a procedure is presented for the common situation where the horizontal diaphragm is expected to yield prior to yield occurring in the vertical shear walls or braced frames. However, if a RWFD building is designed for the vertical elements of the seismic-force-resisting system to yield in-plane and the diaphragm to remain elastic, the nonlinear displacement demands on the vertical elements need to be established. The in-plane yielding of the walls can occur due to "frame" action of a wall panel with large openings, rocking of the wall, or yielding at wall-to-slab or wall-to-foundation shear transfer connections.

Although ASCE 7-10 has response modification coefficients for the wall systems that in theory account for wall yielding and rocking, the appropriateness of these values should be studied because they were set based on committee opinion rather than rigorous analyses. A disconnect exists because the same response modification coefficients have been used to date for wall systems with either rigid or flexible diaphragms even though the flexible diaphragms have the potential to increase inelastic displacement demand on the walls.

If the walls, geometry, and masses of two buildings are equal but one has a rigid diaphragm and the other has a flexible diaphragm, the building with the flexible diaphragm will have a greater spectral displacement than that for the building with a rigid diaphragm. For the elastic range of motion, displacements occur in both the diaphragm and the walls. Once the walls yield, the displacement contribution of the diaphragm will be limited to the displacement associated with the overstrength of the wall system. At accelerations greater than that associated with the wall overstrength, the displacement will increase in the wall system but not the diaphragm. This has the potential to drive additional nonlinear displacements into the wall system relative to the building with a completely rigid diaphragm. The displacement demands on the vertical elements of the seismic-force-resisting system can be studied using the simplified numerical model developed in conjunction with this project.

8.4 Irregular Plan Shapes and Abrupt Changes along Exterior Walls

RWFD often have re-entrant corners and other abrupt changes in geometry. For example, small wall pop-outs of about 3-ft provide architectural relief for long walls. The effect of re-entrant corners, small wall pop-outs, and other abrupt changes would benefit from a study that looks at how these conditions

affect forces acting on nearby diaphragm connectors and the effect on diaphragm chords and collectors. These issues are best studied with three-dimensional models.

8.5 Combining Connector Forces from Shear Acting in Two Orthogonal Directions

Diaphragm shears from two orthogonal directions both load a diaphragm connector. ASCE 7-10 does not require that connectors be designed for forces from orthogonal shears acting simultaneously. A study using three-dimensional nonlinear response models of diaphragms with individual diaphragm connectors modeled could be used to determine if these forces should be combined at the connector level. If so, then the models could be used to study how best to combine the forces.

8.6 Forces on Continuity Ties

Steel deck panels often serve as the wall anchorage continuity ties in the direction that the deck spans. At end laps continuity tie forces are transferred through the framing connectors that attach the ends of deck panels to one another and to the support framing. These same connectors resist shear forces from the main diaphragm shear. Clarification of how exactly to combine forces to the connectors from the diaphragm shear and continuity tie forces would be beneficial.

8.7 Three-Dimensional Modeling Calibrated to the Response of Buildings and Tests

Several instrumented RWFD buildings have been exposed to strong ground shaking, and several nonlinear response analyses by others have been performed in an attempt to replicate the measured response. Several of these analyses have been relatively successful, but more detailed models that include individual nonlinear connector response would be useful. Most, if not all, of the instrumented RWFD buildings have wood diaphragms. For RWFD buildings with steel deck, there is no response data with strong motions. For steel deck diaphragms, a three-dimensional model could be compared to the approximately 70-ft long diaphragms tested by Massarelli, et al [Massarelli, et. al, 2012]. Also, instrumentation of additional RWFD buildings including ones with wood diaphragms and ones with steel deck diaphragms is desirable.

8.8 Deflection of Wood Diaphragms

A simple means of computing or estimating the diaphragm deflection could likely be obtained from the analysis results performed to date. In comparison to the analyses of the archetypes, deflections computed in accordance with the 2008 SDPWS appear to overestimate diaphragm displacement. Although overestimating deflection is conservative for computing second order effects and building separations, it would be unconservative if one used it to compute a period and used that period to determine design forces. This is the reason that in Section 6.1, the estimated period of the diaphragm

using Wilson's shear beam formula (Equation 1, $T_{diaph} = (0.066\delta_{max})^{0.5}$ where δ_{max} is based on 1.0g of acceleration), which is more than $T_{diaph} = 0.002L$ for wood structural panel diaphragms, or other means of computing the period should not be used to determine design forces. The data from the archetype analyses could be studied to develop a means of estimating the diaphragm displacement at the design level and maximum considered earthquakes. The results could be compared to analysis results of the three-dimensional model described in Section 8.7.

8.9 Applicability to Buildings with Lightweight Enclosures and Steel Bracing

The archetypes developed in conjunction with this project were selected to represent typical RWFD buildings in the United States. It is recognized that the alternate design methodology may apply to other systems not necessarily modeled, such as stiff braced frame buildings with steel stud and/or steel siding envelopes. It would be beneficial to conduct further studies with these other building types to better evaluate their performance under this alternate design procedure. Many of the concepts of the alternate procedure are expected to be relevant; however, the lightweight wall typically used with braced frames may require a period equation different than the period equation presented in this report. Also, the significant difference in mass due to the lightweight walls may lead to different behavior than that of the archetypes modeled in the studies that led to the alternate design procedure.

8.10 Applicability to Multi-Story Buildings

The principles discussed under this design methodology could also be transferred to certain multi-story buildings, but with caution. Often two-story tilt-up concrete or masonry buildings are built with large flexible diaphragms, and their behavior may be similar to that modeled under this project. Higher mode shapes and interaction between the two diaphragms remain a concern and should be studied further before extrapolating this alternate design procedure to multiple stories.

8.11 Implications of Diaphragm Deflections on Structural and Nonstructural Elements

Buildings with large flexible diaphragms can experience portions of the building displacing significant distances horizontally compared with buildings with rigid diaphragms. In buildings with rigid diaphragms, the diaphragm's horizontal displacement is likely only a little larger than the supporting frame or shear wall system; and the drift of these supporting SFRS's is limited by ASCE 7-10. Therefore, internal horizontal displacements of the rigid diaphragms are indirectly controlled.

However, the limitations on flexible diaphragm displacements are less prescriptive than the drift limits for the SFRS, relying much upon the engineer's judgment of deformation compatibility discussed in Section 6.3. Furthermore as demonstrated in Section 6.4, investigating second-order effects (P-Δ) due to

large diaphragm displacements involves modifying existing code provisions not originally intended for horizontal diaphragms usage.

While the mainstay of RWFD buildings has traditionally been warehouse shells, their use in office buildings or commercial retailing with numerous tenant improvements and partitions has become very common. The susceptibility of these two different building inventories to damage due to large displacements is quite different, and limitations will likely be warranted.

8.12 Large-Scale Diaphragm Tests

Large-scale cyclically loaded diaphragm tests or diaphragms tests for response to earthquake records could be performed to better understand the behavior of flexible diaphragms. Tests are desirable for both wood and steel deck diaphragms. The effect of connection ductility on global diaphragm ductility could be explored along with means of improving the spread of ductility. The location of first yield and how to control this location could also be explored. Deformation compatibility issues could also be explored along with the diaphragm tests though focused sub-assemblage tests are likely also needed.

THIS PAGE INTENTIONALLY LEFT BLANK

Chapter 9 Conclusions

This report has presented an alternate procedure to design single-story RWFD buildings with wood structural panel diaphragms within the existing framework of the current 2012 IBC and ASCE 7-10. The alternate design procedure presented is relatively simple to implement and is based on yielding and energy dissipation in the diaphragm rather than yielding, rocking, or sliding of the walls. FEMA P695 based analytical studies have demonstrated improved seismic performance of buildings designed using the alternate procedure, beyond the seismic performance anticipated using currently adopted seismic design provisions.

The flow of goods and the sale of goods in the United States is heavily dependent upon RWFD buildings. Big box retail stores and logistical storage facilities can be at risk if the building code provisions that govern seismic design do not appropriately address how earthquakes affect them. With this disconnect between the intent of the provisions and the behavior of these buildings, difficulty exists in evaluating this building stock for seismic vulnerabilities. The alternate procedure presented in this report is intended to fill this gap.

At this time, the alternate seismic design procedure is not adopted by a building code or included in ASCE 7-10. Designs using this alternate design procedure may not comply with IBC 2012 and ASCE 7-10. For an existing building, using this procedure may not result in a building that complies with ASCE 41-13. For new buildings the Alternate Materials and Methods of Construction of ASCE 7-10 Section 11.1.4, could be used but would require approval from the authority having jurisdiction. Although strictly following the alternative design procedure may not meet current code, the principles could be applied to a building that meets current code by modifying the procedure to include strengthening above current code requirements in the end zones (amplified shear boundary zones) without including reduction of the design forces in the other areas of the diaphragm.

A version of the alternate design procedure presented herein has been adopted by the 2015 NEHRP Provisions [FEMA, 2015] as a Part 3 resource paper. Eventually, this procedure or a version of it will be proposed as a change to a future edition of ASCE 7. It was not brought forward in the current standard update cycle in order to allow designers of these buildings to gain trial experience with the procedure, and so that relevant issues as discussed in Chapter 8 could be further discussed.

Recommendations for future study and research are provided in Chapter 8. The intention of including these recommendations is to provide focus to future studies and research so it directly benefits development of design provisions for RWFD buildings.

THIS PAGE INTENTIONALLY LEFT BLANK

References

ACI, 2011. *Building Code Requirements for Structural Concrete,* ACI 318-11, American Concrete Institute (ACI), Farmington Hills, MI.

ACI Committee 551, 2010. *Design Guide for Tilt-Up Concrete Panels* (ACI 551.2R-10), Tilt-Up Concrete Technical Committee, American Concrete Institute (ACI), Farmington Hills, MI.

ASCE, 2010. *Minimum Design Loads for Buildings and Other Structures* (ASCE 7-10). American Society of Civil Engineers, Reston, VA.

ASCE, 2013. *Seismic Evaluation and Retrofit of Existing Buildings* (ASCE 41-13). American Society of Civil Engineers, Reston, VA.

AWC, 2008. *Special Design Provisions for Wind and Seismic* (SDPWS)*,* American Wood Council, Leesburg, Virginia.

Brandow, G.E., 2010. SEI Case Study: Large Retail Building, Yucca Valley, California, Structural Engineering Institute, Reston, VA. http://www.asce.org/uploadedFiles/sei/Certification/KMARTCaseStudy.pdf

Bouwkamp, J.B., Hamburger, R.O., Gillengerten, J.D., 1994. "Degradation of Plywood Roof Diaphragms Under Multiple Earthquake Loading," Data Utilization Report CSMIP/94-02, California Strong Motion Instrumentation Program, February 1994.

Carr, J., 2007. RUAUMOKO, University of Canterbury.

Celebi, M., Bongiovanni, G., Safak, E., Brady, A.G., 1989. "Seismic Response of a Large-Span Roof Diaphragm," Earthquake Spectra, Vol. 5, No. 2, 1989.

Christovasilis, I. P., Filiatrault, A., and Wanitkorkul, A., 2009. "Seismic Testing of a Full-Scale Two-Story Light-Frame Wood Building: NEESWOOD Benchmark Test." Technical Report MCEER-09-0005.

Coyne, T., 2007. "UB-REU student project."

EERI, 1985. "The Morgan Hill Earthquake of April 24, 1984," *Earthquake Spectra*. Volume 1, Number 3, Earthquake Engineering Research Institute, Berkeley, CA.

EERI, 1988. "The Whittier Narrow Earthquake of October 1, 1987," *Earthquake Spectra*. Volume 4, Number 2, Earthquake Engineering Research Institute, El Cerrito, California.

FEMA, 2009. *Quantification of Building Seismic Performance Factors* (FEMA P695). Federal Emergency Management Agency, Washinghton, DC.

FEMA, 2011. *Quantification of Building Performance Factors: Component Equivalency Methodology* (FEMA P795). Federal Emergency Management Agency, Washington, DC.

FEMA, 2015. *NEHRP Recommended Seismic Provisions for New Buildings and Other Structures*, FEMA P-1050, prepared for FEMA by the Building Seismic Safety Council of the National Institute of Building Sciences. Federal Emergency Management Agency, Washington, D.C.

Folz, B., and Filiatrault, A., 2001. "Cyclic analysis of wood shear walls." Journal of Structural Engineering, 127(4), 433-441.

Fonseca, F. S., S.K., R., and Campbell, S. H., 2002. "Nail, Wood Screw, and Staple Fastener Connections." CUREE Publication No. W-16.

Freeman, S.A., Gilmartin, U.A., and Searer, G.R., 1995. Tilt-up Construction: Proposed Seismic Design Procedures Developed from Strong Motion Research. In Proceedings of the NEHRP Conference and Workshop on Research on the Northridge, California Earthquake of January 17, 1994. Richmond, CA: Consortium of Universities for Research in Earthquake Engineering.

Freeman, S, Searer, G, and Gilmartin, U, 2002. "Proposed Seismic Design Provisions for Rigid Shear Wall / Flexible Diaphragm Structures," *Proceedings of the Seventh U.S. National Conference on Earthquake Engineering* (7NCEE). Earthquake Engineering Research Institute, Oakland, CA.

Guenfoud, N., Tremblay, R., Rogers, C.A., 2010. "Shear Capacity and Tension Capacity of Arc-Spot Welds for Multi-Overlap Deck Panels," Journal of Constructional Steel Research 66 (2010) 1018-1029.

ICBO, 1988. *Uniform Building Code*, 1988 Edition, International Conference of Building Officials, Whittier, CA.

ICBO, 1997. *Uniform Building Code*, 1997 Edition, International Conference of Building Officials, Whittier, CA.

ICC, 2012. *International Building Code*. International Code Council, Country Club Hills, IL.

Koliou M, 2014. *Seismic Analysis and Design of Rigid Wall - Flexible Diaphragm Structures* [Ph.D.]. University at Buffalo - The State University of New York; Buffalo, NY.

Koliou, M., Filiatrault, A., Kelly, D.J. and Lawson, J., 2014. "Distributed Yielding Concept for Improved Seismic Collapse Performance of Rigid Wall-Flexible Diaphragm Buildings", ASCE Journal of Structural Engineering (Under Review).

Lawson J, 2013. *Seismic Design of Timber Panelized Roof Structures.* WoodWorks, Wood Products Council, Washington DC.

Massarelli R, Franquet J, Shrestha K, Tremblay R, and Rogers C, 2012. "Seismic Testing and Retrofit of Steel Deck Roof Diaphragms for Building Structures," *Thin-Walled Structures*, Volume 61, Elsevier, Philadelphia, PA.

MATLAB version 8.10.1.604 Natick, 2013. The MathWorks Inc, Massachusetts.

Mays T, and Steinbicker J, 2013. *Engineering Tilt-Up*, Tilt-Up Concrete Association, Mount Vernon, IA

Newmark, N.M. and Hall, W.J., 1973. "Seismic design criteria for nuclear reactor facilities," Building Practices for Disaster Mitigation, Report No. 46, National Bureau of Standards, U.S. Department of Commerce.

NIST, 2004, *Voluntary Product Standard PS 2-04*, *Performance Standard for Wood-Based Structural-Use Panels*, United States Department of Commerce, National Institute of Standards and Technology, Gaithersburg, MD, 2004

NOAA, 1973. *San Fernando, California, Earthquake of February 9, 1971*, Volume I. National Oceanic and Atmospheric Administration, United States Department of Commerce, Washington DC.

NRC, 1973. *The Great Alaska Earthquake of 1964*, National Research Council: Committee on the Alaska Earthquake, National Academy of Sciences, Washington DC.

Olund, O., 2009. "Analytical Study to Investigate the Seismic Performance of Single Story Tilt-Up Structures." Master of Applied Science, University of British Columbia, British Columbia, Canada.

PEER, 2004. *Evaluation and Application of Concrete Tilt-up Assessment Methodologies* (PEER Lifelines Task 509), Degenkolb Engineers, San Francisco, CA.

Phipps M, and Jirsa J, 1990. "Performance of Industrial Facilities and Implications for Design of New Structures and Upgrading of Existing Hazardous Buildings," *Proceedings: Putting the Pieces Together – The Loma Prieta Earthquake One Year Later,* Bay Area Regional Earthquake Preparedness Project (BAREPP), San Francisco.

Rogers, C.A., Tremblay, R., 2003a. "Inelastic Seismic Response of Frame Fasteners for Steel Roof Deck Diaphragms," Journal of Structural Engineering, American Society of Civil Engineers, December 2003.

Rogers, C. A., and Tremblay, R., 2003b. "Inelastic Seismic Response of Side Lap Fasteners for Steel Roof Deck Diaphragms." Journal of Structural Engineering, 129(12), 1637-1646.

SDI, 2004. *Steel Deck Institute Diaphragm Design Manual* (DDM03), Steel Deck Institute.

SEAOC, 2008. "Tilt-up Buildings" The SEAOC Blue Book: Seismic Design Recommendations, Structural Engineers Association of California, 2008.

SEAOC, 2010. 2009 IEBC Structural/Seismic Design Manual: Existing Building Seismic Hazard Reduction Design Examples, Structural Engineers Association of California, 2010.

SEAOC Seismology Committee, 1999. *Recommended Lateral Force Requirements and Commentary – 7th edition,* Structural Engineers Association of California, Sacramento, CA.

SEAONC, 2001. Guidelines for Seismic Evaluation and Rehabilitation of Tilt-Up Buildings and Other Rigid Wall/Flexible Diaphragm Structures, Structural Engineers Association of Northern California, San Francisco, CA and International Conference of Building Officials (ICBO).

Shipp J, 2010. "Case Studies – Documentation to Support a Separate Structural Engineering Practice Act." Structures Congress 2010, Structural Engineering Institute, ASCE. http://www.asce.org/uploadedFiles/sei/Certification/CaseStudies16Dec09.pdf

SSC, 1995. *Northridge Earthquake, Turning Loss to Gain*, SSC Report No. 95-01. Seismic Safety Commission, State of California, Sacramento, CA.

Stewart, W. G., (1987), "The Seismic Design of Plywood Sheathed Shear Walls." Ph.D. Dissertation, University of Canterbury, Christchurch, New Zealand.

Tremblay, R., Martin, E., and Yang, W., 2004. "Analysis, Testing and Design of Steel Roof Deck Diaphragms for Ductile Earthquake Resistance." Journal of Earthquake Engineering, 8(5), 775-816.

Vamvatsikos, D., and Cornell, A. C., 2002. "Incremental Dynamic Analysis." Earthquake Engineering and Structural Dynamics, 31, 491-514.

Wilson A, Quenneville P, and Ingham J, 2013. "Natural Period and Seismic Idealization of Flexible Timber Diaphragms." *Earthquake Spectra*, Volume 29, Number 3, Earthquake Engineering Research Institute, Oakland, CA.

APPENDIX A Alternate Design Procedure Discussion and Commentary

An alternate procedure for design of rigid wall-flexible diaphragm buildings for earthquake effects is proposed in Section 4.5 of this report. When using this procedure, diaphragm yielding is expected. The alternate procedure requires proportionally strengthened end regions of the diaphragm, which encourages the spread of yielding within the diaphragm as described in Section A.4. The alternate procedure is based on the results of a study in which the performance of archetype buildings was improved by weakening the diaphragm away from the end region Koliou, et al. (2014). At this time, the alternate design procedure is meant to apply to RWFD buildings with wood structural panel diaphragms nailed to wood framing.

The alternate design procedure is one of three design paths applicable to buildings with rigid walls and flexible diaphragms. The three design paths are:

1. Yielding and energy dissipation of a ductile diaphragm is expected with the walls remaining essentially elastic,

2. Yielding and energy dissipation of the vertical elements is expected with the diaphragm remaining essentially elastic, and

3. The location of yielding and energy dissipation is not specifically determined and may occur in either the diaphragm or walls, or both.

In this report, only Path 1 is addressed. Path 2 is difficult to achieve because of the inherent in-plane strength and stiffness of the walls relative to the strength and stiffness of the diaphragm. Path 3 could have design requirements based on the equivalent lateral force procedure and a two-stage approach similar to that proposed for Path 1. However, a response modification coefficient applicable to the diaphragm, R_{diaph}, is likely required in the range of 2 to 3.5. This is based on fewer restrictions on diaphragm geometry than Path 1 and a projection of the results of the analyses of diaphragms with only one nailing pattern throughout as presented in Appendix K. Path 3 would require confirmation analyses. An engineer would choose the design path based on the expected behavior of the diaphragm relative to the wall. At this time, only Path 1 is fully developed, so the remainder of this Appendix only addresses Path 1.

A.1 Commentary on Alternate Design Procedure with Diaphragm Yielding

Two-stage analysis procedure: RWFD buildings with the flexible diaphragm supported by much stiffer perimeter walls are similar to podium buildings for which a flexible wood framed upper structure is supported by a much stiffer podium structure of reinforced concrete with concrete or masonry shear walls. The two-stage analysis procedure of Section 12.2.3.2 of ASCE 7-10, is often used to design podium structures. The alternate design procedure proposed in Section 4.5 of this report is a two-stage analysis procedure: first, design the diaphragm using its own period, response modification coefficient

and detailing rules, and second, design the vertical elements using the existing design provisions of ASCE 7-10 with minor modifications.

The listed commentary statements below match the alternate design procedure steps presented in Section 4.5.

C.1 **Response modification coefficient:** A response modification coefficient for the diaphragm was determined based on a FEMA P695 evaluation of the alternate procedure. The evaluation is described in Appendix G, Archetype building types are described in Appendix H, and the analysis results are presented in Appendix I.

C.2 **Period for the wood diaphragm:** The formula for the wood diaphragm is obtained from Appendix D, Section D.3. It is based on diaphragms designed for high-seismicity using the current design procedure and was confirmed to be valid with this alternate procedure at all seismic hazard levels. The formula yields a shorter period than would be obtained for diaphragms designed for moderate seismicity so it can conservatively be applied to all levels of seismicity. The period of the diaphragm alone, i.e. without the period lengthening effect of including wall flexibility, is used rather than the total building period to be conservative in picking the spectral acceleration for the diaphragm design. The analyses demonstrated that the diaphragm periods were substantially independent of diaphragm depth. Alternate procedures that compute a diaphragm period that is longer than the period obtained from the proposed equation should not be used.

C.3 **Seismic response coefficient, C_s:** The seismic response coefficient is determined in accordance with the equivalent lateral force procedure in Section 12.8.1 of ASCE 7-10 but using R_{diaph} in place of R and T_{diaph} in place of T_a. For large diaphragm spans, T_{diaph} is typically longer than T_a computed in accordance with Eq. 12.8-7 of ASCE 7-10 and will often be longer than the transition period, T_s, resulting in spectral accelerations that are in the constant velocity portion of the design spectrum.

C.4 **Diaphragm design shears:** In general, diaphragm design shears are less than those computed using the current practice for intermediate precast concrete shear wall buildings, except along the 10% edge regions of the diaphragm.

C.5 **Shear amplification in edge regions:** Diaphragm design shears are increased by an amplification factor of 1.5 for the end 10% of the diaphragm span length (amplified shear boundary zone). This is shown in Figure A1. The value of 1.5 was confirmed with the analyses presented in Appendices G, H and I.

C.6 **Diaphragm Chords:** The diaphragm chords required with this alternate design procedure are generally smaller than those designed using current practice because the seismic response coefficient, C_s, is generally lower for the alternate design procedure.

C.7 **Collectors:** The design of collectors and their connections for buildings assigned to SDC C and higher requires that the collected force be amplified by an overstrength factor. The diaphragm overstrength factor, $\Omega_{o\ diaph}$, should be used rather than the wall overstrength factor because the diaphragm rather than the walls limit the strength of the system.

C.8 **Vertical elements of the SFRS:** The vertical elements of the SFRS, i.e., shear walls, are designed as Stage 2 of the two-stage analysis procedure. Forces from the diaphragm are amplified by the ratio $(R_{diaph}/\rho_{diaph})/(R_{wall}/\rho_{wall})$ as they are applied to the walls. This is similar to the requirement of Item d of the Two-Stage Analysis Procedure in Section 12.2.3.2 of ASCE 7-10. The response modification coefficient, R, is assigned the value for the type of vertical system being engineered but not greater than R_{diaph} to ensure that the diaphragm will yield first. The approximate period for the walls is computed using ASCE 7-10 Equation 12.8-9 for the walls. This formula typically results in a period that is less than that computed using ASCE 7-10 Equation 12.8-7. This results in design forces for wall mass based on a spectral acceleration that is almost always on the plateau of the design spectrum, i.e. the constant acceleration portion of the design spectrum.

C.9 **Deflections:** Deflection computations are required to confirm that structural integrity of attached structural elements is maintained, attached or supported nonstructural items are not damaged to the point of causing falling hazards, and the structure does not pound against adjacent structures. For example, diaphragm deflection may cause prying at perimeter roof connections, as shown in Figure A2, and in current practice, this condition is not accounted for. Although study is required to determine how critical this is, it does demonstrate the type of concern that should be addressed. The elastic diaphragm deflection is amplified by a deflection amplification factor for the diaphragm, $C_{d\ diaph}$. The basis for $C_{d\ diaph} = 4.5$ is presented in Appendix G Section G.3.

C.10 **Second order/P-Δ effects:** Both diaphragm and wall deflections should be considered when checking for second-order or P-Δ effects. The diaphragm deflection component can be reduced to approximately two-thirds of the maximum diaphragm deflection because the diaphragm tributary seismic weight on average moves approximately two-thirds of the diaphragm deflection plus the deflection of the walls.

C.11 **Out-of-plane wall forces and out-of-plane top-of-wall anchorage forces:** Out-of-plane wall forces and out-of-plane wall anchorage are in accordance with current code requirements except as that k_a is set equal to 2 for all diaphragm spans. The basis for this change is described in Appendix J.

C.12 **Additional requirements.** As Discussed in Section 5.6, two additional design requirements apply to transfer of shear between the diaphragm and vertical element of the SFRS. First, the amplified unit shear stress (in plf) in the diaphragm end zone is to be used for design of the shear connection between the diaphragm and the vertical elements. Second, where wood structural panel sheathing is fastened directly to a wood ledger, the unit shear stress (in plf) is required to be further amplified by Ω_0.

C.13

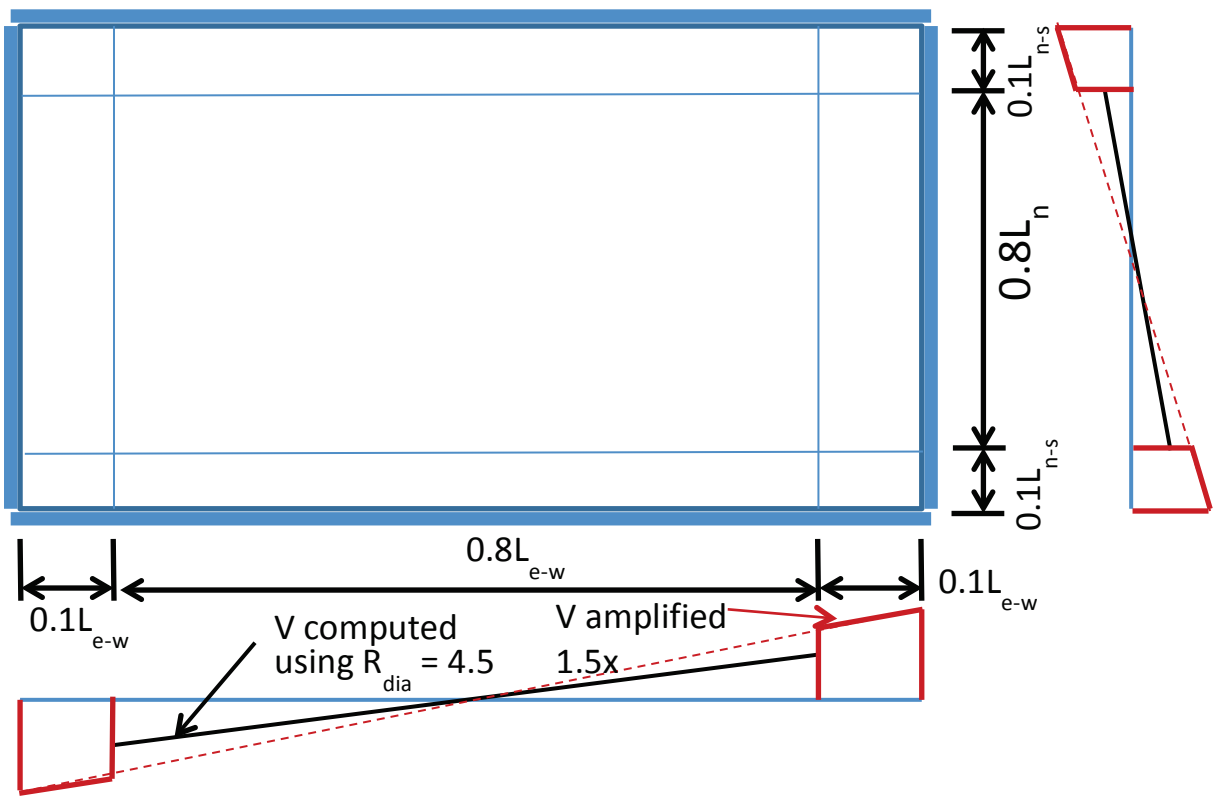

Figure A1. Amplified Shear Boundary Zones for the Alternate Procedure

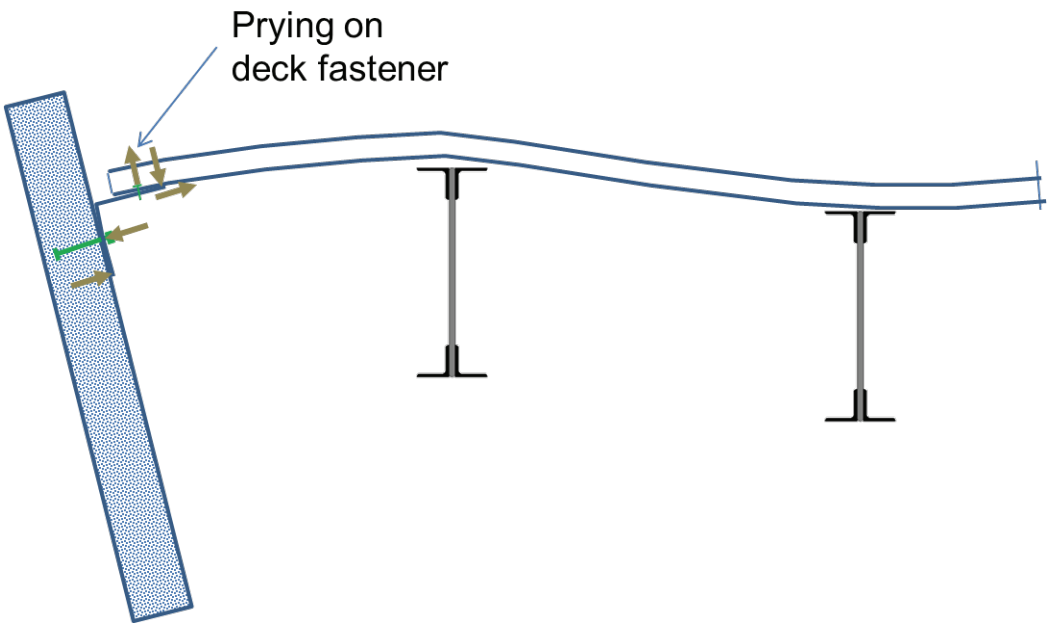

Figure A2. Deformations and Change in Angle between Roof Diaphragm and Wall

A.2 Limitations of the Alternate Design Procedure

The alternate design procedure is limited to one-story buildings whose plan geometry can be divided into self-supported rectangular diaphragm segments. Each diaphragm segment must be supported laterally on all four sides, i.e., this does not apply to diaphragms that cantilever or resist load in rotation, but can apply to multi-span diaphragm systems. The alternate procedure is not applicable to irregular-shaped diaphragms that are not devisable into rectangular sections because defining how to spread ductility in a non-rectangular diaphragm configuration is beyond the scope of the study reported in this report. For buildings with irregular configurations or as an alternative for rectangular-shaped diaphragms, a design procedure in which R_{diaph} on the order of 2 to 3.5 is used without strengthened edges, Design Path 3 listed in Section A.1 might be appropriate but would require additional analyses to confirm the adequacy of such a procedure.

The alternate procedure is only applicable to diaphragms that will perform equivalent to the diaphragms studied to develop the alternate design procedure. For wood diaphragms, the connectors studied were common nails that connect the wood structural panels to wood framing members or nailers on steel framing. Steel deck diaphragms were also studied but as will be discussed in Section A.3, the alternate procedure should not be used for them at this time.

A.3 Applicability of Alternate Design Procedure to RWFD Buildings with Steel Deck Diaphragms

At this time the alternate design procedure is not intended to apply to RWFD buildings with steel deck diaphragms. There are several reasons for not recommending its use even though it has been studied (Koliou, 2014). Reasons include (1) test results of a large scale diaphragm show significantly less distribution of yielding than the analytical results show when loaded parallel to deck edges (Massarelli, et al., 2012), (2) steel deck diaphragms were never intended to be yielding elements as such design strengths are based on monotonic tests, (3) data for reverse cyclically loaded connections is sparse and missing for many commonly used deck gages, (4) the post-yield stiffness of connectors is positive for only a short deformation, 1 to 2 mm, (5) few reverse cyclically loaded diaphragm tests have been performed while FEMA P695 requires comprehensive test data, and (6) many diaphragms in high seismic regions are designed using proprietary sidelap connections for which no test data was available to include in the study. Additionally, the behavior of connectors simultaneously resisting forces from diaphragm shear for which ductile connector behavior is expected and forces from out-of-plane wall anchorage for which elastic connector behavior is expected must be understood. This issue will likely require design limitations that have yet to be identified.

Archetypes studied and reported by Koliou included 20 and 22 ga steel deck diaphragms with puddle welds, powder actuated fasteners and self-drilling screws for framing connectors. Sidelap connectors included in the study were button punches, self-drilling screws, and top seam welds. There is a potential that the alternate design procedure could be applied to 20 and 22 ga diaphragms with the connectors studied. However, the concern of yielding not spreading as reported by Massarelli, et al. (2012) for diaphragms loaded parallel to the direction that the deck sheets span must be understood and addressed. It could also be applied to new or proprietary connectors with positive post-yield stiffness to an acceptable deformation limit. Currently that limit is not known exactly but a value of 10 mm is likely sufficient.

Once a set of non-proprietary connections can be shown to result in acceptable diaphragm performance, additional connectors could be approved using the procedures of FEMA P795 (2011) *Quantification of Building Performance Factors: Component Equivalency Methodology*.

If the alternate design procedure were to be applicable to diaphragms with welded connections the weld quality must be consistent with the weld quality used for the cyclic testing that led to the applicability. Detailed welding requirements would be required as part of the procedure. Recommendations for welding are provided in Guenfoud, et al. (2010). The factors to control for arc-spot welds (puddle welds) are high current setting, electrode type (ASTM E6011), and proper welding technique. Recommendations are made to increase the welding times relative to those recommended in SDI Manual (2004) for 1/8 in. electrodes.

A.4 Discussion of Diaphragm Yielding

Use of the alternate procedure has the potential to provide improved diaphragm yielding relative to that of a diaphragm designed with current design procedures. However, the degree of improvement is dependent on how diaphragm shear strength is distributed for each design.

Diaphragm yielding spreads towards the center of the diaphragm span because of the post-yield strength characteristics of common nails used as connectors. Common nails connecting wood structural panels to wood framing or wooden nailers exhibit positive post-yield stiffness that results in substantial increases in strength above its yield strength. This strength gain above the yield strength allows higher forces and yielding to develop in the diaphragm in the direction toward the center of the diaphragm span.

The spread of yielding also depends on the nonlinear distribution of shears in the diaphragm. The degree to which the yielding spreads towards the diaphragm center depends on the distribution of diaphragm shears for a particular time-history and the changes in diaphragm nailing along the length of the diaphragm. A diaphragm with many nailing zones that approximately follow a linearly varying distribution of diaphragm shear strength will distribute yielding more than a diaphragm with fewer nailing zones between the amplified shear end regions.

A.5 Quality of Design, Construction and Inspection

Like many seismic-force-resisting systems, the effectiveness of the alternate design procedure will depend on how well the design requirements are met. Fortunately, the design requirements are relatively simple in comparison to many other systems. The main change from current design practice is how shear strength is proportioned along the diaphragm span. As described in Section A.4, improved distribution of yielding can be obtained by using multiple zones of diaphragm strength but the procedure is not dependent on providing multiple zones of yielding.

Diaphragm designs using the alternate design procedure are no more likely to be constructed improperly than current diaphragm designs. A common concern is the use of the wrong nailing patterns or wrong nail type. If this is a concern, inspection of the nailing pattern and type of nails should be included in the project inspection requirements or structural observation program. Special inspection is already a requirement for most diaphragms in SDC C and above and for high-load wood diaphragm designs utilizing Table 4.2B in the SDPWS in all SDCs.

A.6 Diaphragm Modifications and Deterioration

After initial construction, diaphragm strength can be affected by modifications and deterioration. The most common modification that reduces strength is adding openings through the diaphragm, which will reduce the strength approximately in proportion to the size of the openings in a line relative to the overall depth of the diaphragm. Large openings or many small ones can further reduce the strength and cause a concentration of deformations. This is also a concern with current practice, and is usually addressed by the engineer by adding extra diaphragm strength to offset the weakening from the penetrations [Lawson J, 2013]. Openings near the center of the diaphragm are likely to have little or no effect on performance. Openings at the transition between unamplified and amplified shears or close to this transition but towards the center of the diaphragm span will have a detrimental effect as this region is likely to have the greatest yielding. Openings within the amplified shear end regions are also likely to have a detrimental effect, particularly if they are near the diaphragm ends where weakening can result in a concentration of yielding at the diaphragm end.

Deterioration of a diaphragm can occur due to roof leaks or moisture condensation. These can lead to damage to wood structural panels and to corrosion of nails or steel deck diaphragms. Roof leak damage is usually concentrated at or near the diaphragm-to-wall connections and at openings through the diaphragm. Deterioration is a concern but it is no greater for the alternate design than it is for current practice.

A.7 Possible Code Provisions

12.2 STRUCTURAL SYSTEM SELECTION

12.2.1 Selection and Limitations

The basic lateral and vertical seismic force-resisting system shall conform to one of the types indicated in Table 12.2-1 or a combination of systems as permitted in Sections 12.2.2, 12.2.3, and 12.2.4. Each type is subdivided by the types of vertical elements used to resist lateral seismic forces. The structural systems used shall be in accordance with the structural system limitations and the limits on structural height, h_n, contained in Table 12.2-1. The appropriate response modification coefficient, R; overstrength factor, Ω_0; and the deflection amplification factor, C_d, indicated in Table 12.2-1 shall be used in determining the base shear, element design forces, and design story drift.

<u>Single-story buildings with a flexible wood structural panel diaphragm and reinforced-concrete or reinforced-masonry shear walls that meet the restrictions of 12.15.* are permitted to be designed using the two-stage analysis procedure of Section 12.15.</u>
Each selected seismic force-resisting system shall be designed and detailed in accordance with the specific requirements for the system as set forth in the applicable reference document listed in Table 12.2-1 and the additional requirements set forth in Chapter 14.

Seismic force-resisting systems not contained in Table 12.2-1 are permitted provided analytical and test data are submitted to the authority having jurisdiction for approval that establish their dynamic characteristics and demonstrate their lateral force resistance and energy dissipation capacity to be equivalent to the structural systems listed in Table 12.2-1 for equivalent values of response modification coefficient, R; overstrength factor, Ω_0; and deflection amplification factor, C_d.

The following is the proposed addition of Section 12.15 to ASCE 7-10. The content of this section is all new text so strikeout and underline formatting is not used.

12.15 TWO-STAGE DESIGN PROCEDURE SINGLE-STORY BUILDINGS WITH FLEXIBLE WOOD STRUCTURAL PANEL DIAPHRAGMS AND WITH A REINFORCED-CONCRETE OR REINFORCED-MASONRY SHEAR WALL SYSTEM

12.15.1 Restrictions

Single-story buildings with flexible wood structural panel diaphragms and with a reinforced-concrete or reinforced-masonry shear wall system shall be permitted to be designed in accordance with the Two-Stage Design Procedure of Section 12.15.2 to 12.15.* if the following restrictions are met.

1. The wood structural panel diaphragm is without rigid topping, and is designed with nail fasteners in conformance with the 2008 NDS Special Design Provisions for Wind and Seismic [AWC, 2008].
2. The vertical elements are intermediate or special reinforce concrete shear walls or special reinforced masonry shear walls.
3. The diaphragm is without horizontal structural irregularities except for Type 2 in accordance with Table 12.3-1.
4. The diaphragm can be divided into rectangular segments with lateral support at each edge.
5. The period of the diaphragm, T_{diaph}, computed in accordance with 12.15.2.2 is greater than or equal to 3 times the period of the wall system, T_{walls}, computed in accordance with 12.15.2.3.
6. $C_{s\ wall}$ falls on the plateau of the response spectrum.

12.15.2 Stage One – Diaphragm Design

12.15.2.1 Design Coefficients and Factors for Diaphragm

The diaphragm is assigned a response modification coefficient, R_{diaph} equal to 4.5, an overstrength factor, $\Omega_{o\ diaph}$, equal to 2, and a deflection amplification factor, C_d, equal to 4.5.

12.15.2.2 Diaphragm Period

1. The wood diaphragm period is determined using Eq. 12.15-1.

2. $$T_{diaph} = 0.002L_f \qquad (12.15\text{-}1)$$

3. where

4. L_f = the span, in feet, of the horizontal flexible diaphragm being considered; the span is measured between vertical elements that provide lateral support to the diaphragm in the direction being considered.

12.15.2.3 Diaphragm Design Force

Design forces for the diaphragm shall be computed in accordance with Sections 12.15.3.1 to 12.15.3.*.

12.15.2.3.1 Calculation of Seismic Response Coefficient

The seismic response coefficient, C_s, is determined in accordance with the equivalent lateral force procedure in Section 12.8.1 of ASCE 7-10 but using R_{diaph} in place of R and T_{diaph} in place of T.

12.15.2.3.2 In-plane Diaphragm Force

The in-plane diaphragm force shall be in accordance with Eq. 12.15-2.

$$F_p = C_s w_p \qquad (12.15\text{-}2)$$

where

F_p= the force acting on the diaphragm per unit length.

w_p= the tributary seismic weight applicable per unit length of diaphragm including the tributary weight of the out-of-plane walls.

12.15.2.3.3 Direction of Loading

The seismic design forces are permitted to be applied independently in each of two orthogonal directions and orthogonal interaction effects are permitted to be neglected.

12.15.2.3.4 Diaphragm Shears

The diaphragm design shear shall be computed using the force computed with Eq. 12.15-2. For shear design of the diaphragm, the design shears in the end 10% regions of the diaphragm span in each orthogonal direction shall be amplified 1.5 times.

12.15.2.3.5 Diaphragm Chords and Chord Forces

Diaphragm chords shall be located at opposite edges to resist the diaphragm's flexural forces.. Flexural moments in the diaphragm shall be computed using forces computed in accordance with Eq. 12.15-2. The chord axial force shall be determined assuming a force couple develops between the chords at opposite edges of the diaphragm segment.

12.15.2.3.6 Collector Elements and Their Connections

Collector elements shall be provided that are capable of transferring the seismic forces originating in other portions of the structure to the vertical wall elements providing the resistance to those forces. Structures assigned to Seismic Design Categories C through F shall be designed to resist the forces calculated using the seismic load effects including overstrength factor of Section 12.4.3 but using $\Omega_{o\ diaph}$ for the overstrength and using the seismic forces determined from Eq. 12.15-2.

12.15.3 Stage Two – Wall System Design

12.15.3.1 Design Coefficients and Factors for Shear Walls

A seismic force-resisting system that includes reinforced-concrete or reinforced-masonry shear walls and is listed in Table 12.2-1 shall be assigned seismic parameters in accordance with Section 12.2.1. The appropriate response modification coefficient, R, overstrength factor, Ω_o, and deflection amplification factor shall be in accordance with the value assigned in Table 12.2-1 except that R shall not be greater than R_{diaph}. The response modification coefficient, R, shall be referred to as R_{wall}, the overstrength factor, Ω_o, shall be referred to as $\Omega_{o\ wall}$, and the deflection amplification factor, C_d, shall be referred to as $C_{d\ wall}$. The detailing requirements and system limitations of Table 12.2-1 apply even though the R_{wall} may have been reduced to be less than or equal to R_{diaph}.

12.15.3.2 Period for Walls

The period of the wall system, T_{wall}, shall be computed assuming the diaphragm is rigid and using Eq. 12.8-9.

12.15.3.3 Design Force for Wall System

The vertical wall elements of the seismic force-resisting system shall be designed for in-plane forces using the equivalent lateral force procedure of Section 12.8 but with the force from the diaphragm amplified by $(R_{diaph}/\rho_{diaph})/(R_{wall}/\rho_{wall})$ but not less than 1.0, R_{wall} in place of R, and T_{wall} in place of T.

12.15.4 Deflections

12.15.4.1 Diaphragm Deflection

Elastic diaphragm deflection, $\delta_{e\ diaph}$, shall be computed using the force level, F_p, in Section 12.15.2.3.2. The maximum inelastic diaphragm deflection, δ_{diaph}, shall be computed using Eq. 12.15-3.

$$\delta_{diaph} = \frac{C_{d\ diaph}\delta_{e\ diaph}}{I_e} \qquad (12.15\text{-}3)$$

12.15.4.2 In-Plane Wall Deflection

Elastic in-plane wall deflection, $\delta_{e\ wall}$, shall be computed using the force level in Section 12.15.3.3. The maximum inelastic wall deflection, δ_{wall}, shall be computed using Eq. 12.15-4.

$$\delta_{wall} = \frac{C_{d\ wall}\delta_{e\ wall}}{I_e} \qquad (12.15\text{-}4)$$

12.15.4.3 P-Delta Effects

P-Δ effects on diaphragm shear shall be investigated in accordance with 12.8-7. The design story drift, Δ, shall equal two-thirds of the maximum diaphragm displacement δ_{diaph} computed in accordance with Eq. 12.15-3 plus the deflection of the wall system δ_{wall} computed in accordance with Eq. 12.15-4.

12.15.4.4 Deflection Limitation

The maximum inelastic deflection equal to the in-plane deflection of the diaphragm, δ_{diaph}, plus the in-plane deflection of the wall system, δ_{wall}, in the direction under consideration shall not exceed the permissible deflection of the attached elements. Permissible deflection shall be that deflection that will permit the attached element to maintain its structural integrity under the individual loading and continue to support the prescribed loads.

12.15.4.5 Structural Separation

Structural separations shall be computed in accordance with 12.12.3 except that the maximum inelastic response displacement , δ_M, shall be a combination of the diaphragm plus in-plane wall displacements ($\delta_{diaph} + \delta_{wall}$).

12.15.5 Structural Walls and Their Anchorage

The walls and their anchorages shall be designed in accordance with Section 12.11 except that k_a shall be assigned a value of 2.0 for all diaphragm span lengths.

APPENDIX B Evaluating RWFD Buildings Using FEMA P695 Methodology

The FEMA P695 methodology is used to reliably quantify building system performance and provide guidance in the selection of appropriate design criteria when ASCE 7-10 linear design methods are applied. The primary objectives of FEMA P695 are to obtain an acceptably low probability of collapse of the SFRS under maximum considered earthquake (MCE) ground motions, and to provide uniform protection against collapse across various structural systems. An appropriate P695 evaluation must use a representative nonlinear model that includes both detailed design information of the system as well as comprehensive test data on the post-yield performance of system components and subassemblies.

When using FEMA P695, a structural system and design methodology are evaluated through the use of collapse fragility curves. Incremental Dynamic Analyses (IDA) are conducted on a representative sample of nonlinear numerical building models that account for the range of the design space using a pre-determined ensemble of earthquake ground motions. Collapse fragility curves are then developed from the IDAs. The number of archetypes selected is based on building an appropriate representation of typical RWFD buildings including the range of variation reasonably expected and likely to affect performance. The archetypes are assigned to performance groups for the evaluation process.

Evaluations of archetypes are performed for seismicity levels being considered for a building system. For RWFD buildings archetypes are designed for high and moderate seismic risk. For the evaluations, high-seismic risk is defined as having design acceleration parameters S_{DS} equal to 1.0 and S_{D1} equal to 0.60. These acceleration parameters are used for the SDC D_{max} evaluation in accordance with FEMA P695. Moderate-seismic risk is defined as having design acceleration parameters S_{DS} equal to 0.499 and S_{D1} equal to 0.199, which are the boundary values for SDCs C and D and is referred to SDC C_{max} for the evaluations.

For this study, the FEMA P695 Far Field Ground Motion Set (FEMA P695, 2009) was used. This set contains twenty-two historical ground motions listed in the table below from all over the world with two horizontal components each recorded at the same station. This results in
forty-four ground motion records to use to analyze each archetype. This ground motion ensemble is considered representative of the seismicity in the Western United States.

Table B1 – FEMA P695 Earthquake Ground Motion Ensemble

EQ. Index	Earthquake Event				Recording Station	PGA(g)*
	Name		Year	M_w		
	EQ_ID.	Earthquake				
1	12011	Northridge	1994	6.7	Beverly Hills – Mulhol	0.52
2	12012	Northridge	1994	6.7	Canyon Country–WLC	0.48
3	12041	Duzce, Turkey	1999	7.1	Bolu	0.82
4	12052	Hector Mine	1999	7.1	Hector	0.34
5	12061	Imperial Valley	1979	6.5	Delta	0.35
6	12062	Imperial Valley	1979	6.5	El Centro Array#11	0.38
7	12071	Kobe, Japan	1995	6.9	Nishi – Akashi	0.51
8	12072	Kobe, Japan	1995	6.9	Shin – Osaka	0.24
9	12081	Kocaeli, Turkey	1999	7.5	Duzce	0.36
10	12082	Kocaeli, Turkey	1999	7.5	Arcelik	0.22
11	12091	Landers	1992	7.3	Yermo Fire Station	0.24
12	12092	Landers	1992	7.3	Coolwater	0.42
13	12101	Loma Prieta	1989	6.9	Capitola	0.53
14	12102	Loma Prieta	1989	6.9	Gilroy Array#3	0.56
15	12111	Manjil, Iran	1990	7.4	Abbar	0.51
16	12121	Superstition Hills	1987	6.5	El Centro Imp. Co.	0.36
17	12122	Superstition Hills	1987	6.5	Poe Road (temp)	0.45
18	12132	Cape Mendocino	1992	7.0	Rio Dell Overpass	0.55
19	12141	Chi-Chi, Taiwan	1999	7.6	CHY 101	0.44
20	12142	Chi-Chi, Taiwan	1999	7.6	TCU045	0.51
21	12151	San Fernando	1971	6.6	LA – Hollywood Stor.	0.21
22	12171	Friuli, Italy	1976	6.5	Tolmezzo	0.35

The collapse margin ratio (CMR) is determined from the IDA and fragility curves. It is defined as the median spectral collapse intensity at the fundamental elastic period of the building archetype under analysis, $S_{CT}[T]$ obtained from nonlinear dynamic analyses divided by the ground motion spectral demand $S_{MT}[T]$ at the maximum considered earthquake (MCE) intensity level at the same fundamental elastic period. The collapse margin ratio is multiplied by a spectral shape factor (SSF) to obtain an adjusted collapse margin ratio (ACMR). The spectral shape factor is a function of the fundamental period, the period-based ductility, μ_T, and the applicable seismic design category of the archetype under analysis. The ACMR for both individual archetypes and the archetype performance groups are compared to acceptable ACMRs that account for uncertainties judged to be within the evaluation process. The acceptable ACMR for a performance group targets less than 10% probability of collapse in an MCE event, and the acceptable ACMR for individual archetypes targets less than 20% probability of collapse in an MCE event.

For this study, the acceptable ACMRs are computed using the uncertainty (beta) factors listed in Table B2. Note that the value for the design requirement uncertainty is based on an assumed improved design procedure so a larger value might be more appropriate for evaluating the current design procedure. The combined uncertainty, β_{Total}, is computed as the square root sum of the squares of the individual

uncertainties. For β_{Total} equal to 0.66, the acceptable ACMR is 1.73 and 2.30 for 20% and 10% probability of collapse at Maximum Considered Earthquake (MCE) ground motion, respectively. The acceptable ACMR applicable for the performance of individual archetypes is 1.73, and the acceptable ACMR of performance groups is 2.30.

Table B2. Beta factors for determining acceptable collapse margin ratios.

Description	Beta factor	Value of β
Record-to-record uncertainty	β_{TR}	0.40
Design requirements uncertainty	B_{DR}	0.20
Test data uncertainty	β_{TD}	0.35
Modeling uncertainty	B_{MDL}	0.35
Combined uncertainty	$\boldsymbol{\beta_{Total}}$	**0.66**

B.1 Modeling Framework

Large wood structural panel and steel deck diaphragms can have thousands of connectors. Yielding of these connectors is the primary means of obtaining ductility and dissipating energy. Although modeling the nonlinear behavior of all or many of these connectors in a detailed three-dimensional analysis would be the ideal means of evaluating RWFD systems, taking this approach is unrealistic at this time given the thousands of hours of computer run time it would require. For example, such a model took more than three hours to run one-half of a comparatively short record. Because the computer run time necessary to perform nonlinear response history analyses of detailed three dimensional models is too long, a modeling framework was developed that allows for a relatively simplified model to be used. The modeling framework developed to analyze RWFD buildings includes three steps as illustrated in Figure B1. These three steps are as follows:

1. Create a database of connectors that have been cyclically tested. Based on the test results, determine the hysteretic parameters of Wayne-Stewart (Stewart 1987) or SAWS (Folz and Filiatrault, 2001) nonlinear cyclic springs for each connector. A representation of the parameters for the Wayne-Stewart and SAWS springs are shown in Figure B2. Examples for nailed and welded framing connectors are illustrated in Figures B3 and B4.

2. Create a mathematical model in MATLAB of one-half of each archetype's diaphragm that accounts for the stiffness of the panels, diaphragm chords, and each diaphragm connector. Divide the diaphragm model into horizontal segments and load the diaphragm by a cyclic point load at its mid-span. Combine the response of the elements and connectors within each diaphragm segment to form a single nonlinear hysteretic spring that represents the cyclic response of the segment. This step is illustrated in Figure B5. Variable connector spacing is accounted for in this model.

3. Create a model in RUAUMOKO2D (Carr, 2007) that consists of one-half of the archetype and includes a spring and mass for each horizontal diaphragm segment, beam elements with nonlinear

hinges to represent the out-of-plane wall response, and springs and masses to represent the in-plane wall at the end of the diaphragm. A representation of the simplified model is shown in Figure B6. P-delta effects are incorporated into the model by applying the roof weight on leaning columns between the ground and the roof diaphragm. Localized effects that account for shear concentration in subdiaphragms, at corners, at openings, or at regions receiving wall anchorage forces are not accounted for in this analysis. This model also cannot account for loading from the two orthogonal directions acting simultaneously.

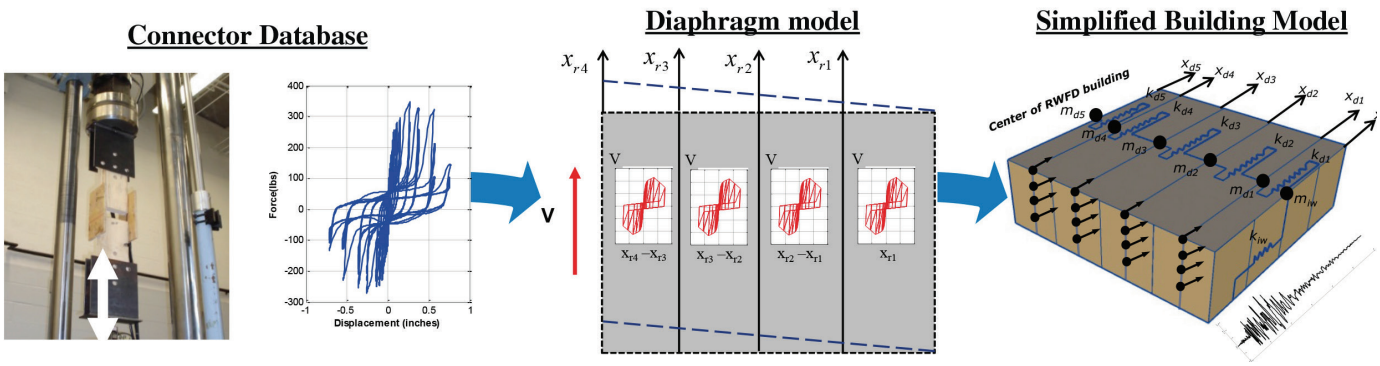

Figure B1. Three-step modeling framework.

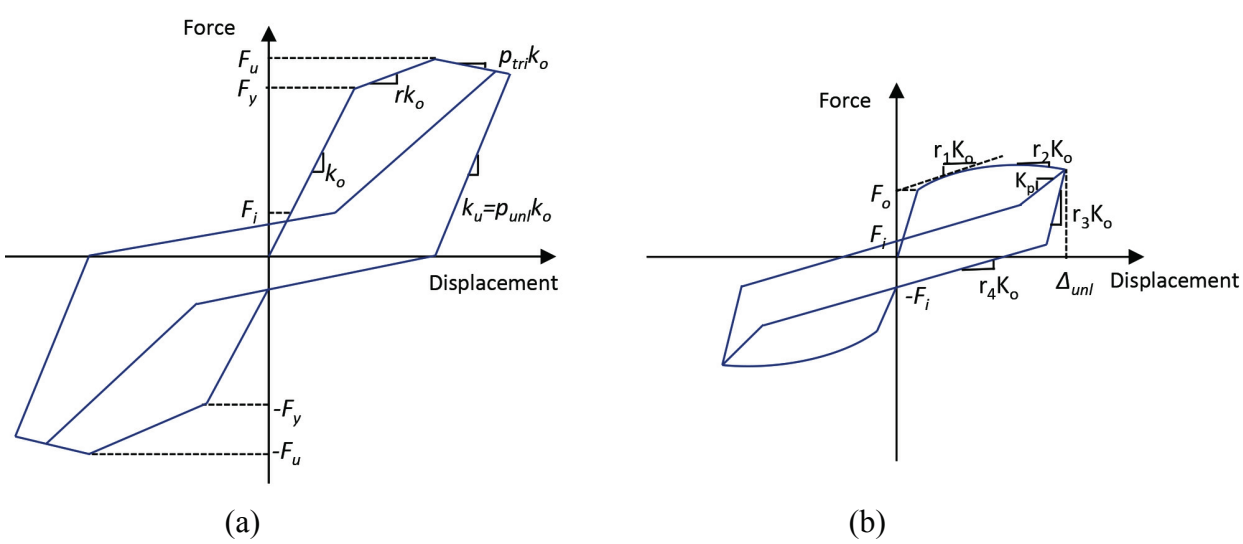

Figure B2. Illustration of hysteretic models: (a) Wayne-Stewart (Stewart, 1987) and (b) CUREE-SAWS (Folz and Filiatrault, 2001).

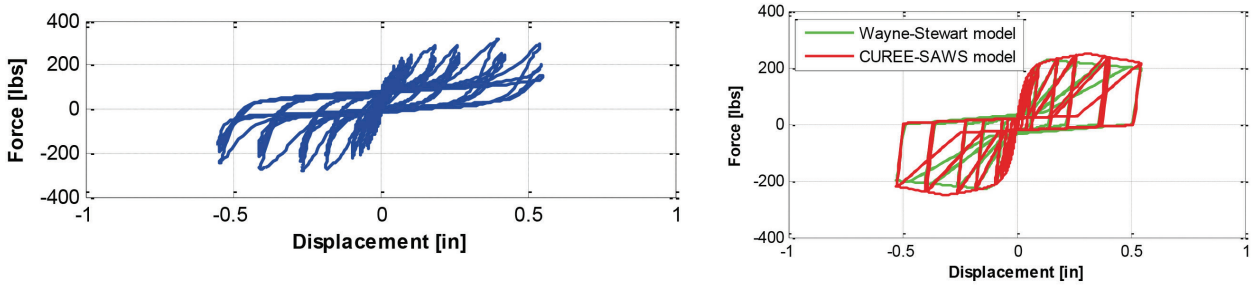

(a) (b)

Figure B3. Comparison of hysteretic response for 10d common nail and wood deck: (a) example of experimental data (Coyne, 2007) and (b) best fit numerical model based on data from several tests (Koliou, 2014).

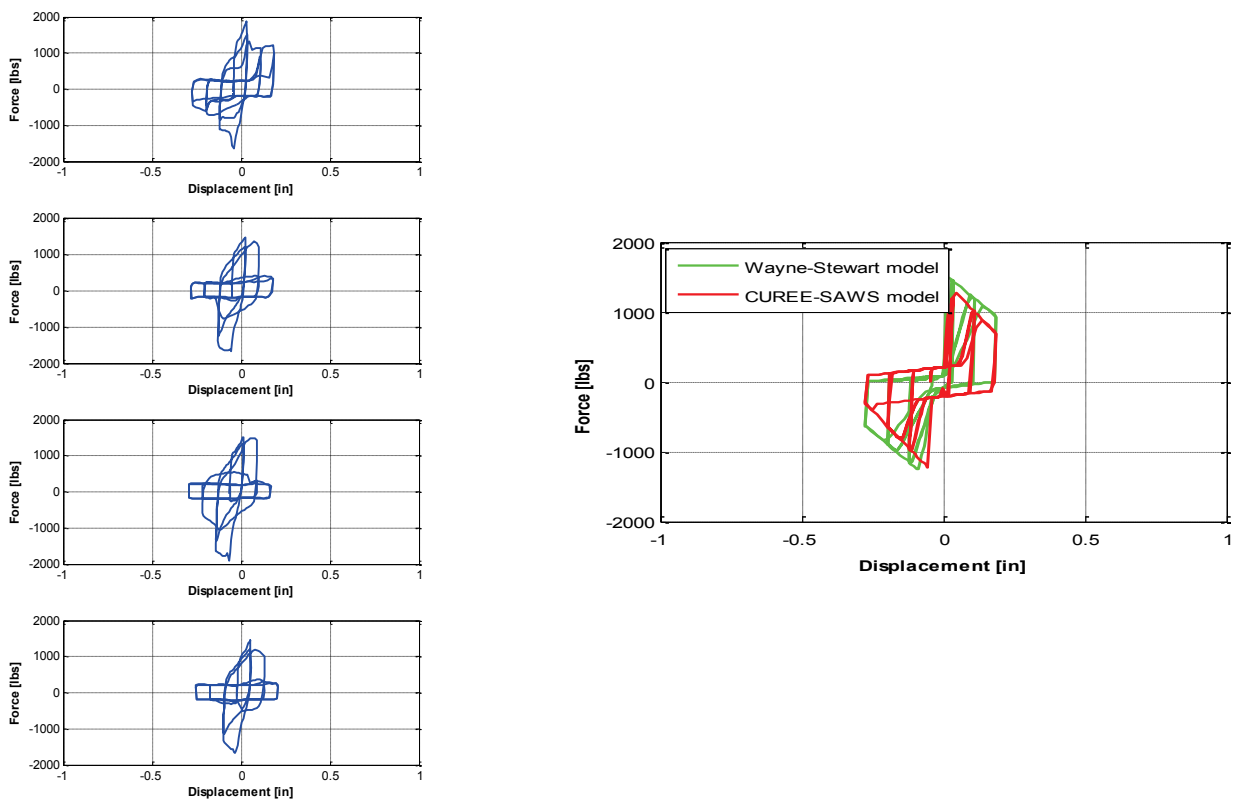

(a) (b)

Figure B4. Comparison of hysteretic response for 2-ply-22-gauge framing welds to 0.25 in. plate: (a) experimental (Guenfoud, et. al., 2010) and (b) fitted optimal hysteretic models

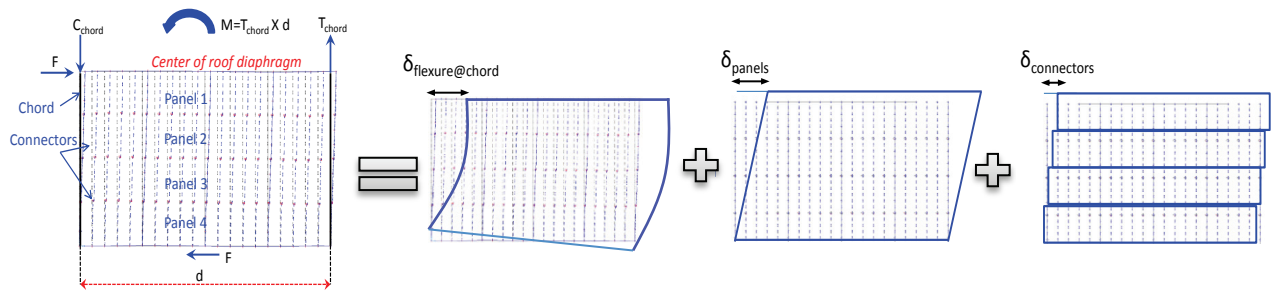

Figure B5. In-plane displacement components of the analytical inelastic roof diaphragm model.

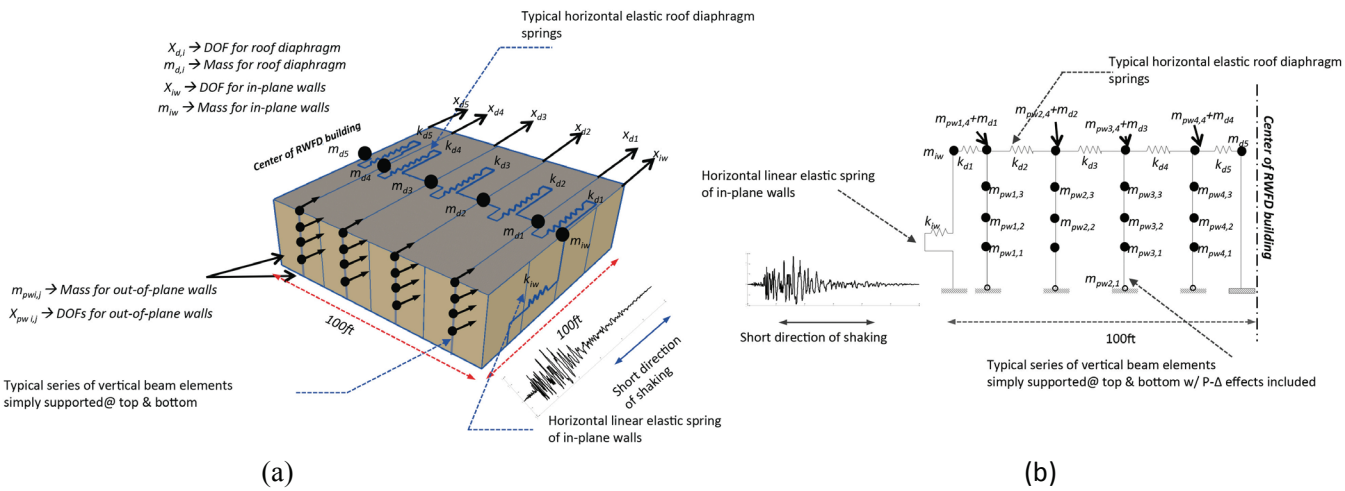

Figure B6. Illustration of a simplified rigid wall flexible diaphragm (RWFD) building model developed in the RUAUMOKO2D platform.

Cyclic test data for the 10d common nails are from Coyne (2007), Fonseca and Campbell (2002), and Christovasilis, et al (2009). Cyclic data for button punch, screw, and top seam weld sidelap connectors between deck sheets are from Rogers and Tremblay (2003b). Cyclic data for welds, powder actuated fasteners, and screws that connect steel deck to steel plates are from Guenfoud, et al. (2010) and from Rogers and Tremblay (2003a). A list of the database of cyclic test data for nails and steel deck connectors is included in Tables C1, C2, and C3 of Appendix C.

B.2 Modeling Framework Validation

The two-dimensional model of the diaphragm, Step 2, was validated by comparing predicted results to cyclic diaphragm test results of Tremblay et al. (2004). The predicted and tested shear for monotonic loading are normalized to the applicable maximum shear and compared in Figure B7. The results of shear versus deformation for one main cycle predicted by the diaphragm sub model versus the test results are compared in Figure B8. Results for the simplified model, Step 3, are compared to those of a detailed finite element model by Olund (2009).

The periods are obtained from eigenvalue analyses using the simplified building model and are initial elastic periods. The natural periods of the simplified model for the first and second modes are about 3% longer than those predicted by Olund's detailed model.

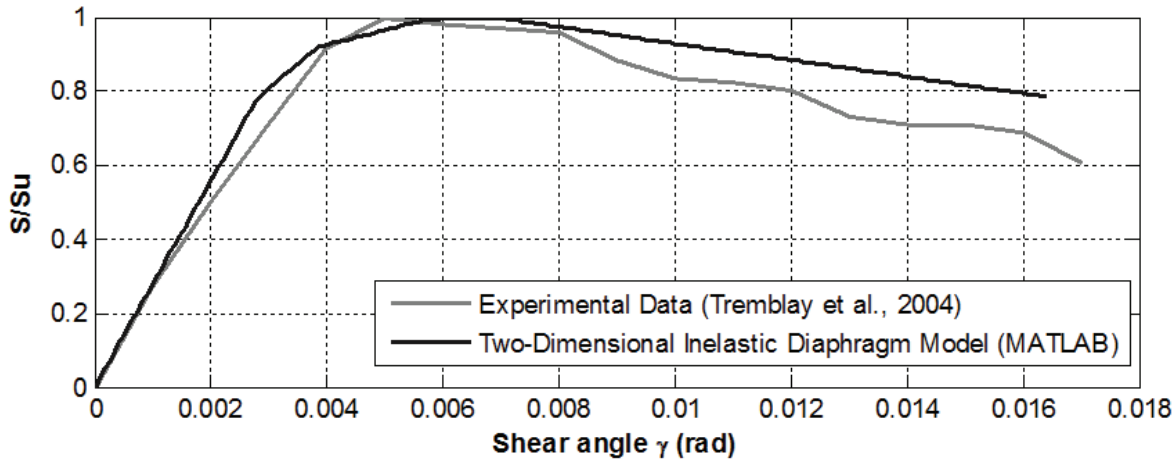

Figure B7. Validation/comparison of inelastic roof diaphragm for monotonic loading.

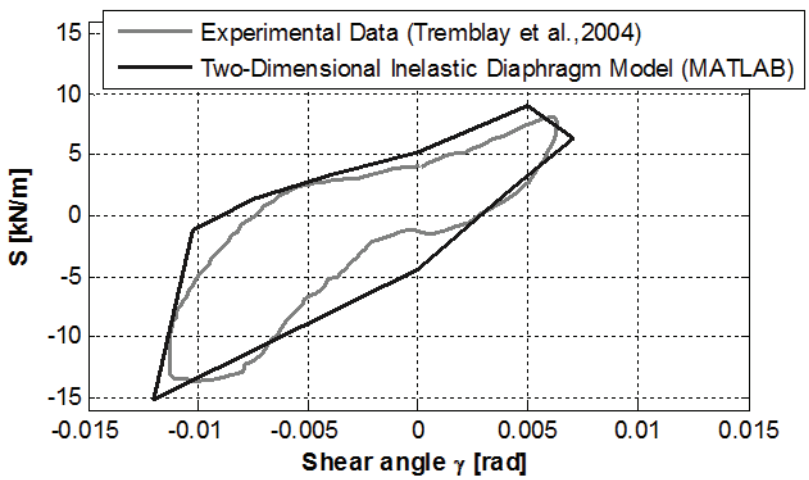

Figure B8. Validation/comparison of inelastic roof diaphragm for cyclic loading (one main cycle).

The collapse assessment of the rigid wall flexible diaphragm (RWFD) building was evaluated by conducting Incremental Dynamic Analyses (IDA) (Vamvatsikos and Cornell, 2002) using the FEMA P695 Far Field Ground Motion Ensemble (FEMA P695, 2009) and computing the median collapse intensity. To monitor the state of the structure at the end of each nonlinear time history dynamic analysis, the diaphragm (roof) drift ratio was considered as the damage measure (DM), while the intensity measure (IM) was defined by the spectral acceleration ($S_a(T_1)$) at the fundamental period of the RWFD building; T_1 is the fundamental period obtained from eigenvalue analyses of the initially elastic simplified building model. Olund (2009) set the limit state for a RWFD as a roof drift equal to 3%. For the purpose of comparing results of Olund's detailed model to those of the simplified building model the

limit state is set equal to 3% diaphragm drift, but for analysis results for the FEMA P695 evaluations, the limit state is equated to a load-displacement (P-delta) sidesway instability. As shown in Figure B9, the simplified building model slightly underestimates (by approximately 9%) the median collapse intensity compared to the detailed FEM developed by Olund (2009).

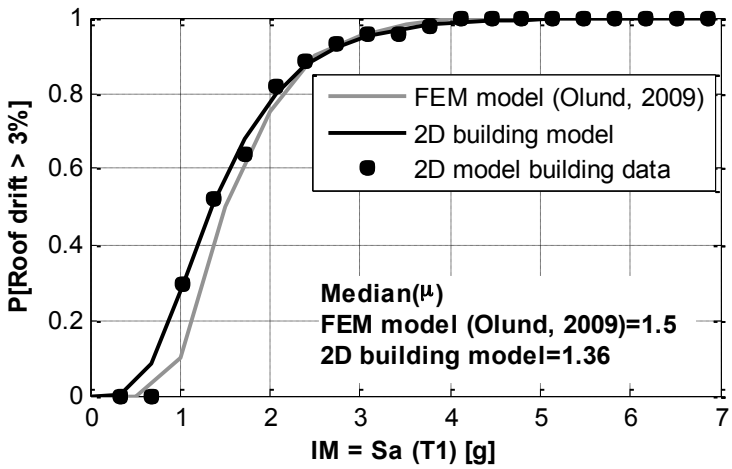

Figure B9. Incremental dynamic analysis results/comparison.

A limitation of the modeling framework is that it cannot account for the simultaneous loading of framing connectors at ends of steel deck sheets from the in-plane diaphragm shears and the continuity tie or out-of-plane wall anchorage forces. Therefore, the archetypes designed and analyzed are based on the requirements to resist shear only. However, the magnitudes of these two sources of loading are not compatible with one another. Specifically, out-of-plane wall forces are not reduced to account for ductility and the connections supporting the wall are expected to behave elastically, while the forces acting on these same connectors from diaphragm shear resistance are based on an assumption that the connections will yield. There seems to be a philosophical conflict in the intended behavior of the fastener when exposed to both diaphragm shear forces and wall anchorage forces, which occur simultaneously in some regions of the diaphragm. For steel deck diaphragms, consideration should be given to supporting the out-of-plane wall forces with separate continuity ties rather than transferring them into the deck sheets. Further analyses beyond those for the FEMA P695 evaluations are recommended to study this issue. Studying this issue will require nonlinear response history analyses of detailed, three-dimensional models with nonlinear connections, but it will be unrealistic to apply the entire suite of time-histories typically used for FEMA P695 evaluations.

APPENDIX C List of Connectors in Database

Cyclic test data are essential for analyzing flexible diaphragms. At this time, the data for common nail connectors are relatively complete. More cyclic test data of steel deck diaphragm connectors is needed. The connections included in the database assembled by Koliou (2014) and the sources of the test data are included in Tables C1, C2, and C3. The fitted parameters for the Wayne-Stewart hysteretic model and the CUREE-SAWS hysteretic model are included in Chapter 3 of Koliou (2014).

Table C1. Cyclic test data for nails

Connection type	Specimen characteristics	Number of specimens tested	Source
6d common nails (d=0.113in, l=2.0in)	7/16 OSB std.	10	Coyne (2007)
8d common nails (d=0.113in, l=2.5in)	2x4 Hem Fir. & 7/16 OSB std.	19	Christovasilis et al. (2009)
	2x6 Hem Fir. & 7/16 OSB std.	17	
8d common nails (d=0.131in, l=2.5in)	7/16 OSB std.	10	Coyne (2007)
10d common nails (d=0.148in, l=3.0in)	7/16 OSB std.	10	
	5/8 OSB std.	10	
	3/4 OSB std.	10	
10d box nails (d=0.131in, l=3.0in)	DF-L & 19/32 T&G	20	Fonseca et al. (2002)
	DF-L & 19/32 OSB std.	20	
#10 Rolled – Hardened screws (d=0.113in, l=2.0in)	DF-L & 7/16 OSB std.	20	

Table C2. Cyclic test data for steel deck sidelap connectors

Connection type	Specimen characteristics	Number of specimens tested	Corresponding Publication
Button punch (0.39in. diameter)	22 ga deck	2	Rogers and Tremblay (2003b)
	20 ga deck	2	
Screws (10-14x7/8 in.)	22 ga deck	2	
	20 ga deck	2	
Welds (1.38in. length)	22 ga deck	2	

Table C3. Cyclic test data for steel deck framing connectors

Connection type	Specimen characteristics	Number of specimens tested	Corresponding Publication
Powder-Actuated Fasteners (Hilti EDNK22-THO12 and Buildex BX12)	22 ga deck to 0.12 in. plate	4	Rogers and Tremblay (2003a)
	20 ga deck to 0.12 in. plate	4	
Powder-Actuated Fasteners (Hilti ENPH2-21-L15 and Buildex BX14)	22 ga deck to 0.79 in. plate	4	
	20 ga deck to 0.79 in. plate	4	
Buildex Screws (12-14x in.)	22 ga deck to 0.12 in. plate	2	
	20 ga deck to 0.12 in. plate	2	
Hilti Screws (12-24x7/8 in.)	22 ga deck to 0.12 in. plate	2	
	20 ga deck to 0.12 in. plate	2	
Welds (0.63 in. arc spot) & Washer	22 ga deck to 0.12 in. plate	1	
Welds (0.63 in. arc spot)	22 ga deck to 0.12 in. plate	2	
	22 ga deck to 0.79 in. plate	1	
	20 ga deck to 0.12 in. plate	2	
Welds (0.63in. – 0.75in. arc spot)	2 ply – 16 ga deck to 0.25 in. plate	4	Guenfoud, Tremblay & Rogers (2010)
	2 ply – 18 ga deck to 0.25 in. plate	4	
	2 ply – 20 ga deck to 0.25 in. plate	4	
	2 ply – 22 ga deck to 0.25 in. plate	4	
	4 ply – 16 ga deck to 0.25 in. plate	4	
	4 ply – 18 ga deck to 0.25 in. plate	3	
	4 ply – 20 ga deck to 0.25 in. plate	4	
	4 ply – 22 ga deck to 0.25 in. plate	4	

APPENDIX D Evaluation of Current Design Procedure

Although the current design procedure is based on the assumption of inelastic response in the vertical elements (walls, rigid frames), yielding of the diaphragm commonly dominates the inelastic response of the buildings to earthquakes. Archetype buildings using the current design procedure were designed and P695 analyses (FEMA P695, 2009) were applied to these designs to provide a baseline of performance and to demonstrate that changes to the design procedure are necessary.

D.1 Description of Archetypes

Evaluations were performed on archetypes as described for high and moderate risk. For these evaluations, archetypes were designed with either steel deck or wood structural panel diaphragms. The archetype naming convention is shown in Figure D1. Summary tables and tables with detailed descriptions of diaphragm zones for the archetypes are in Appendix E. The walls for these archetypes are reinforced-concrete wall panels 25 ft in width, 33 ft tall measured from the top of the slab-on-grade, and 9-1/4 in. thick for high seismic risk and 7-1/4 in. thick for moderate seismic risk. The roof level is at 30 ft above the top of the slab-on-grade with the walls cantilevering as a parapet 3 ft higher than the roof level.

The archetypes are grouped by diaphragm type, either wood or steel deck, and whether the diaphragm is relatively large or small. The archetypes have plan aspect ratios of 1:1, 2:1 and 1:2. Large diaphragms are 400 ft long and either 400 ft or 200 ft wide. The small diaphragms with aspect ratios of 2:1 and 1:2 are 200 ft long by 100 ft wide, and for the 1:1 aspect ratios the diaphragms are 100 ft by 100 ft. The wood diaphragms are wood structural panels nailed to wood nailers that are attached to open web steel joists, commonly called a hybrid panelized roof structure. The steel deck diaphragms are attached to the joists with arc spot welds, powder actuated fasteners, or self-drilling screws. Adjacent steel deck sheets are attached along their sides (sidelaps) with top seam welds, button punches, or self-drilling screws. Many steel deck diaphragms include proprietary sidelap connections in the western portion of the U.S., which includes regions of high seismicity. Archetypes are not included with the proprietary sidelap connections because cyclic test data for the response of these connectors is not available. The steel deck diaphragms were designed using 22 and 20 gage deck because connection data was available for connectors with these deck gages. Note that thicker gage deck results in less ductile connections so the steel deck diaphragm results presented herein are limited to only diaphragms with 22 or 20 gage deck.

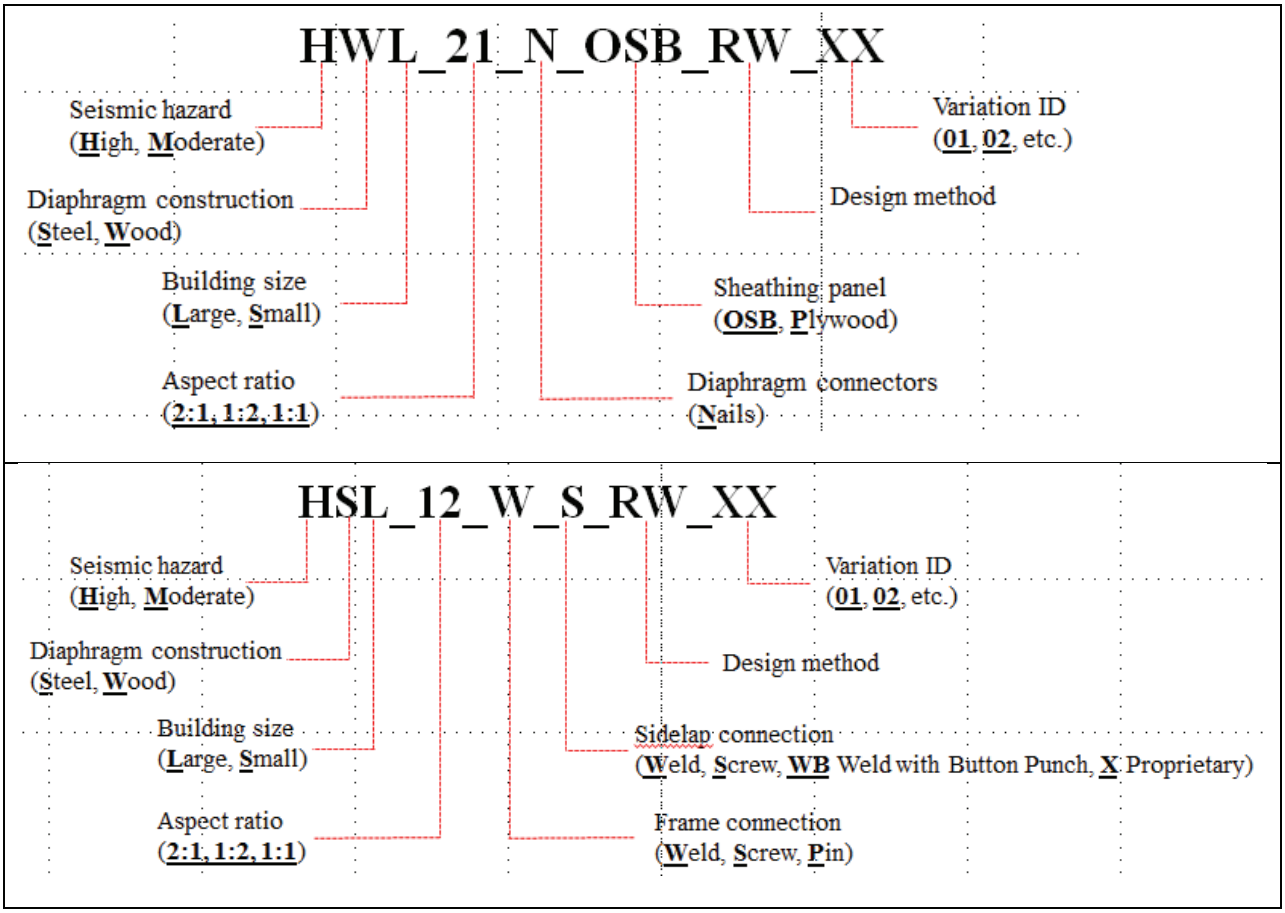

Figure D1. Archetype Naming Convention.

The archetypes were designed as intermediate precast shear walls with a response modification coefficient of 4. The period for each direction of each archetype was computed using the approximate period equation, ASCE 7-10 Eq. 12.8-7, for T_a, which is consistent with current practice. For the 30 ft roof height of the archetypes, the approximate period is 0.26 seconds. This value is less than the transition period, T_s, equal to 0.60 seconds for high-seismic risk (SDC D) archetypes and 0.40 seconds for moderate seismic-risk (SDC C_{max}) archetypes. Therefore, the archetypes for the existing design procedure, i.e., current code, are designed using a base shear coefficient of 0.25 for the high-seismic risk (SDC D) archetypes and for a base shear coefficient of 0.125 for the moderate seismic risk (SDC C_{max}) cases.

The diaphragms for the archetypes are zoned with different fastener spacings similar to zoning commonly used in practice. For the wood diaphragms, the diaphragms are zoned as follows:

- Large wood diaphragms with 1:1 aspect ratio – four zones of concentric squares for high-seismic risk and two zones of concentric squares for moderate seismic risk.
- Large wood diaphragm with 2:1 and 1:2 aspect ratio for high-seismic risk – six zones total with the first two zones near the center of diaphragm as concentric rectangles and the remaining zones banded for loading in the transverse direction
- Large wood diaphragm with 2:1 and 1:2 aspect ratio for moderate seismic risk – three banded zones for loading in the transverse direction
- Small wood diaphragm with 1:1 aspect ratio – two zones of concentric squares
- Small wood diaphragms with 2:1 and 1:2 aspect ratio – five banded zones for high-seismic risk and two banded zones for moderate seismic risk for loading in the transverse direction

For the steel deck diaphragms, the diaphragms are zoned as follows:

- Large steel deck diaphragm with 1:1 aspect ratio – three zones of concentric squares
- Large steel deck diaphragm with 2:1 and 1:2 aspect ratio – three zones banded for transverse direction loading
- Small steel deck diaphragms with 1:1 aspect ratio – one zone used for entire diaphragm
- Small steel deck diaphragms with 2:1 and 1:2 aspect ratio – two zones banded for transverse direction loading

D.2 Summary of FEMA P695 Analysis Results for Current Design

Incremental Dynamic Analyses (IDA) (Vamvatsikos and Cornell, 2002) using the FEMA P695 Far Field Ground Motion Ensemble (FEMA P695, 2009) were performed using the simplified building models to compute the median collapse intensity. For the analysis results, the median collapse intensity is defined as the median spectral intensity at the fundamental period that causes side-sway P-delta instability. Summaries of collapse results for individual wood and steel deck diaphragm archetypes are included in Appendix F. Values for the median collapse intensity, $S_{CT}[T]$, ground motion spectral demand, $S_{MT}[T]$, building drift ratios (BDR) for the design level earthquake and maximum considered earthquake, the spectral shape factor (SSF), fundamental elastic period, and period based ductility, μ_T, are provided. The BDR, which equals the sum of the wall drift ratio (WDR) and the diaphragm drift ratio (DDR), is used as measure of building damage for this study. Collapse margin ratios (CMRs), adjusted collapse margin ratios (ACMRs), and acceptable ACMRs for the individual archetypes and the archetype groups are also included in Appendix F. The acceptable ACMR applicable for the performance of individual archetypes is 1.73, and the acceptable ACMR of performance groups is 2.30. Summaries of the collapse margin ratio results for the performance groups of wood and steel archetypes are provided in Tables D2 and D3.

The current design procedure did not pass the FEMA P695 collapse criteria for the small archetype performance groups with wood diaphragms. Each small wood diaphragm archetype had an individual ACMR that exceeded the acceptable value of 1.73 indicating each archetype passed the criterion. However, the small archetype performance groups for both high- and moderate-seismic risk had ACMR values of 2.11 and 1.98, respectively, which is less than the acceptable ACMR of 2.30, so these performance groups did not pass the criterion. The small archetypes had short periods and remained in the short period range as yielding occurred. In this region, period shifts can result in resonance with large spikes in the short period range that can lead to much larger spectral accelerations and displacements than predicted using the design spectrum plateau. This issue of short-period structures having higher seismic demands leading to the lowest level of collapse performance has been well documented, starting with Newmark and Hall (1973). Section 9.5.1 of FEMA P695 (2009) describes this issue with short-period structures in greater detail.

The larger archetype wood diaphragm performance groups had ACMRs of 2.68 and 2.80 for the high- and moderate risk performance groups, which exceed the acceptable ACMR of 2.30 to pass the criteria. Each large wood diaphragm archetype had an individual ACMR that exceeded the acceptable value of 1.73. The large wood archetypes performed better because the elastic periods were often off of the design response spectrum's plateau but the diaphragm was designed as though it was on the plateau of the spectrum. Also, as the diaphragm yields its period lengthens, which in general leads to lower forces.

Both the large and small steel deck diaphragm performance groups did not pass the criteria. For individual archetypes with high-seismic risk 5 of 7 large archetypes and 1 of 9 small archetypes had ACMRs less than the acceptable ACMR of 1.73, and for individual archetypes with moderate-seismic risk 3 of 12 large archetypes and 3 of 9 small archetypes had ACMRs less than acceptable. The ACMRs for the large archetype groups of 1.71 and 1.87 for high-seismic risk and 1.95 and 1.88 for moderate seismic risk performed slightly worse than the small archetype groups. The small archetype groups had values of 2.23 and 1.92 for high-seismic risk and a value of 1.86 for moderate seismic risk. The reason for the difference relative to what was observed for the wood diaphragms is that the larger steel diaphragms were relatively stiffer than the larger wood diaphragms and had periods that were on or close to the design spectrum plateau. Differences in ACMRs of the archetypes with various combinations of welds, PAFs, screws and button punches were not significant enough to distinguish definitive differences in performance of the connectors.

Table D1. Summary of collapse margin ratio results for wood diaphragm archetype performance groups for current design

Performance Group	Seismicity	Size	Computed ACMR	Acceptable ACMR	Pass/Fail
PG-1E	High	Large	2.68	2.30	Pass
PG-2E	High	Small	2.11		Fail
PG-3E	Moderate	Large	2.80		Pass
PG-4E	Moderate	Small	1.98		Fail

Table D2. Summary of collapse margin ratio results for steel deck diaphragm archetype performance groups

Performance Group	Seismicity	Size	Framing Connectors	Sidelaps	Computed ACMR	Acceptable ACMR	Pass/Fail
PG-5E	High	Large	Welds	Welds / button punches	1.71	2.30	Fail
PG-6E	High	Large	PAFs / screws	Screws	1.87		Fail
PG-7E	High	Small	Welds	Button punches	2.23		Fail
PG-8E	High	Small	PAFs / screws	Screws	1.92		Fail
PG-9E	Moderate	Large	Welds / PAFs/ screws	Screws	1.95		Fail
PG-10E	Moderate	Large	Welds / PAFs/ screws	Welds	1.88		Fail
PG-11E	Moderate	Small	Welds /PAFs / screws	Screws	1.86		Fail

The results indicate that the current design rules are not adequate based on the FEMA P695 methodology for both wood structural panel and steel deck diaphragms. Therefore, a modified or new design procedure is needed. The results also indicate that if a single response modification coefficient were to be used for the diaphragm parallel to current design of SFRS, its value would need to be less than 4. For the wood diaphragms, considering that the lowest ratio of ACMR to acceptable ACMR (1.98/2.3) is 0.86 leads to the expectation that current design using a response modification coefficient *R* (0.86x4) of about 3 to 3.5 is appropriate. For steel deck diaphragms, consider that the lowest ratio of ACMR to acceptable ACMR (1.71/2.3) is 0.74 leads to the expectation that current design using an *R*-coefficient of about 2.5 to 3 may be appropriate for 20 and 22 ga steel deck diaphragms. However, analyses should be performed to determine the appropriate *R* values. This expectation is not appropriate for steel deck diaphragms with gages of 18 or thicker as they are anticipated to result in less ductile diaphragms.

The analysis results also showed that the diaphragm's inelastic behavior was concentrated at the ends of the diaphragm. The global ductility of the diaphragm is lower than the ductility of the connectors because connector yielding is not spreading well into the diaphragm. Response of these buildings would improve if a means of spreading connection yielding deeper into the diaphragm were developed. For the steel deck diaphragms, the response would also be improved if the post-yield stiffness of the connector were positive to a larger displacement value. Tests indicate positive post-yield stiffness only to 1 or 2 mm. The exact displacement needed for improved behavior is not known at this time but a value such as 10 mm is expected to be more than adequate.

D.3 Fundamental Period of the Archetypes

The results of the simplified building model analyses show that the fundamental period of each archetype is dominated by the diaphragm response. The elastic fundamental periods for the archetypes were obtained from the analyses and are included in Tables F1 and F3 of Appendix F. A summary of the elastic periods are included in Table D3.

Table D3. Summary of Elastic Periods for Archetypes

Wood diaphragm span length	Period for high-seismic archetypes	Period for moderate-seismic archetypes
400 ft	0.85 to 0.87 sec	0.90 to 0.92 sec
200 ft	0.49 to 0.54 sec	0.55 to 0.58 sec
100 ft	0.36 to 0.38 sec	0.43 to 0.45 sec
Steel diaphragm span length		
400 ft	0.49 to 0.56 sec	0.61 to 0.73 sec
200 ft	0.35 to 0.42 sec	0.51 to 0.59 sec
100 ft	0.21 to 0.26 sec	0.28 to 0.33 sec

Using the elastic periods from the analyses of the high-seismic wood diaphragm archetypes and the high-seismic steel deck diaphragm archetypes, empirical formulas were developed for the fundamental periods of wood and steel deck diaphragms, respectively. The following formula is proposed for computing the fundamental period, T_{wood}, of the wood diaphragm buildings with concrete or masonry shear walls.

$$T_{wood} = \frac{0.0019}{\sqrt{C_w}} h_n + 0.002L_f \qquad \text{Equation (D1)}$$

Where, L_f is the diaphragm span in feet between vertical elements of the seismic-force-resisting system, C_w is a coefficient defined by Equation 12.8-10 in ASCE 7-10

$$C_w = \frac{100}{A_B}\sum_{i=1}^{x}\frac{A_i}{\left[1+0.83\left(\frac{h_i}{D_i}\right)^2\right]} \qquad \text{Equation (D2)}$$

A_B is the area of the base of the building in ft^2, A_i is the web area of the in-plane shear wall i in ft^2, D_i is the length of the in-plane shear wall i in ft^2, and h_i is the height of the in-plane shear wall i in ft^2, h_n is the height of the roof framing in ft.

The following formula is proposed for computing the fundamental period, T_{steel}, of the steel deck diaphragm buildings.

$$T_{steel} = \frac{0.0019}{\sqrt{C_w}}h_n + 0.001L_f \qquad \text{Equation (D3)}$$

The proposed period equations are plotted along with the periods determined from the simplified building model analyses in Figure D2 for the wood diaphragm archetypes and in Figure D3 for the steel diaphragm archetypes. Although the periods are derived from analyses of single-span diaphragms, the deformations were shear dominated. Therefore, the period equations are valid for multi-span diaphragms. The archetypes used to develop these formulas included heavy walls. A study on the applicability of these formulas to buildings with light walls is recommended.

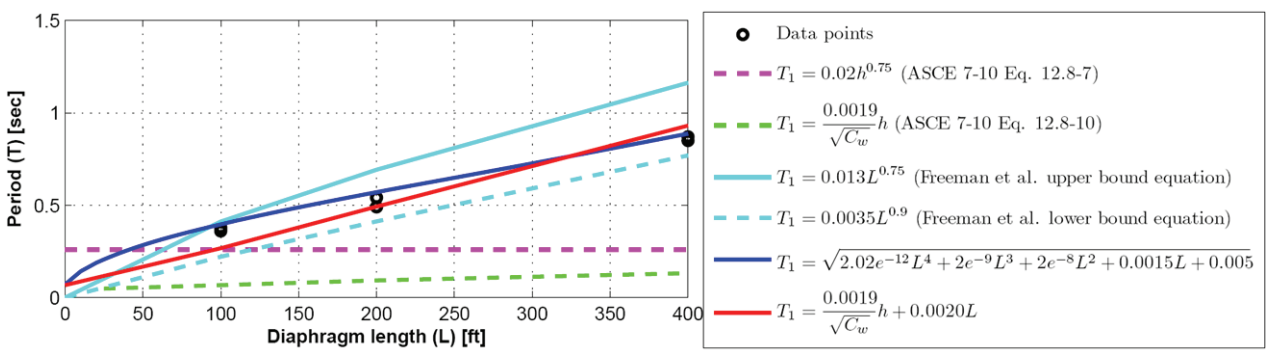

Figure D2. Comparison of fundamental periods from analyses of wood panel archetypes to those predicted by the proposed formula (Equation D1), ASCE 7-10 equations, a best fit curve, and those proposed by Freeman et. al (1995).

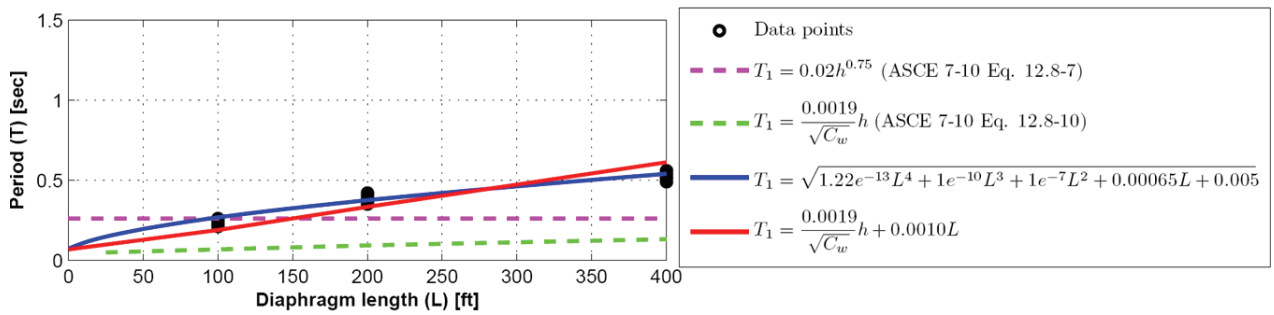

Figure D3. Comparison of fundamental periods from analyses of steel deck archetypes to those predicted by the proposed formula (Equation D3), ASCE 7-10 equations, and a best fit curve.

APPENDIX E Description of Archetypes for Current Design Procedure

Refer to Koliou (2014) for additional information about the archetypes.

Table E1. Archetype Descriptions for Wood Diaphragms

Archetype ID	Diaphragm construction	Building size	Diaphragm aspect ratio	Building dimensions (ft)	Connector type (F=framing S=sidelap)	Seismic design category
HWL_21_N_OSB_RW4_04	Wood	Large	2:1	400x200	Common nails	D_{max}
HWL_12_N_OSB_RW4_02	Wood	Large	1:2	200x400	Common nails	D_{max}
HWL_11_N_OSB_RW4_01	Wood	Large	1:1	400x400	Common nails	D_{max}
HWS_21_N_OSB_RW4_01	Wood	Small	2:1	200x100	Common nails	D_{max}
HWS_12_N_OSB_RW4_01	Wood	Small	1:2	100x200	Common nails	D_{max}
HWS_11_N_OSB_RW4_01	Wood	Small	1:1	100x100	Common nails	D_{max}
HWS_11_N_OSB_RW4_02	Wood	Small	1:1	100x100	Common nails	D_{max}
MWL_11_N_OSB_RW4_01	Wood	Large	1:1	400x400	Common nails	C_{max}
MWL_21_N_OSB_RW4_01	Wood	Large	2:1	400x200	Common nails	C_{max}
MWL_12_N_OSB_RW4_01	Wood	Large	1:2	200x400	Common nails	C_{max}
MWS_11_N_OSB_RW4_01	Wood	Small	1:1	100x100	Common nails	C_{max}
MWS_21_N_OSB_RW4_01	Wood	Small	2:1	200x100	Common nails	C_{max}
MWS_12_N_OSB_RW4_01	Wood	Small	1:2	100x200	Common nails	C_{max}

Table E2. Archetype Descriptions for Steel Diaphragms for High-Seismic Risk – Existing Design

Archetype Designation	Diaphragm Dimensions	Zone	Zone Width (ft)	Connector Pattern / Deck Gage	Framing Connectors	Sidelap Connectors	Sidelap Spacing
High Seismicity – Large Buildings							
HSL_11_P_S_RW4	400 x 400 ft	3	56	36/11 – 22 ga	PAF	#10 screw	6 in.
		2	24	36/9 – 22 ga	PAF	#10 screw	9 in.
		1	120	36/9 – 22 ga	PAF	#10 screw	18 in.
HSL_11_W_WB_RW4	400 x 400 ft	3	56	36/7 – 22 ga	1/2 in. dia. welds	TSW	12 in.
		2	24	36/7 – 22 ga	1/2 in. dia. welds	BP	12 in.
		1	120	36/7 – 22 ga	1/2 in. dia. welds	BP	24 in.
HSL_21_W_WB_RW4_01	400 x 200 ft	3	50	36/7 – 22 ga	1/2 in. dia. Effective area welds (5/8 and 3/4 in. dia. at the surface)	TSW	6 in.
		2	54	36/7 – 22 ga	1/2 in. dia. Effective area welds (5/8 and 3/4 in. dia. at the surface)	TSW	12 in.
		1	96	36/7 – 22 ga	1/2 in. dia. Effective area welds (5/8 and 3/4 in. dia. at the surface)	BP	12 in.
HSL_21_P_S_RW4_01	400 x 200 ft	3	50	36/9 – 20 ga	PAF	#10 screws	3 in.
		2	60	36/9 – 22 ga	PAF	#10 screws	6 in.
		1	90	36/5 – 22 ga	PAF	#10 screws	6 in.
HSL_11_S_S_RW4	400 x 400 ft	3	66	36/11 – 22 ga	#12 or #14 HWH self-drilling screws by Hilti	#10 screws	3 in.
		2	24	36/9 – 22 ga	#12 or #14 HWH self-drilling screws by Hilti	#10 screws	6 in.

Table E2. Archetype Descriptions for Steel Diaphragms for High-Seismic Risk – Existing Design (cont.)

Archetype Designation	Diaphragm Dimensions	Zone	Zone Width (ft)	Connector Pattern / Deck Gage	Framing Connectors	Sidelap Connectors	Sidelap Spacing
		1	120	36/9 – 22 ga	#12 or #14 HWH self-drilling screws by Hilti	#10 screws	9 in.
HSL_12_W_WB_RW4	Refer to HSL_21_W_WB for design						
HSL_12_P_S_RW4	Refer to HSL_21_P_S for design						
High Seismicity – Small Buildings							
HSS_11_W_B_RW4	100 x 100 ft	3	50	36/5 – 22 ga	1/2 in. dia effective welds (5/8 in. and 3/4 in. at the surface)	BP	12 in.
		2	50	36/5 – 22 ga	1/2 in. dia. effective welds (5/8 in. and 3/4 in. at the surface)	BP	12 in.
		1	50	36/5 – 22 ga	1/2 in. dia. effective welds (5/8 in. and 3/4 in. at the surface)	BP	12 in.
HSS_21_W_WB_RW4	200 x 100 ft	3	0	36/7 – 22 ga	1/2 in. dia. effective welds (5/8 in. and 3/4 in. dia. puddle welds at the surface)	TSW	9 in.
		2	40	36/7 – 22 ga	1/2 in. dia. effective welds (5/8 in. and 3/4 in. dia. puddle welds at the surface)	TSW	9 in.

Table E2. Archetype Descriptions for Steel Diaphragms for High-Seismic Risk – Existing Design (cont.)

Archetype Designation	Diaphragm Dimensions	Zone	Zone Width (ft)	Connector Pattern / Deck Gage	Framing Connectors	Sidelap Connectors	Sidelap Spacing
		1	60	36/7 – 22 ga	1/2 in. dia. effective welds (5/8 in. and 3/4 in. dia. puddle welds at the surface)	BP	12 in.
HSS_12_W_WB_RW4	Refer to HSS_21_W_WB_RW4						
HSS_11_P_S_RW4	100 x 100 ft	3	0	36/9 – 22 ga	PAF	#10 screws	18 in.
		2	0	36/9 – 22 ga	PAF	#10 screws	18 in.
		1	50	36/9 – 22 ga	PAF	#10 screws	18 in.
HSS_11_S_S_RW4	100 x 100 ft	3	0	36/9 – 22 ga	#12	#10 screws	9 in.
		2	0	36/9 – 22 ga	#12	#10 screws	9 in.
		1	50	36/9 – 22 ga	#12	#10 screws	9 in.
HSS_21_P_S_RW4	200 x 100 ft	3	0	36/9 – 22 ga	PAF	#10 screws	3 in.
		2	40	36/9 – 22 ga	PAF	#10 screws	3 in.
		1	60	36/9 – 22 ga	PAF	#10 screws	9 in.
HSS_12_P_S_RW4	Refer to HSS_21_P_S_RW4						
HSS_21_S_S_RW4	200 x 100 ft	3	0	36/11 – 20 ga	#12	#10 screws	3 in.
		2	40	36/11 – 20 ga	#12	#10 screws	3 in.
		1	60	36/9 – 22 ga	#12	#10 screws	6 in.
HSS_12_S_S_RW4	Refer to HSS_21_S_S_RW4						

Table E3. Archetype Descriptions for Steel Diaphragms for Moderate-Seismic Risk – Existing Design

Archetype Designation	Diaphragm Dimensions	Zone	Zone Width (ft)	Connector Pattern / Deck Gage	Framing Connectors	Sidelap Con-nectors	Sidelap Spacing
Moderate Seismicity – Large Buildings							
MSL_21_P_S_RW4	400 x 200 ft	3	32	36/9 – 22 ga	PAF	#10 screws	15 in.
		2	36	36/9 – 22 ga	PAF	#10 screws	27 in.
		1	132	36/5 – 22 ga	PAF	#10 screws	15 in.
MSL_12_P_S_RW4	Refer to MSL_21_P_S_RW4						
MSL_21_S_S_RW4	400 x 200 ft	3	32	36/9 – 22 ga	#12 Hilti HWH screws	#10 screws	6 in.
		2	36	36/9 – 22 ga	#12 Hilti HWH screws	#10 screws	12 in.
		1	132	36/5 – 22 ga	#12 Hilti HWH screws	#10 screws	9 in.
MSL_12_S_S_RW4	Refer to MSL_21_S_S_RW4						
MSL_21_W_S_RW4	400 x 200 ft	3	32	36/7 – 22 ga	3/4 in. welds	#10 screws	6 in.
		2	36	36/7 – 22 ga	3/4 in. welds	#10 screws	12 in.
		1	132	36/5 – 22 ga	5/8 in. welds	#10 screws	9 in.
MSL_12_W_S_RW4	Refer to MSL_21_W_S_RW4						
MSL_11_P_S_RW4	400 x 400 ft	3	32	36/5 – 22 ga	PAF	#10 screws	12 in.
		2	36	36/5 – 22 ga	PAF	#10 screws	21 in.
		1	132	36/5 – 22 ga	PAF	#10 screws	36 in.
MSL_11_S_S_RW4	400 x 400 ft	3	32	36/5 – 22 ga	#12 Hilti HWH screws	#10 screws	9 in.
		2	36	36/5 – 22 ga	#12 Hilti HWH screws	#10 screws	12 in.
		1	132	36/5 – 22 ga	#12 Hilti HWH screws	#10 screws	21 in.
MSL_11_W_S_RW4	400 x 400 ft	3	32	36/5 – 22 ga	5/8 in. dia. welds	#10 screws	9 in.
		2	36	36/5 – 22 ga	5/8 in. dia. welds	#10 screws	18 in.
		1	132	36/5 – 22 ga	5/8 in. dia. welds	#10 screws	21 in.
MSL_21_W_W_RW4_01	400 x 200 ft	3	40	36/7 – 22 ga	3/4 in. dia. welds	TSW	18 in.

Table E3. Archetype Descriptions for Steel Diaphragms for Moderate-Seismic Risk – Existing Design (cont.)

Archetype Designation	Diaphragm Dimensions	Zone	Zone Width (ft)	Connector Pattern / Deck Gage	Framing Connectors	Sidelap Connectors	Sidelap Spacing
		2	40	36/5 – 22 ga	3/4 in. dia. welds	TSW	24 in.
		1	120	36/5 – 22 ga	3/4 in. dia. welds	TSW	36 in.
MSL_12_W_W_RW4_01	Refer to MSL_21_W_W_RW4_01						
MSL_11_W_W_RW4_01	400 x 400 ft	3	40	36/5 – 22 ga	3/4 in. dia. welds	TSW	36 in.
		2	40	36/4 – 22 ga	3/4 in. dia. welds	TSW	36 in.
		1	120	36/4 – 22 ga	3/4 in. dia. welds	TSW	72 in.
Moderate Seismicity – Small Buildings							
MSS_11_S_S_RW4	100 x 100 ft	3	0	36/5 – 22 ga	#12 HWH Hilti screw	#10 screws	36 in.
		2	0	36/5 – 22 ga	#12 HWH Hilti screw	#10 screws	36 in.
		1	50	36/5 – 22 ga	#12 HWH Hilti screw	#10 screws	36 in.
MSS_11_P_S_RW4	100 x 100 ft	3	0	36/5 – 22 ga	PAF	#10 screws	36 in.
		2	0	36/5 – 22 ga	PAF	#10 screws	36 in.
		1	50	36/5 – 22 ga	PAF	#10 screws	36 in.
MSS_11_W_S_RW4	100 x 100 ft	3	0	36/5 – 22 ga	5/8 in. puddle welds	#10 screws	36 in.
		2	0	36/5 – 22 ga	5/8 in. puddle welds	#10 screws	36 in.
		1	50	36/5 – 22 ga	5/8 in. puddle welds	#10 screws	36 in.
MSS_21_S_S_RW4	200 x 100 ft	3	22	36/7 – 22 ga	#12 HWH Hilti screw	#10 screws	9 in.
		2	0	36/5 – 22 ga	#12 HWH Hilti screw	#10 screws	12 in.
		1	78	36/5 – 22 ga	#12 HWH Hilti screw	#10 screws	12 in.
MSS_12_S_S_RW4	Refer to MSS_21_S_S_RW4						
MSS_21_P_S_RW4	200 x 100 ft	3	22	36/7 – 22 ga	PAF	#10 screws	12 in.
		2	0	36/5 – 22 ga	PAF	#10 screws	21 in.
		1	78	36/5 – 22 ga	PAF	#10 screws	21 in.
MSS_12_P_S_RW4	Refer to MSS_21_P_S_RW4						
MSS_21_W_S_RW4	200 x 100 ft	3	22	36/7 – 22 ga	5/8 in. puddle welds	#10 screws	9 in.
		2	0	36/5 – 22 ga	5/8 in. puddle welds	#10 screws	12 in.
		1	78	36/5 – 22 ga	5/8 in. puddle welds	#10 screws	12 in.
MSS_12_W_S_RW4	Refer to MSS_21_W_S_RW4						
MSL_21_P_S_RW4	400 x 200 ft	3	32	36/9 – 22 ga	PAF	#10 screws	15 in.

Table E3. Archetype Descriptions for Steel Diaphragms for Moderate-Seismic Risk – Existing Design (cont.)

Archetype Designation	Diaphragm Dimensions	Zone	Zone Width (ft)	Connector Pattern / Deck Gage	Framing Connectors	Sidelap Connectors	Sidelap Spacing
		2	36	36/9 – 22 ga	PAF	#10 screws	27 in.
		1	132	36/5 – 22 ga	PAF	#10 screws	15 in.
MSL_12_P_S_RW4	Refer to MSL_21_P_S_RW4						
MSL_21_S_S_RW4	400 x 200 ft	3	32	36/9 – 22 ga	#12 Hilti HWH screws	#10 screws	6 in.
		2	36	36/9 – 22 ga	#12 Hilti HWH screws	#10 screws	12 in.
		1	132	36/5 – 22 ga	#12 Hilti HWH screws	#10 screws	9 in.
MSL_12_S_S_RW4	Refer to MSL_21_S_S_RW4						
MSL_21_W_S_RW4	400 x 200 ft	3	32	36/7 – 22 ga	3/4 in. welds	#10 screws	6 in.
		2	36	36/7 – 22 ga	3/4 in. welds	#10 screws	12 in.
		1	132	36/5 – 22 ga	5/8 in. welds	#10 screws	9 in.
MSL_12_W_S_RW4	Refer to MSL_21_W_S_RW4						

THIS PAGE INTENTIONALLY LEFT BLANK

APPENDIX F – FEMA P695 Evaluation Results for Current Design Procedure

Results for the FEMA P695 collapse analyses for the current design procedure are presented in this appendix. The following notations and abbreviations are used in the tables:

ACMR	Adjusted Collapse Margin Ratio where: $ACMR = SSF_i \times CMR_i$
BDR	Building Drift Ratio where: $BDR(\%) = DDR(\%) + WDR(\%)$
CMR	Collapse Margin Ratio where: $CMR_i = \frac{S_{CT}}{S_{MT}}$
DE	Design Earthquake
DDR	Diaphragm Drift Ratio (%) where: $DDR(\%) = \frac{X_{mid,roof}}{L_f/_2} \times 100$ $X_{mid,roof}$ is the diaphragm deflection at mid length L_f is the diaphragm span in feet
MCE	Maximum Considered Earthquake
SSF	Spectral Shape Function
S_{CT} [T]	Median collapse intensity obtained from nonlinear dynamic analysis at the fundamental elastic period
S_{MT} [T]	Ground motion spectral demand at maximum considered earthquake (MCE) intensity level at the fundamental elastic period
WDR(%)	In-plane Wall Drift Ratio where: $WDR(\%) = \frac{X_{in-plane\ walls}}{h_{wall}} \times 100$ $X_{in\text{-}plane\ walls}$ is the deflection at the roof level of the in-plane walls h_{wall} is the height of roof above the foundation
μ_T	Period based ductility where: $\mu_T = \frac{\delta_u}{\delta_{y,eff}}$ δ_u is the ultimate building drift ratio (BDR) $\delta_{y,eff}$ is the effective yield building drift ratio (BDR)

Table F1. Summary of collapse results for RWFD buildings incorporating wood roof diaphragm archetype designs

Archetype ID	Design configuration				Pushover and IDA results			Relevant analysis parameters		
	Building size	Diaphragm aspect ratio	Diaphragm construction	Seismic SDC	$S_{MT}[T]$ (g)	$S_{CT}[T]$ (g)	CMR	Period (sec)	Median BDR @ DE (%)	Median BDR @ MCE (%)
Performance Group No. PG-1E (Wood, Large Building, Existing Design)										
HWL_21_N_OSB_RW4_07	Large	2:1	Wood Panelized	D_{max}	1.06	2.00	1.89	0.85	0.29	0.55
HWL_12_N_OSB_RW4_02	Large	1:2	Wood Panelized	D_{max}	1.50	3.36	2.24	0.49	0.42	0.64
HWL_11_N_OSB_RW4_01	Large	1:1	Wood Panelized	D_{max}	1.05	1.68	1.60	0.87	0.32	0.53
Performance Group No. PG-2E (Wood, Small Building, Existing Design)										
HWS_21_N_OSB_RW4_01	Small	2:1	Wood Panelized	D_{max}	1.41	1.98	1.40	0.54	0.56	1.16
HWS_12_N_OSB_RW4_01	Small	1:2	Wood Panelized	D_{max}	1.50	2.64	1.76	0.38	0.72	1.72
HWS_11_N_OSB_RW4_01	Small	1:1	Wood Panelized	D_{max}	1.50	2.21	1.47	0.36	0.65	1.68
HWS_11_N_OSB_RW4_02	Small	1:1	Wood Panelized	D_{max}	1.50	2.32	1.55	0.37	0.68	1.63
Performance Group No. PG-3E (Wood, Large Building, Existing Design)										
MWL_21_N_OSB_RW4_01	Large	2:1	Wood Panelized	C_{max}	0.50	1.28	2.56	0.90	0.31	0.52
MWL_12_N_OSB_RW4_01	Large	1:2	Wood Panelized	C_{max}	0.75	1.75	2.33	0.55	0.39	0.63
MWL_11_N_OSB_RW4_01	Large	1:1	Wood Panelized	C_{max}	0.51	1.09	2.14	0.92	0.35	0.55
Performance Group No. PG-4E (Wood, Small Building, Existing Design)										
MWS_21_N_OSB_RW4_01	Small	2:1	Wood Panelized	C_{max}	0.75	1.15	1.50	0.58	0.51	0.89
MWS_12_N_OSB_RW4_01	Small	1:2	Wood Panelized	C_{max}	0.75	1.35	1.72	0.43	0.55	0.98
MWS_11_N_OSB_RW4_01	Small	1:1	Wood Panelized	C_{max}	0.75	1.47	1.96	0.45	0.59	1.15

Table F2. Adjusted collapse margin ratios and acceptable collapse margin ratios for RWFD buildings incorporating wood roof diaphragm archetype designs

Archetype ID	Design configuration				Collapse margin parameters				Acceptance check	
	Building size	Diaphragm aspect ratio	Diaphragm construction	Seismic SDC	CMR	μ_T	SSF	ACMR	Accept. ACMR	Pass/Fail
Performance Group No. PG-1E (Wood, Large Building, Existing Design)										
HWL_21_N_OSB_RW4_07	Large	2:1	Wood	D_{max}	1.89	8.07	1.43	2.70	1.73	Pass
HWL_12_N_OSB_RW4_02	Large	1:2	Wood	D_{max}	2.24	8.95	1.36	3.05	1.73	Pass
HWL_11_N_OSB_RW4_01	Large	1:1	Wood	D_{max}	1.60	8.42	1.43	2.29	1.73	Pass
Mean of Performance Group:					**1.91**	**8.48**	**1.41**	**2.68**	**2.30**	**Pass**
Performance Group No. PG-2E (Wood, Small Building, Existing Design)										
HWS_21_N_OSB_RW4_01	Small	2:1	Wood	D_{max}	1.40	7.20	1.31	1.84	1.73	Pass
HWS_12_N_OSB_RW4_01	Small	1:2	Wood	D_{max}	1.76	8.95	1.36	2.39	1.73	Pass
HWS_11_N_OSB_RW4_01	Small	1:1	Wood	D_{max}	1.55	8.32	1.36	2.10	1.73	Pass
HWS_11_N_OSB_RW4_02	Small	1:1	Wood	D_{max}	1.55	8.51	1.36	2.11	1.73	Pass
Mean of Performance Group:					**1.57**	**8.25**	**1.35**	**2.11**	**2.30**	**Fail**
Performance Group No. PG-3E (Wood, Large Building, Existing Design)										
MWL_21_N_OSB_RW4_01	Large	2:1	Wood	C_{max}	2.56	8.15	1.14	2.92	1.73	Pass
MWL_12_N_OSB_RW4_01	Large	1:2	Wood	C_{max}	2.33	8.79	1.14	2.66	1.73	Pass
MWL_11_N_OSB_RW4_01	Large	1:1	Wood	C_{max}	2.14	8.54	1.14	2.44	1.73	Pass
Mean of Performance Group:					**2.34**	**8.49**	**1.14**	**2.67**	**2.30**	**Pass**
Performance Group No. PG-4E (Wood, Small Building, Existing Design)										
MWS_21_N_OSB_RW4_01	Small	2:1	Wood	C_{max}	1.50	8.05	1.16	1.74	1.73	Pass
MWS_12_N_OSB_RW4_01	Small	1:2	Wood	C_{max}	1.72	8.49	1.14	1.96	1.73	Pass
MWS_11_N_OSB_RW4_01	Small	1:1	Wood	C_{max}	1.96	8.09	1.14	2.23	1.73	Pass
Mean of Performance Group:					**1.73**	**8.21**	**1.15**	**1.98**	**2.30**	**Fail**

Table F3. Summary of collapse results for RWFD buildings incorporating steel roof diaphragm archetype designs

Archetype ID	Design configuration				Pushover and IDA results			Relevant analysis parameters		
	Building size	Diaphragm aspect ratio	Diaphragm construction	Seismic SDC	$S_{MT}[T]$ (g)	$S_{CT}[T]$ (g)	CMR	Period (sec)	Median BDR @ DE (%)	Median BDR @ MCE (%)
Performance Group No. PG-5E (Steel, Large Building, Welds and Button Punches as sidelap Connectors, Existing Design)										
HSL_21_W_WB_RW4_01	Large	2:1	Steel (WR Deck)	D_{max}	1.50	1.56	0.99	0.52	0.19	0.45
HSL_12_W_WB_RW4_01	Large	1:2	Steel (WR Deck)	D_{max}	1.50	2.85	1.90	0.39	0.28	0.71
HSL_11_W_WB_RW4_01	Large	1:1	Steel (WR Deck)	D_{max}	1.50	1.43	0.95	0.49	0.13	0.42
Performance Group No. PG-6E (Steel, Large Building, Screws as sidelap Connectors, Existing Design)										
HSL_21_P_S_RW4_01	Large	2:1	Steel (WR Deck)	D_{max}	1.50	1.85	1.23	0.54	0.15	0.33
HSL_12_P_S_RW4_01	Large	1:2	Steel (WR Deck)	D_{max}	1.50	3.10	2.07	0.41	0.25	0.56
HSL_11_P_S_RW4_01	Large	1:1	Steel (WR Deck)	D_{max}	1.50	1.69	1.13	0.56	0.18	0.34
HSL_11_S_S_RW4_01	Large	1:1	Steel (WR Deck)	D_{max}	1.50	1.73	1.15	0.51	0.16	0.29
Performance Group No. PG-7E (Steel, Small Building, Button Punches as sidelap Connectors, Existing Design)										
HSS_11_W_B_RW4_01	Small	1:1	Steel (WR Deck)	D_{max}	1.50	2.59	1.73	0.21	0.17	0.39
HSS_21_W_B_RW4_01	Small	2:1	Steel (WR Deck)	D_{max}	1.50	2.13	1.42	0.35	0.21	0.44
HSS_12_W_B_RW4_01	Small	1:2	Steel (WR Deck)	D_{max}	1.50	2.85	1.90	0.26	0.15	0.35
Performance Group No. PG-8E (Steel, Small Building, Screws as sidelap Connectors, Existing Design)										
HSS_11_P_S_RW4_01	Small	1:1	Steel (WR Deck)	D_{max}	1.50	2.33	1.55	0.23	0.16	0.41
HSS_11_S_S_RW4_01	Small	1:1	Steel (WR Deck)	D_{max}	1.50	2.15	1.43	0.25	0.14	0.36

Table F3. Summary of collapse results for RWFD buildings incorporating steel roof diaphragm archetype designs (cont.)

Archetype ID	Design configuration				Pushover and IDA results			Relevant analysis parameters		
	Building size	Diaphragm aspect ratio	Diaphragm construction	Seismic SDC	$S_{MT}[T]$ (g)	$S_{CT}[T]$ (g)	CMR	Period (sec)	Median BDR @ DE (%)	Median BDR @ MCE (%)
HSS_21_P_S_RW4_01	Small	2:1	Steel (WR Deck)	D_{max}	1.50	1.99	1.33	0.37	0.19	0.35
HSS_12_P_S_RW4_01	Small	1:2	Steel (WR Deck)	D_{max}	1.50	2.56	1.71	0.24	0.17	0.31
HSS_21_S_S_RW4_01	Small	2:1	Steel (WR Deck)	D_{max}	1.50	1.87	1.25	0.42	0.15	0.42
HSS_12_S_S_RW4_01	Small	1:2	Steel (WR Deck)	D_{max}	1.50	2.13	1.42	0.22	0.14	0.39
Performance Group No. PG-9E (Steel, Large Building, Screws as sidelap Connectors, Existing Design)										
MSL_21_P_S_RW4_01	Large	2:1	Steel (WR Deck)	D_{max}	0.68	0.93	1.35	0.66	0.29	0.41
MSL_12_P_S_RW4_01	Large	1:2	Steel (WR Deck)	D_{max}	0.75	1.50	2.01	0.53	0.19	0.33
MSL_21_S_S_RW4_01	Large	2:1	Steel (WR Deck)	D_{max}	0.63	0.96	1.52	0.71	0.22	0.35
MSL_12_S_S_RW4_01	Large	1:2	Steel (WR Deck)	D_{max}	0.75	1.41	1.88	0.55	0.21	0.32
MSL_21_W_S_RW4_01	Large	2:1	Steel (WR Deck)	D_{max}	0.62	1.15	1.41	0.73	0.20	0.31
MSL_12_W_S_RW4_01	Large	1:2	Steel (WR Deck)	D_{max}	0.75	1.47	1.96	0.52	0.23	0.34
MSL_11_P_S_RW4_01	Large	1:1	Steel (WR Deck)	D_{max}	0.70	1.27	1.81	0.65	0.24	0.39
MSL_11_S_S_RW4_01	Large	1:1	Steel (WR Deck)	D_{max}	0.70	1.10	1.58	0.65	0.21	0.45
MSL_11_W_S_RW4_01	Large	1:1	Steel (WR Deck)	D_{max}	0.67	1.11	1.66	0.68	0.25	0.47

Table F3. Summary of collapse results for RWFD buildings incorporating steel roof diaphragm archetype designs (cont.)

Archetype ID	Design configuration				Pushover and IDA results			Relevant analysis parameters		
	Building size	Diaphragm aspect ratio	Diaphragm construction	Seismic SDC	$S_{MT}[T]$ (g)	$S_{CT}[T]$ (g)	CMR	Period (sec)	Median BDR @ DE (%)	Median BDR @ MCE (%)
Performance Group No. PG-10E (Steel, Large Building, Welds as sidelap Connectors, Existing Design)										
MSL_21__W_W_RW4_01	Large	2:1	Steel (WR Deck)	C_{max}	0.73	1.02	1.39	0.62	0.19	0.35
MSL_12__W_W_RW4_01	Large	1:2	Steel (WR Deck)	C_{max}	0.75	1.50	1.99	0.51	0.24	0.41
MSL_11__W_W_RW4_01	Large	1:1	Steel (WR Deck)	C_{max}	0.74	1.13	1.52	0.61	0.18	0.36
Performance Group No. PG-11E (Steel, Small Building, Screws as sidelap Connectors, Existing Design)										
MSS_11_S_S_RW4_01	Small	1:1	Steel (WR Deck)	C_{max}	0.75	1.26	1.67	0.32	0.15	0.36
MSS_11_P_S_RW4_01	Small	1:1	Steel (WR Deck)	C_{max}	0.75	1.34	1.78	0.30	0.17	0.41
MSS_11_W_S_RW4_01	Small	1:1	Steel (WR Deck)	C_{max}	0.75	0.98	1.30	0.28	0.14	0.37
MSS_21_S_S_RW4_01	Small	2:1	Steel (WR Deck)	C_{max}	0.75	1.05	1.39	0.54	0.19	0.48
MSS_12_S_S_RW4_01	Small	1:2	Steel (WR Deck)	C_{max}	0.75	1.39	1.85	0.31	0.15	0.29
MSS_21_P_S_RW4_01	Small	2:1	Steel (WR Deck)	C_{max}	0.75	1.17	1.55	0.59	0.20	0.44
MSS_12_P_S_RW4_01	Small	1:2	Steel (WR Deck)	C_{max}	0.75	1.48	1.97	0.28	0.16	0.32
MSS_21_W_S_RW4_01	Small	2:1	Steel (WR Deck)	C_{max}	0.75	1.08	1.43	0.55	0.18	0.36
MSS_12_W_S_RW4_01	Small	1:2	Steel (WR Deck)	C_{max}	0.75	1.28	1.71	0.33	0.17	0.31

Table F4. Computed and acceptable adjusted collapse margin ratios for RWFD buildings incorporating steel roof diaphragm archetype designs

Archetype ID	Design configuration				Collapse margin parameters				Acceptance check	
	Building Size	Diaphragm aspect ratio	Diaphragm construction	Seismic SDC	CMR	μ_T	SSF	ACMR	Accept. ACMR	Pass/Fail
Performance Group No. PG-5E (Steel, Large Building, Welds and Button Punches as sidelap Connectors, Existing Design)										
HSL_21_W_WB_RW4_01	Large	2:1	Steel	D_{max}	0.99	8.09	1.34	1.33	1.73	Fail
HSL_12_W_WB_RW4_01	Large	1:2	Steel	D_{max}	1.90	8.26	1.33	2.53	1.73	Pass
HSL_11_W_WB_RW4_01	Large	1:1	Steel	D_{max}	0.95	8.16	1.33	1.27	1.73	Fail
Mean of Performance Group:					**1.28**	**8.17**	**1.33**	**1.71**	**2.30**	**Fail**
Performance Group No. PG-6E (Steel, Large Building, Screws as sidelap Connectors, Existing Design)										
HSL_21_P_S_RW4_01	Large	2:1	Steel	D_{max}	1.23	8.24	1.35	1.67	1.73	Fail
HSL_12_P_S_RW4_01	Large	1:2	Steel	D_{max}	2.07	8.14	1.33	2.75	1.73	Pass
HSL_11_P_S_RW4_01	Large	1:1	Steel	D_{max}	1.13	8.26	1.36	1.53	1.73	Fail
HSL_11_S_S_RW4_01	Large	1:1	Steel	D_{max}	1.15	8.01	1.33	1.53	2.73	Fail
Mean of Performance Group:					**1.40**	**8.16**	**1.34**	**1.87**	**2.30**	**Fail**
Performance Group No. PG-7E (Steel, Small Building, Button Punches as sidelap Connectors, Existing Design)										
HSS_11_W_B_RW4_01	Small	1:1	Steel	D_{max}	1.73	7.94	1.32	2.28	1.73	Pass
HSS_21_W_B_RW4_01	Small	2:1	Steel	D_{max}	1.42	8.05	1.33	1.89	1.73	Pass
HSS_12_W_B_RW4_01	Small	1:2	Steel	D_{max}	1.90	7.91	1.32	2.51	1.73	Pass
Mean of Performance Group:					**1.68**	**7.97**	**1.32**	**2.23**	**2.30**	**Fail**
Performance Group No. PG-8E (Steel, Small Building, Screws as sidelap Connectors, Existing Design)										
HSS_11_P_S_RW4_01	Small	1:1	Steel	D_{max}	1.55	8.02	1.33	2.07	1.73	Pass
HSS_11_S_S_RW4_01	Small	1:1	Steel	D_{max}	1.43	8.15	1.33	1.91	1.73	Pass
HSS_21_P_S_RW4_01	Small	2:1	Steel	D_{max}	1.33	8.33	1.33	1.76	1.73	Pass
HSS_12_P_S_RW4_01	Small	1:2	Steel	D_{max}	1.71	8.25	1.33	2.27	1.73	Pass
HSS_21_S_S_RW4_01	Small	2:1	Steel	D_{max}	1.25	7.85	1.32	1.65	1.73	Fail
HSS_12_S_S_RW4_01	Small	1:2	Steel	D_{max}	1.42	8.06	1.33	1.89	1.73	Pass
Mean of Performance Group:					**1.45**	**8.11**	**1.33**	**1.92**	**2.30**	**Fail**

Table F4. Computed and acceptable adjusted collapse margin ratios for RWFD buildings incorporating steel roof diaphragm archetype designs (cont.)

Archetype ID	Design configuration				Collapse margin parameters				Acceptance check	
	Building Size	Diaphragm aspect ratio	Diaphragm construction	Seismic SDC	CMR	μ_T	SSF	ACMR	Accept. ACMR	Pass/Fail
Performance Group No. PG-9E (Steel, Large Building, Screws as sidelap Connectors, Existing Design)										
MSL_21_P_S_RW4_01	Large	2:1	Steel	C_{max}	1.35	8.32	1.15	1.55	1.73	Fail
MSL_12_P_S_RW4_01	Large	1:2	Steel	C_{max}	2.01	7.85	1.13	2.27	1.73	Pass
MSL_21_S_S_RW4_01	Large	2:1	Steel	C_{max}	1.52	8.02	1.18	1.80	1.73	Pass
MSL_12_S_S_RW4_01	Large	1:2	Steel	C_{max}	1.88	8.38	1.15	2.16	1.73	Pass
MSL_21_W_S_RW4_01	Large	2:1	Steel	C_{max}	1.41	8.20	1.18	1.66	1.73	Fail
MSL_12_W_S_RW4_01	Large	1:2	Steel	C_{max}	1.96	8.02	1.15	2.25	1.73	Pass
MSL_11_P_S_RW4_01	Large	1:1	Steel	C_{max}	1.81	7.99	1.15	2.08	1.73	Pass
MSL_11_S_S_RW4_01	Large	1:1	Steel	C_{max}	1.58	8.15	1.15	1.81	1.73	Pass
MSL_11_W_S_RW4_01	Large	1:1	Steel	C_{max}	1.66	8.22	1.17	1.94	1.73	Pass
Mean of Performance Group:					**1.69**	**8.13**	**1.16**	**1.95**	**2.30**	**Fail**
Performance Group No. PG-10E (Steel, Large Buildings, Welds as Sidelap connectors, Existing Design)										
MSL_21__W_W_RW4_01	Large	2:1	Steel	C_{max}	1.39	7.76	1.15	1.59	1.73	Fail
MSL_12__W_W_RW4_01	Large	1:2	Steel	C_{max}	1.99	8.15	1.14	2.27	1.73	Pass
MSL_11__W_W_RW4_01	Large	1:1	Steel	C_{max}	1.52	8.09	1.16	1.76	1.73	Pass
Mean of Performance Group:					**1.63**	**8.00**	**1.15**	**1.88**	**2.30**	**Fail**
Performance Group No. PG-11E (Steel, Small Building, Screws as sidelap Connectors, Existing Design)										
MSS_11_S_S_RW4_01	Small	1:1	Steel	C_{max}	1.67	8.15	1.14	1.91	1.73	Pass
MSS_11_P_S_RW4_01	Small	1:1	Steel	C_{max}	1.78	8.26	1.14	2.03	1.73	Pass
MSS_11_W_S_RW4_01	Small	1:1	Steel	C_{max}	1.30	7.78	1.13	1.47	1.73	Fail
MSS_21_S_S_RW4_01	Small	2:1	Steel	C_{max}	1.39	8.05	1.15	1.60	1.73	Fail
MSS_12_S_S_RW4_01	Small	1:2	Steel	C_{max}	1.85	8.56	1.14	2.11	1.73	Pass
MSS_21_P_S_RW4_01	Small	2:1	Steel	C_{max}	1.55	8.12	1.16	1.80	1.73	Pass
MSS_12_P_S_RW4_01	Small	1:2	Steel	C_{max}	1.97	7.88	1.14	2.25	1.73	Pass
MSS_21_W_S_RW4_01	Small	2:1	Steel	C_{max}	1.43	7.97	1.15	1.65	1.73	Fail
MSS_12_W_S_RW4_01	Small	1:2	Steel	C_{max}	1.71	8.02	1.14	1.95	1.73	Pass
Mean of Performance Group:					**1.63**	**8.09**	**1.14**	**1.86**	**2.30**	**Fail**

APPENDIX G Evaluation of Alternate Design Procedure

To validate the alternate design procedure, archetype buildings were designed and P695 analyses were performed.

G.1 Description of Archetypes

Evaluations were performed on archetypes designed for high and moderate seismic risk as defined in Appendix B. For these evaluations, archetypes were designed with either steel deck or wood panel diaphragms. Summary tables with detailed descriptions of diaphragm zones for the archetypes are in Appendix H for the wood diaphragms. The results of the steel deck diaphragms are included in Koliou (2014). The walls for these archetypes are reinforced-concrete wall panels 25 ft in length, 33 ft tall measured from the top of slab-on-grade, and
9-1/4 in. thick for high seismic risk and 7-1/4 in. thick for moderate seismic risk. The roof level is at 30 ft above the top of slab-on-grade with parapet walls cantilevering 3 ft higher than the roof level.
The archetypes are grouped by whether the diaphragm is large or small. The archetypes have plan aspect ratios of 1:1, 2:1 and 1:2. Large diaphragms are 400 ft long and either 400 ft or 200 ft wide. The small diaphragms with aspect ratios of 2:1 and 1:2 are 200 ft long by 100 ft wide, and for the 1:1 aspect ratios the diaphragms are 100 ft by 100 ft. The wood diaphragms are wood structural panels nailed to wood nailers that are attached to open web steel joists.

G.2 Summary of FEMA P695 Analysis Results for the Alternate Design Procedure

Incremental Dynamic Analyses (IDA) (Vamvatsikos and Cornell, 2002) using the FEMA P695 Far Field Ground Motion Ensemble (FEMA P695, 2009) were performed using the simplified models to compute the median collapse intensity. Summaries of collapse results for individual wood diaphragm archetypes are included in Appendix I. Adjusted collapse margin ratios (ACMR) and acceptable ACMR values for the individual archetypes and the archetype groups are also included in Appendix I. The acceptable ACMR values are computed using the beta factors listed in Table D1. The combined uncertainty, βTotal, is computed as the square root sum of the squares of the individual uncertainties. For βTotal equal to 0.66, the acceptable ACMR is 1.73 and 2.30 for 20% and 10% probability of collapse at Maximum Considered Earthquake (MCE) ground motion, respectively. The acceptable ACMR applicable for the performance of individual archetypes is 1.73, and the ACMR of performance groups is 2.30. Summaries of the adjusted collapse margin ratio results for the performance groups of wood archetypes are provided in Table G1. The acceptable ACMR of at least 2.30 is achieved for each performance group.

Table G1. Summary of collapse margin ratio results for wood structural panel diaphragm archetype performance groups

Performance Group	Seismicity	Size	Computed ACMR	Acceptable ACMR	Pass/Fail
PG-1N	High	Large	3.68	2.30	Pass
PG-2N	High	Small	2.51		Pass
PG-3N	Moderate	Large	3.90		Pass
PG-4N	Moderate	Small	3.07		Pass

The elastic periods for the archetypes designed in accordance with the alternate design procedure are listed in Table G2. In almost all cases the range of periods are 0 to 20% longer than the computed equivalent periods in Table D3 for the archetypes designed using the current code design procedure.

The archetypes with larger diaphragms did better than the archetypes with small diaphragms, and the archetypes designed for moderate seismicity performed better than the ones designed for high seismicity. The small archetypes designed for high seismicity had the lowest ACMR. The range of fundamental elastic periods indicated in Table G2 is less than the transition period of 0.6 sec. for most of these 100 and 200 ft long diaphragms. Thus, these archetypes are experiencing the short period issue described in Section D.1.2 regarding the FEMA P695 analyses for the archetypes using the current design procedure. The ACMR for small archetypes designed for moderate seismicity have longer periods than those designed for high seismicity and the transition period is only 0.4 sec. The short period issue is less of a factor for the small buildings designed for moderate seismicity. The elastic period values in Table G2 are all well above the transition period for the wood archetypes that are 400 ft long, thus, the high ACMRs for the large wood diaphragm performance groups, PG1 and PG3.

Table G2. Summary of Elastic Periods for Archetypes Designed Using the Alternate Design Procedure

Wood diaphragm span length	Period for high-seismic archetypes	Period for moderate-seismic archetypes
400 ft	0.92 to 0.96 sec	0.92 to 0.93 sec
200 ft	0.53 to 0.65 sec	0.57 to 0.61 sec
100 ft	0.39 to 0.42 sec	0.45 to 0.46 sec

The ranges of building drift ratios (BDR) for the performance groups are provided in Table G3. The BDR is the sum of the wall drift ratio (WDR) and the diaphragm drift ratio (DDR) and serves as a damage index. The WDR is computed as the in-plane wall deformation divided by the height of the roof, and the DDR is computed as the diaphragm displacement divided by one-half of the diaphragm span. In general shorter diaphragm spans result in larger BDRs, especially for the wood diaphragms. This likely results from the wall drift ratio (WDR) being a larger percentage of the BDR for the smaller buildings.

Table G3. Range of building drift ratios (BDRs) for the wood diaphragm performance groups

Performance Group	Seismicity	Size	Median BDR @ DE (%)	Median BDR @ MCE (%)
PG-1N	High	Large	0.34 to 0.52	0.54 to 0.81
PG-2N	High	Small	0.79 to 0.85	1.14 to 1.31
PG-3N	Moderate	Large	0.34 to 0.39	0.55 to 0.65
PG-4N	Moderate	Small	0.53 to 0.61	0.90 to 1.21

G.3 Overstrength and Deflectio Amplificatio Factors for the Diaphragm

Values for the overstrength factor, Ωo, and deflection amplification factor, Cd, computed from the analysis results are included in Table I3. The smallest overstrength factor of all performance groups proposed for the system equal to 1.70, but rounded to half unit intervals, it would be equal to 2.0. The deflection amplification was computed as 5.6 in accordance with FEMA P695. Normally, deflection amplification factors are not taken greater than the response modification coefficient, R; however, in this case, an amplification factor higher than R was required because only 2% damping was assumed. An initial stiffness damping value of 2% of critical damping was chosen rather than the commonly assumed value of 5% for buildings because these buildings generally incorporate fewer non-structural components than conventional frame and wall buildings. Additional explanation is provided in Koliou [2014]. The deflection amplification factor was computed as Rdiaph/0.8 to account for the low damping. For Rdiaph = 4.5, Cd = 5.6. To test the validity of this value, the ratio of the median diaphragm drift caused by the design level ground motion to the median diaphragm drift at the "code" level force was computed for each archetype. The results are presented in Table I4. The mean ratio for Performance Group 1, which is large footprints and high seismic risk, was 3.3, which was the highest value for any of the performance groups. The highest ratio for an individual archetype was 4.3. These results indicate that the damping was more than 2% and that Cd equal to Rdiaph is appropriate.

THIS PAGE INTENTIONALLY LEFT BLANK

Appendix H Description of Archetypes for the Alternate Design Procedure

H.1 Description of Archetypes for the Alternate Design Procedure

Table H1. Archetype Descriptions for Wood Diaphragms for High- and Moderate-Seismic Risk – Alternate Design

Archetype ID	Diaphragm Dimensions	Zone	Zone Width (ft)	Sheathing	10d Common Nail Spacing		
					Boundaries and Contin-uous Edges	Other Edges	Intermediate Field Area
High-Seismicity Wood, Large Buildings							
HWL_21_N_OSB_RD4.5-1.5_01 HWL_12_N_OSB_RD4.5-1.5_01	400 x 200 ft	End	40 ft	15/32” OSB	2 in. o.c.	3 in. o.c.	12 in. o.c.
		Middle	320 ft	15/32” OSB	2-1/2 in. o.c.	4 in. o.c.	12 in. o.c.
HWL_21_N_OSB_RD4.5-1.5_02 HWL_12_N_OSB_RD4.5-1.5_02	400 x 200 ft	End	40 ft	15/32” OSB	2 lines each at 2-1/2 in. o.c.	2 lines each at 4 in. o.c.*	12 in. o.c.
		Middle	320 ft	15/32” OSB	2-1/2 in. o.c.	4 in. o.c.	12 in. o.c.
HWL_21_N_OSB_RD4.5_1.5_03	400 x 200 ft	End	40 ft	15/32” OSB	2 lines each at 2-1/2 in. o.c.	2 lines each at 3 in. o.c.*	12 in. o.c.
		Middle	320 ft	15/32” OSB	2 in. o.c.	3 in. o.c.	12 in. o.c.
HWL_21_N_OSB_RD4.5_1.5_04	400 x 200 ft	End	40 ft	15/32” OSB	2 lines each at 2-1/2 in. o.c.	2 lines each at 4 in. o.c.*	12 in. o.c.
		Middle	320 ft	15/32” OSB	2-1/2 in. o.c.	4 in. o.c.	12 in. o.c.
HWL_11_N_OSB_RD4.5-1.5_01	400 x 400 ft	End	40 ft	15/32” OSB	2 in. o.c.	3 in. o.c.**	12 in. o.c.
		Middle	320 ft	15/32” OSB	4 in. o.c.	6 in. o.c.	12 in. o.c.

Table H1. Archetype Descriptions for Wood Diaphragms for High- and Moderate-Seismic Risk – Alternate Design (cont.)

Archetype ID	Diaphragm Dimensions	Zone	Zone Width (ft)	Sheathing	10d Common Nail Spacing		
					Boundaries and Continuous Edges	Other Edges	Intermediate Field Area
High-Seismicity Wood, Large Buildings							
HWL_21_N_OSB_RD4.5-1.5_01 HWL_12_N_OSB_RD4.5-1.5_01	400 x 200 ft	End	40 ft	15/32" OSB	2 in. o.c.	3 in. o.c.	12 in. o.c.
		Middle	320 ft	15/32" OSB	2-1/2 in. o.c.	4 in. o.c.	12 in. o.c.
HWL_21_N_OSB_RD4.5-1.5_02 HWL_12_N_OSB_RD4.5-1.5_02	400 x 200 ft	End	40 ft	15/32" OSB	2 lines each at 2-1/2 in. o.c.	2 lines each at 4 in. o.c.*	12 in. o.c.
		Middle	320 ft	15/32" OSB	2-1/2 in. o.c.	4 in. o.c.	12 in. o.c.
HWL_21_N_OSB_RD4.5_1.5_03	400 x 200 ft	End	40 ft	15/32" OSB	2 lines each at 2-1/2 in. o.c.	2 lines each at 3 in. o.c.*	12 in. o.c.
		Middle	320 ft	15/32" OSB	2 in. o.c.	3 in. o.c.	12 in. o.c.
HWL_21_N_OSB_RD4.5_1.5_04	400 x 200 ft	End	40 ft	15/32" OSB	2 lines each at 2-1/2 in. o.c.	2 lines each at 4 in. o.c.*	12 in. o.c.
		Middle	320 ft	15/32" OSB	2-1/2 in. o.c.	4 in. o.c.	12 in. o.c.
HWL_11_N_OSB_RD4.5-1.5_01	400 x 400 ft	End	40 ft	15/32" OSB	2 in. o.c.	3 in. o.c.**	12 in. o.c.
		Middle	320 ft	15/32" OSB	4 in. o.c.	6 in. o.c.	12 in. o.c.
HWL_11_N_OSB_RD4.5-1.5_02	400 x 400 ft	End	40 ft	15/32" OSB	2 lines each at 2-1/2 in. o.c.	2 lines each at 4 in. o.c.*	12 in. o.c.
		Middle	320 ft	15/32" OSB			
High-Seismicity Wood, Small Buildings							
HWS_21_N_OSB_RD4.5-1.5_01 HWS_12_N_OSB_RD4.5-1.5_01	200 x 100 ft	End	20 ft	15/32" OSB	2 lines each at 2-1/2 in. o.c.	2 lines each at 3 in. o.c.*	12 in. o.c.
		Middle	160 ft	15/32" OSB	2 in. o.c.	3 in. o.c.**	12 in. o.c.

Table H1. Archetype Descriptions for Wood Diaphragms for High- and Moderate-Seismic Risk – Alternate Design (cont.)

Archetype ID	Diaphragm Dimensions	Zone	Zone Width (ft)	Sheathing	10d Common Nail Spacing		
					Boundaries and Continuous Edges	Other Edges	Intermediate Field Area
HWS_11_N_OSB_RD4.5_1.5_01	100 x 100 ft	End	10 ft	15/32" OSB	2-1/2 in. o.c.	4 in. o.c.	12 in. o.c.
		Middle	80 ft	15/32" OSB	4 in. o.c.	6 in. o.c.	12 in. o.c.
Moderate-Seismicity Wood, Large Buildings							
MWL_21_N_OSB_RD4.5-1.5_01 MWL_12_N_OSB_RD4.5-1.5_01	400 x 200 ft	End	0 ft	15/32" OSB	6 in. o.c.	6 in. o.c.	12 in. o.c.
		Middle	400 ft	15/32" OSB	6 in. o.c.	6 in. o.c.	12 in. o.c.
MWL_11_N_OSB_RD4.5-1.5_01	400 x 400 ft	End	0 ft	15/32" OSB	6 in. o.c.	6 in. o.c.	12 in. o.c.
		Middle	400 ft	15/32" OSB	6 in. o.c.	6 in. o.c.	12 in. o.c.
Moderate-Seismicity Wood, Small Buildings							
MWS_21_N_OSB_RD4.5-1.5_01 MWS_12_N_OSB_RD4.5-1.5_01	200 x 100 ft	End	20 ft	15/32" OSB	4 in. o.c.	6 in. o.c.	12 in. o.c.
		Middle	160 ft	15/32" OSB	6 in. o.c.	6 in. o.c.	12 in. o.c.
MWS_11_N_OSB_RD4.5-1.5_01	100 x 100 ft	End	0 ft	15/32" OSB	6 in. o.c.	6 in. o.c.	12 in. o.c.
		Middle	100 ft	15/32" OSB	6 in. o.c.	6 in. o.c.	12 in. o.c.

*Special 4x4 subpurlins at other edges in lieu of 2x4s

**Special 3x4 subpurlins at other edges in lieu of 2x4s

THIS PAGE INTENTIONALLY LEFT BLANK

Appendix I FEMA P695 Evaluation Results for the Alternate Design Procedure

I.1 FEMA P695 Evaluation Results for Alternate Design Procedure

Table I1. Summary of collapse results for RWFD buildings incorporating wood roof diaphragm archetype designs

Archetype ID	Design Configuration				Pushover and IDA Results			Relevant Analysis Parameters		
	Building Size	Diaphragm Aspect Ratio	Diaphragm Const.	Seismic SDC	SMT[T] (g)	SCT[T] (g)	CMR	Period (sec)	Median BDR @ DE (%)	Median BDR @ MCE (%)
Performance Group No. PG-1N (Wood, Large Building, New Design)										
HWL_21_N_OSB_RD4.5-1.5_01	Large	2:1	Wood	D_{max}	0.95	2.56	2.69	0.93	0.44	0.60
HWL_21_N_OSB_RD4.5-1.5_02	Large	2:1	Wood	D_{max}	0.92	2.91	3.16	0.94	0.41	0.56
HWL_21_N_OSB_RD4.5-1.5_03	Large	2:1	Wood	D_{max}	0.96	2.65	2.59	0.92	0.43	0.60
HWL_21_N_OSB_RD4.5-1.5_04	Large	2:1	Wood	D_{max}	0.94	2.94	3.13	0.94	0.42	0.54
HWL_12_N_OSB_RD4.5-1.5_01	Large	1:2	Wood	D_{max}	1.50	3.65	2.43	0.53	0.51	0.78
HWL_12_N_OSB_RD4.5-1.5_02	Large	1:2	Wood	D_{max}	1.50	3.63	2.42	0.55	0.52	0.81
HWL_11_N_OSB_RD4.5-1.5_01	Large	1:1	Wood	D_{max}	0.91	2.11	2.32	0.96	0.34	0.57
HWL_11_N_OSB_RD4.5-1.5_02	Large	1:1	Wood	D_{max}	0.93	2.15	2.39	0.95	0.35	0.59
Performance Group No. PG-2N (Wood, Small Building, New Design)										
HWS_21_N_OSB_RD4.5-1.5_01	Small	2:1	Wood	D_{max}	1.36	2.45	1.80	0.65	0.83	1.14
HWS_12_N_OSB_RD4.5-1.5_01	Small	1:2	Wood	D_{max}	1.50	2.95	1.97	0.42	0.85	1.24
HWS_11_N_OSB_RD4.5-1.5_01	Small	1:1	Wood	D_{max}	1.50	2.84	1.89	0.39	0.79	1.31
Performance Group No. PG-3N (Wood, Large Building, New Design)										
MWL_21_N_OSB_RD4.5-1.5_01	Large	2:1	Wood	C_{max}	0.49	1.68	3.43	0.92	0.34	0.55
MWL_12_N_OSB_RD4.5-1.5_01	Large	1:2	Wood	C_{max}	0.75	2.08	2.77	0.57	0.41	0.65
MWL_11_N_OSB_RD4.5-1.5_01	Large	1:1	Wood	C_{max}	0.48	1.76	3.52	0.93	0.39	0.57
Performance Group No. PG-4N (Wood, Small Building, New Design)										
MWS_21_N_OSB_RD4.5-1.5_01	Small	2:1	Wood	C_{max}	0.74	1.61	2.18	0.61	0.53	0.90
MWS_12_N_OSB_RD4.5-1.5_01	Small	1:2	Wood	C_{max}	0.75	2.08	2.77	0.45	0.67	0.99
MWS_11_N_OSB_RD4.5-1.5_01	Small	1:1	Wood	C_{max}	0.75	2.35	3.13	0.46	0.61	1.21

Table I2. Adjusted collapse margin ratios and acceptable collapse margin ratios for RWFD buildings incorporating wood roof diaphragm archetype designs

Archetype ID	Design Configuration				Collapse Margin Parameters				Acceptance Check	
	Building Size	Diaphragm Aspect Ratio	Diaphragm Construction	Seismic SDC	CMR	μ_T	SSF	ACMR	Accept. ACMR	Pass/Fail
Performance Group No. PG-1N (Wood, Large Building, New Design)										
HWL_21_N_OSB_RD4.5-1.5_01	Large	2:1	Wood	D_{max}	2.69	8.44	1.45	3.91	1.73	Pass
HWL_21_N_OSB_RD4.5-1.5_02	Large	2:2	Wood	D_{max}	3.16	8.37	1.45	4.59	1.73	Pass
HWL_21_N_OSB_RD4.5-1.5_03	Large	2:1	Wood	D_{max}	2.65	8.43	1.45	3.84	1.73	Pass
HWL_21_N_OSB_RD4.5-1.5_04	Large	2:1	Wood	D_{max}	3.13	8.35	1.45	4.54	1.73	Pass
HWL_12_N_OSB_RD4.5-1.5_01	Large	1:2	Wood	D_{max}	2.43	8.84	1.34	3.26	1.73	Pass
HWL_12_N_OSB_RD4.5-1.5_02	Large	1:2	Wood	D_{max}	2.45	8.87	1.34	3.29	1.73	Pass
HWL_11_N_OSB_RD4.5-1.5_01	Large	1:1	Wood	D_{max}	2.32	8.34	1.45	3.36	1.73	Pass
HWL_11_N_OSB_RD4.5-1.5_02	Large	1:1	Wood	D_{max}	2.39	8.38	1.45	3.46	2.73	Pass
Mean of Performance Group:					**2.58**	**8.50**	**1.42**	**3.68**	**2.58**	**8.50**
Performance Group No. PG-2N (Wood, Small Building, New Design)										
HWS_21_N_OSB_RD4.5-1.5_01	Small	2:1	Wood	D_{max}	1.80	7.59	1.35	2.43	1.73	Pass
HWS_12_N_OSB_RD4.5-1.5_01	Small	1:2	Wood	D_{max}	1.97	8.15	1.33	2.62	1.73	Pass
HWS_11_N_OSB_RD4.5-1.5_01	Small	1:1	Wood	D_{max}	1.89	8.44	1.33	2.52	1.73	Pass
Mean of Performance Group:					**1.88**	**8.06**	**1.34**	**2.51**	**2.30**	**Pass**
Performance Group No. PG-3N (Wood, Large Building, New Design)										
MWL_21_N_OSB_RD4.5-1.5_01	Large	2:1	Wood	C_{max}	3.42	8.22	1.22	4.18	1.73	Pass
MWL_12_N_OSB_RD4.5-1.5_01	Large	1:2	Wood	C_{max}	2.77	8.87	1.15	3.19	1.73	Pass
MWL_11_N_OSB_RD4.5-1.5_01	Large	1:1	Wood	C_{max}	3.52	8.64	1.23	4.33	1.73	Pass
Mean of Performance Group:					**3.23**	**8.58**	**1.20**	**3.90**	**2.30**	**Pass**
Performance Group No. PG-4N (Wood, Small Building, New Design)										
MWS_21_N_OSB_RD4.5-1.5_01	Small	2:1	Wood	C_{max}	2.18	8.16	1.16	2.49	1.73	Pass
MWS_12_N_OSB_RD4.5-1.5_01	Small	1:2	Wood	C_{max}	2.77	8.54	1.14	3.16	1.73	Pass
MWS_11_N_OSB_RD4.5-1.5_01	Small	1:1	Wood	C_{max}	3.13	8.25	1.14	3.57	1.73	Pass
Mean of Performance Group:					**2.69**	**8.32**	**1.15**	**3.07**	**2.30**	**Pass**

Table I3. Overstrength and Deflection Amplification Parameters for the Alternate Design Procedure

Archetype ID	Design configuratio					
	Building Size	Diaphragm aspect ratio	Diaphragm construction	Seismic SDC	Ω	Cd
Performance Group No. PG-1N (Wood, Large Building, Alternate Design)						
HWL_21_N_OSB_RD4.5-1.5_01	Large	2:1	Wood	Dmax	2.46	5.625
HWL_21_N_OSB_RD4.5-1.5_02	Large	2:1	Wood	Dmax	2.44	5.625
HWL_21_N_OSB_RD4.5-1.5_03	Large	2:1	Wood	Dmax	2.44	5.625
HWL_21_N_OSB_RD4.5-1.5_04	Large	2:1	Wood	Dmax	2.45	5.625
HWL_12_N_OSB_RD4.5-1.5_01	Large	1:2	Wood	Dmax	1.58	5.625
HWL_12_N_OSB_RD4.5-1.5_02	Large	1:2	Wood	Dmax	1.61	5.625
HWL_11_N_OSB_RD4.5-1.5_01	Large	1:1	Wood	Dmax	2.25	5.625
HWL_11_N_OSB_RD4.5-1.5_02	Large	1:1	Wood	Dmax	2.20	5.625
				Mean	2.18	N/A
Performance Group No. PG-2N (Wood, Small Building, Alternate Design)						
HWS_21_N_OSB_RD4.5-1.5_01	Small	2:1	Wood	Dmax	1.68	5.625
HWS_12_N_OSB_RD4.5-1.5_01	Small	1:2	Wood	Dmax	1.71	5.625
HWS_11_N_OSB_RD4.5-1.5_01	Small	1:1	Wood	Dmax	1.70	5.625
				Mean	1.70	N/A
Performance Group No. PG-3N (Wood, Large Building, Alternate Design)						
MWL_21_N_OSB_RD4.5-1.5_01	Large	2:1	Wood	Cmax	4.68	5.625
MWL_12_N_OSB_RD4.5-1.5_01	Large	1:2	Wood	Cmax	2.77	5.625
MWL_11_N_OSB_RD4.5-1.5_01	Large	1:1	Wood	Cmax	4.32	5.625
				Mean	3.92	N/A
Performance Group No. PG-4N (Wood, Small Building, Alternate Design)						
MWS_21_N_OSB_RD4.5-1.5_01	Small	2:1	Wood	Cmax	2.65	5.625
MWS_12_N_OSB_RD4.5-1.5_01	Small	1:2	Wood	Cmax	2.22	5.625
MWS_11_N_OSB_RD4.5-1.5_01	Small	1:1	Wood	Cmax	2.25	5.625
				Mean	2.37	N/A

Table I4. Ratio of the medial diaphragm drift caused by the design level ground motion to the median diaphragm drift at the "code" level force

Archetype ID	C_d
Performance Group No. PG-1N	
HWL_21_N_OSB_RD4.5-1.5_01	4.0
HWL_21_N_OSB_RD4.5-1.5_02	3.4
HWL_21_N_OSB_RD4.5-1.5_03	4.3
HWL_21_N_OSB_RD4.5-1.5_04	4.0
HWL_12_N_OSB_RD4.5-1.5_01	2.2
HWL_12_N_OSB_RD4.5-1.5_02	2.3
HWL_11_N_OSB_RD4.5-1.5_01	3.4
HWL_11_N_OSB_RD4.5-1.5_02	2.5
Mean of Performance Group:	3.3
Performance Group No. PG-2N	
HWS_21_N_OSB_RD4.5-1.5_01	3.8
HWS_12_N_OSB_RD4.5-1.5_01	2.1
HWS_11_N_OSB_RD4.5-1.5_01	2.0
Mean of Performance Group:	2.6
Performance Group No. PG-3N	
MWL_21_N_OSB_RD4.5-1.5_01	3.4
MWL_12_N_OSB_RD4.5-1.5_01	1.9
MWL_11_N_OSB_RD4.5-1.5_01	3.3
Mean of Performance Group:	2.8
Performance Group No. PG-4N	
MWS_21_N_OSB_RD4.5-1.5_01	3.5
MWS_12_N_OSB_RD4.5-1.5_01	3.4
MWS_11_N_OSB_RD4.5-1.5_01	2.4
Mean of Performance Group:	3.1

APPENDIX J Out-of-Plane Wall and Wall Anchorage Forces

The wall's out-of-plane force level and force level for anchorage of the wall to the diaphragm are separately derived and account for amplified ground accelerations as identified by Bouwkamp, et al. (1994) and Celebi, et al. (1989), observed failures, and consideration of whether yielding should be allowed. While some out-of-plane yielding of the wall is considered acceptable, top of wall anchorage forces are expected to be resisted by connections and members that behave nearly elastically.

J.1 Out-of-Plane Wall and Wall Anchorage Forces; Current Design

During an earthquake, the ground shakes and moves the base of walls in-plane and out-of-plane, which generates inertial forces in the wall. The wall movement causes the diaphragm to move, which generates inertial forces in the diaphragm. The diaphragm movement causes movement of the tops of the walls, which also leads to inertial forces generated in the walls. These out-of-plane wall anchorage forces can be much larger as determined by the percentage of effective mass than the overall forces for the SFRS.

ASCE 7-10 requires that walls be designed for an out-of-plane force, F_p, in accordance with the following formula.

$$F_p = 0.4S_{DS}I_eW_p \geq 0.1W_p \qquad \text{ASCE 7-10, Section 12.11-1}$$

Where W_p is the weight of the wall.

ASCE 7-10 requires that the anchorage of walls and transfer of forces into the diaphragm be designed for an out-of-plane wall force in accordance with the following formulas.

$$F_p = 0.4S_{DS}k_aI_eW_p \geq 0.2k_aI_eW_p \qquad \text{ASCE 7-10, Section 12.11-1}$$

$$k_a = 1.0 + \frac{L_f}{100} \leq 2.0 \qquad \text{ASCE 7-10, Section 12.11-2}$$

Where k_a is an amplification factor for diaphragm flexibility, and

L_f is the span, in feet, of a flexible diaphragm between resisting walls or rigid frames.

In ASCE 7-10, Section 12.11-1 and 12.11-2, k_a and L_f account for diaphragm flexibility. If a diaphragm is rigid, L_f equals 0 but if it is flexible, L_f equals the span length. For many buildings with rigid walls and flexible roof diaphragms, the diaphragm span between supporting walls or frames will be longer than 100 ft so k_a will often be equal to 2.0. For diaphragms in which k_a equals 2.0, the acceleration parameter used to compute the out-of-plane wall anchorage force is $0.8S_{DS}$, which is 80% of the maximum design spectral acceleration parameter. The intent is that the wall anchorage force is resisted

elastically for a force level computed using the maximum design spectral acceleration. The 0.8 factor is included to recognize that some connection and member overstrength may be relied upon to resist the top of wall anchorage force [SEAOC Seismology Committee, 1999].

ASCE 7-10, Section 12.11-1 allows for top of wall anchorage forces less than those computed using the maximum design response spectrum parameter for cases in which the diaphragm span is less than 100 ft. This reduction is inconsistent with the common condition in which a short span diaphragm often has significant overstrength that can result in greater forces developing at the top of wall support.

J.2 Out-of-plane Wall Anchorage Force Study

A study was performed to determine the magnitude of the force required to anchor the top of walls for out-of-plane forces. Archetype HSL_21_W_WB_RW4 was analyzed to determine the out-of-plane wall forces. This archetype is 400 ft long by 200 ft wide with the roof height at 30 ft. The wall panels are 9-1/4 in. thick and 33 ft tall. The roof diaphragm is steel deck with welded framing connectors, top seam weld sidelap connectors in the outer two zones and button punches at the center zone. The top of wall anchorage force computed in accordance with ASCE 7-10 Eq. 12.11-1, is 1,680 lbs/ft, which is based on the design level earthquake. The model of the archetype was loaded with the forty-four ground-motion records from FEMA P695 and incrementally amplified to spectral acceleration intensities up to 2.5g. The median out-of-plane wall anchorage forces for the forty-four records at the roof level are shown in Figures J1 and J2 respectively for the transverse and longitudinal direction of loading. In the figures, the solid blue lines represent out-of-plane anchorage forces for analyses that account for wall flexibility and the solid red lines represent out-of-plane anchorage forces for analyses that have infinitely rigid walls. The out-of-plane wall anchorage forces that include wall flexibility in the analyses, solid blue lines, should be referred to for determining the median out-of-plane wall anchorage force. The analyses with infinitely rigid walls, red lines, are used to help understand the amplified forces near corners, which is discussed later in this section. The MCE intensities are where the dashed vertical blue lines cross the curves.

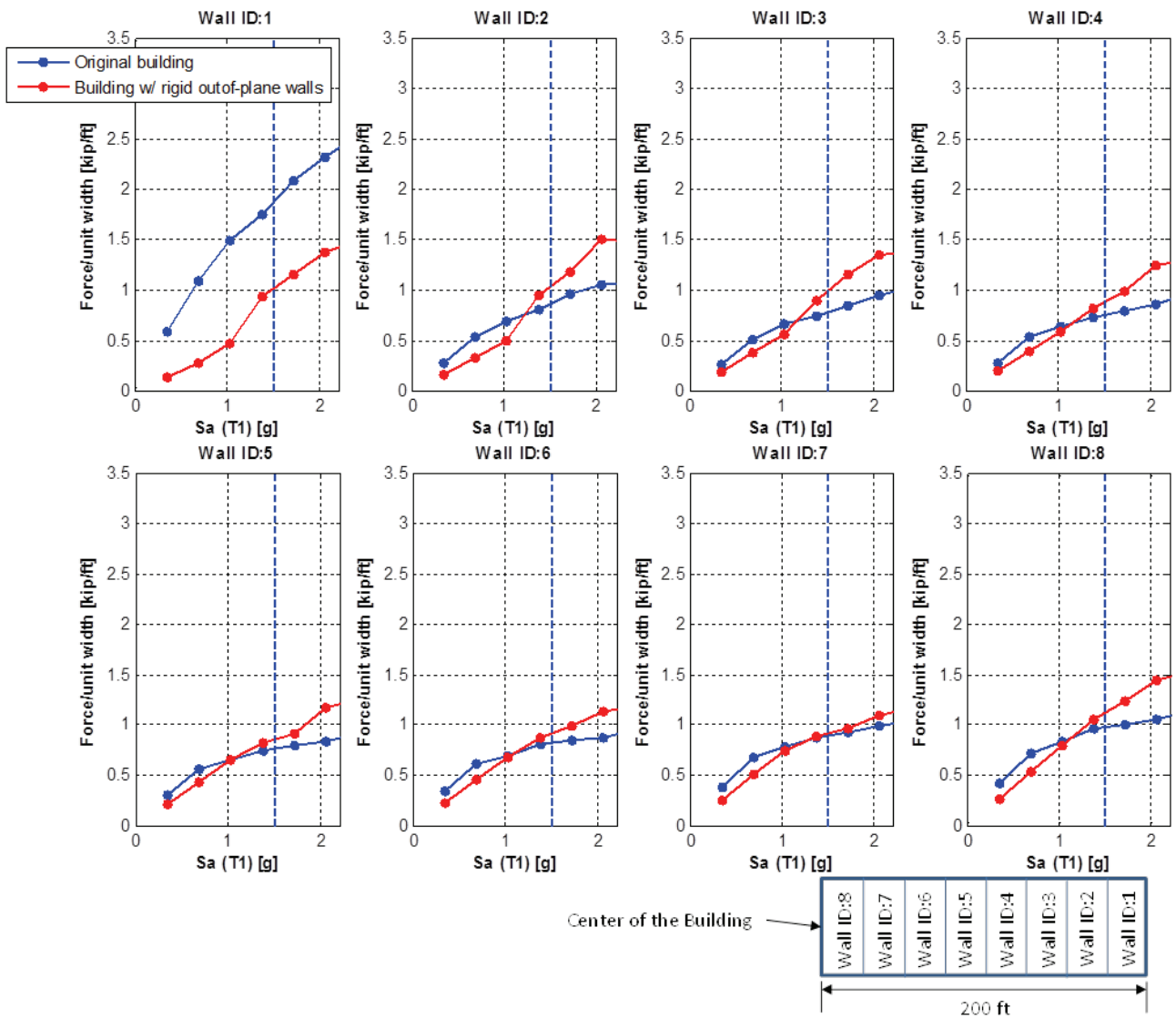

Figure J1. Median out-of-plane wall anchorage force for transverse direction of loading.

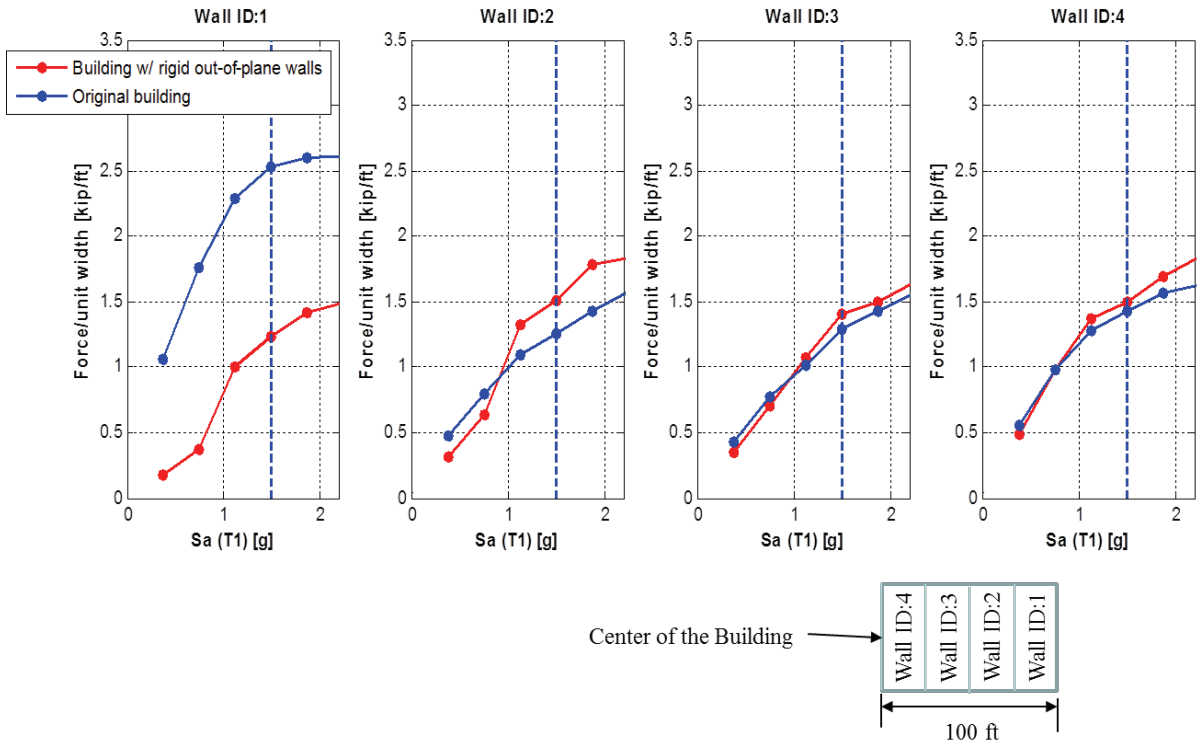

Figure J2. Median out-of-plane wall anchorage force for longitudinal direction of loading.

The study showed that anchorage forces are higher for walls loaded out-of-plane when the diaphragm is loaded in the longitudinal direction than they are for walls loaded out-of-plane when the diaphragm is loaded in the transverse direction. At the center of the diaphragm span, the out-of-plane wall anchorage forces are about 1.2 kips/ft for the transverse direction loading and 1.5 kips/ft in the longitudinal direction loading for MCE level of shaking. Out-of-plane anchorage forces in the longitudinal direction are likely greater than in the transverse direction because the diaphragm has more overstrength in the longitudinal versus the transverse direction.

The study also showed that anchorage forces were higher at the corners than in the middle of the diaphragm. This occurs because input motions between the bottom and the top of the wall panels are more likely to be in-phase adjacent to the corners, which dynamically amplifies the wall accelerations near the corner. This dynamic amplification is evident in the comparison of the out-of-plane anchorage forces for analyses that include wall flexibility, solid blue line, and those that assume the wall is rigid, solid red line. Near corners eliminating wall flexibility greatly reduces the out-of-plane anchorage forces but has little effect near the center of the diaphragm span. Also, the magnitude of the panel flexibility affects the load developed near the corners more than away from the corners.

Median forces generated in the analyses are less than the required design forces computed in accordance with ASCE 7-10 using Eq. 12.11-1 except at the corner in the longitudinal direction. The results suggest

that overstrength in the diaphragm and corner conditions result in higher out-of-plane anchorage forces. Therefore, smaller footprint buildings, which often have significant diaphragm overstrength, may generate higher forces than obtained with the formula for out-of-plane wall anchorage.

J.3 Stiffness of Wall Anchorage Connections

The stiffness of wall-to-diaphragm connections is also considered in design. In previous earthquakes wall-to-diaphragm connections have experienced premature failures and loss of wall support. Strap anchors have buckled and fractured prematurely. Also, as the straps elongate, wood ledgers have been loaded in cross grain bending from the diaphragm nailing. A similar issue occurs with hold-down wall anchors that have oversized bolt holes. The slip that occurs as the hold-down moves to engage the bolt can also allow the diaphragm nailing to load the wood ledger board in cross grain bending. When using wood ledgers, designs should include wall-to-diaphragm anchorage connections that have adequate stiffness to avoid cross grain bending of wood ledger boards, buckling and subsequent fracture of straps, and other detrimental effects of connections that are too flexible.

Current practice for connecting diaphragms to walls avoids some of the potential problems. For example, steel angles have largely replaced wood ledgers. This eliminates the possibility of ledger cross grain bending. The popularity of the hybrid panelized roof system in parts of the United States has significantly reduced the number of diaphragms with wood framing, thus reducing the use of hold-downs. For steel deck diaphragms, the welded connections are stiff. Although other issues may exist with the improved connections, such issues may not become evident until the next major earthquake occurs.

J.4 Transfer of Wall Anchorage Forces to Continuous Diaphragm Ties

Although the interaction of the diaphragm and walls is dynamic in nature, following the flow of forces as if only static forces were involved makes it easier to understand how the connections and roof elements should be designed for support of the walls out-of-plane. For wood diaphragms, the static simplification of the load path for support of out-of-plane wall forces has wall anchorage forces being transferred to sub-diaphragms in the end regions of the diaphragm that transfer anchorage forces into continuity ties that distribute forces into the main diaphragm. Current practice is for the sub-diaphragm to be designed for the top of wall anchorage forces but the shears generated within the sub-diaphragm are not combined with the shears from the main diaphragm even though they occur simultaneously. For steel deck diaphragms, some designers use sub-diaphragms similar to the approach used for wood diaphragms. More commonly for steel deck diaphragms, the static simplification of the load path for support of out-of-plane wall forces has wall anchorage forces transferred to the end of the deck sheets for out-of-plane forces parallel to the direction that the deck sheets span and into the joists for out-of-plane forces perpendicular to the direction that the joists span.

For buildings with concrete and masonry walls, Section 12.11.2.2 of ASCE 7-10 requires continuous diaphragm ties that resist the out-of-plane top of wall connection forces. Many engineers interpret the provision to require that the force at the edge of the wall be transferred across the entire diaphragm through the continuity ties. Other engineers interpret the requirement as allowing the force in the continuity tie to be reduced as the force is transferred into the main diaphragm. This approach is very common when analyzing existing buildings. If using this approach of variable tie force, the required tie strength is small near the center of the diaphragm assuming equal wall mass at each diaphragm edge acting with motions in phase. To address the small tie force, engineers should use a minimum tie force equal to that required by Section 12.1.3 (SEAOC 2008 and SEAOC 2010).

Section 12.1.3 ASCE 7-10 requires that all parts of buildings between seismic separation joints be interconnected. If the minimum force level determined using this section is applied, the ties must also be designed for a seismic force, F_p, equal to 0.133 times short period acceleration, S_{DS}, times the weight of the smaller portion of the building being connected to the larger portion but not less than 5% of the weight of the smaller portion. For one-story buildings, the weight includes the wall and roof weights. Therefore, the maximum tie force will be located where the weight to each side of the tie is equal. For symmetrical buildings, this will be the center of the diaphragm.

APPENDIX K Analysis of Archetypes Using Uniform Nailing

Table K1 includes a comparison of archetypes designed using the alternate design procedure versus those using uniform nailing. For the archetypes with uniform nailing, the nailing in the edge zone, where the shear is amplified by 1.5, was extended across the diaphragm. This is essentially designing for R_{diaph} equal to 3.0 without reducing the nailing across the diaphragm. This nailing is likely to cause a concentration of yielding along the diaphragm edge with little opportunity for yielding to spread into the diaphragm. For the archetypes studied, the less desirable nailing lowered the ACMR but in no case did it reduce it below the acceptable level of 1.73 for an individual archetype. This result indicates that adequate overstrength and ductility exists for this less than desirable nailing. It also means that the location of the transition of amplified shear to unamplified can be extended toward the center of the diaphragm if necessary with only modest reductions in the seismic performance.

Table K1. Comparison of archetypes

Performance group ID	Design Configuration				Collapse margin		Pass/Fail
	Archetype ID	Building Size	Diaphragm Construction	Seismic SDC	ACMR	Acceptable ACMR	
PG-1	HWL_12_N_OSB_RD4.5-1.5_01	Large	Wood Panelized	Dmax	3.26	1.73	Pass
	HWL_12_N_OSB_RD3_01	Large	Wood Panelized	Dmax	2.93		Pass
	Perfomance Group (ACMR=3.78)	***Projected ACMR of PG=ACMR*(2.93/3.26)***			**3.40**	**2.30**	**Pass**
PG-2	HWS_21_N_OSB_RD4.5-1.5_01	Small	Wood Panelized	Dmax	2.43	1.73	Pass
	HWS_21_N_OSB_RD3_01	Small	Wood Panelized	Dmax	2.25		Pass
	Perfomance Group (ACMR=2.52)	***Projected ACMR of PG=ACMR*(2.11/2.43)***			**2.33**	**2.30**	**Pass**
PG-3	MWL_12_N_OSB_RD4.5-1.5_01	Large	Wood Panelized	Cmax	3.19	1.73	Pass
	MWL_12_N_OSB_RD3_01	Large	Wood Panelized	Cmax	2.76		Pass
	Perfomance Group (ACMR=3.90)	***Projected ACMR of PG=ACMR*(2.76/3.19)***			**3.37**	**2.30**	**Pass**
PG-4	MWS_21_N_OSN_RD4.5-1.5_01	Small	Wood Panelized	Cmax	2.49	1.73	Pass
	MWS_21_N_OSN_RD3_01	Small	Wood Panelized	Cmax	2.05		Pass
	Perfomance Group (ACMR=3.07)	***Projected ACMR of PG=ACMR*(2.05/2.49)***			**2.53**	**2.30**	**Pass**

THIS PAGE INTENTIONALLY LEFT BLANK

THIS PAGE INTENTIONALLY LEFT BLANK

FEMA

FEMA P-1026
Catalog No. 14353-2